SYNTHESIS OF MOLECULES AND CLUSTERS WITH ACTINIDE-CHALCOGEN BONDS

By

MATTHEW ADAM STUBER

A dissertation submitted to the

School of Graduate Studies

Rutgers, The State University of New Jersey

In partial fulfillment of the requirements

For the degree of

Doctor of Philosophy

Graduate Program in Chemistry and Chemical Biology

Written under the direction of

John G. Brennan

And approved by

_____

_____

_____

_____

New Brunswick, New Jersey

January 2021

ABSTRACT OF THE DISSERTATION

SYNTHESIS OF MOLECULES AND CLUSTERS WITH ACTINIDE-CHALCOGEN BONDS

By Matthew A. Stuber

Dissertation Director:

John G. Brennan

The synthesis of novel actinide coordination complexes and polymetallic actinide clusters with chalcogen based anions is the focus of this thesis. Thorium and uranium compounds with bidentate ligands have been prepared via in situ oxidation of Th or U with various ligands that include I_2, PhEEPh, $C_6F_5EEC_6F_5$ (E = S, Se), and pySSpy. Four compounds, $(bipy)_2Th(SeC_6F_5)_4$, $(py)Th(Spy)_4$, $(py)U(Spy)_4$, and $(py)_2UI_2(Spy)_2$ were isolated in good yield and characterized by X-ray diffraction. Two bimetallic compounds, $py_4Th_2I_2(Spy)_2(Se_2)_2$ and $py_7Th_2F_5(SC_6F_5)_3$ were synthesized from the reaction of heteroleptic intermediates "$Th(EPh)_x(SR)_{4-x}$" (E = S, Se; R = C_6F_5, py) with elemental selenium and silver(I) fluoride respectively. The first two pyridinethiolate compounds of thorium have been synthesized and discussed in this chapter. Actinide chalcogenolate clusters supported by fluorinated ligands is also discussed.

Tetrametallic thorium clusters with a distorted Th_4E_4 (E = S, Se) cube-like core are prepared by ligand based redox reduction of elemental E with heteroleptic thorium intermediates "$Th(EPh)_x(E'C_6F_5)_{4-x}$" and oxidation of EPh^- to PhEEPh. Four compounds, $(py)_8Th_4(\mu_3\text{-}S)_4(\mu_2\text{-}SPh)_4(SC_6F_5)_4$, $(py)_8Th_4(\mu_3\text{-}Se)_4(\mu_2\text{-}SePh)_4(SeC_6F_5)_4$, $(py)_8Th_4(\mu_3\text{-}S)_4(\mu_2\text{-}SPh)_4(SeC_6F_5)_4$, and $(py)_8Th_4(\mu_3\text{-}Se)_4(\mu_2\text{-}SePh)_4(SC_6F_5)_4$ were

isolated and characterized by NMR spectroscopy and X-ray diffraction. Heterochalcogen clusters could only be isolated when μ_3-E = μ_2-E(Ph) in the core. These compounds show the impact of ring fluorination, with less nucleophilic EC_6F_5 ligands only occupying terminal binding sites, and this reads as the terminal binding sites effect uniform crystal packing and intermolecular π…π and H-bonding interactions throughout each compound. ^{77}Se NMR spectroscopy reveals the solid-state structure of the tetrametallic clusters are maintained in solution.

Tetrametallic uranium clusters with distorted U_4E_4 (E = S, Se) cube-like core are prepared similarly to the thorium tetrametallic clusters. Four compounds, $(py)_8U_4(\mu_3\text{-}S)_4(\mu_2\text{-}SPh)_4(SC_6F_5)_4$, $(py)_8U_4(\mu_3\text{-}Se)_4(\mu_2\text{-}SePh)_4(SeC_6F_5)_4$, $(py)_8U_4(\mu_3\text{-}S)_4(\mu_2\text{-}SPh)_4(SeC_6F_5)_4$, and $(py)_8U_4(\mu_3\text{-}Se)_4(\mu_2\text{-}SePh)_4(SC_6F_5)_4$ were isolated and characterized by X-ray diffraction and magnetic susceptibility measurements. These compounds show similar reactivity where isolatable compounds form only when μ_3-E = μ_2-E(Ph) in the core. The tetrameric uranium core with four μ_3-E bridging ligands offers a unique look at magnetic susceptibility studies, as reports on U(IV)-E-U(IV) environments are limited to mono- and bimetallic compounds. Magnetic susceptibility studies suggest antiferromagnetic coupling at low temperatures.

ACKNOWLEDGEMENTS

First and foremost, I would like to offer my deepest gratitude to my advisor, Dr. John Brennan. Throughout my graduate career, his knowledge and insight into the world of actinide chemistry and supportive guidance has helped me grow as a chemist and independent researcher.

I would like to thank my committee members, Dr. Martha Greenblatt, Dr. Alan Goldman, and Dr. Norman Edelstein for their valuable insight and critiques.

I am grateful to Dr. Thomas Emge for his aid in collecting and processing single crystal X-ray diffraction data, powder X-ray diffraction data, as well as his many insightful discussions on crystallography.

Special thanks to Dr. Anna Kornienko for her help in the day-to-day operations of the lab, as well as her help with specific air-sensitive techniques when I first joined the lab. I am appreciative of our discussions and your support with my ideas for new directions with my research and helped buff out my roughest ideas into executable projects.

I am also thankful to Dr. Weiwei Xie and Dr. Xin Gui for their help with magnetic susceptibility measurements and their invaluable insight on the magnetic phenomena of my compounds.

I would also like to thank my lab mates, Dr. Marissa Ringgold, Dr. Wen Wu, and Garret Gotthelf for keeping me motivated and engaged with my work. I am fortunate for our many lunch excursions, fun conversations, and for just being around to prevent graduate student life from getting too lonely. Marissa synthesized compounds $(bipy)_2Th(SPh)_4$ and $(bipy)_2Th(SePh)_4$ and Wen synthesized

$(bipy)_2Th(SC_6F_5)_4$, for which I was able to compare to the compound $(bipy)_2Th(SC_6F_5)_4$ described in this thesis.

Finally, I would like to thank my friends and family for their amazing support throughout my graduate studies. Their love has kept my light shining even on the darkest of days. I am grateful for the many phone calls of support and have truly helped motivate me throughout this journey. My family has especially been a force of positivity. I am truly grateful for the lessons and values my family has instilled in me as they have made me into the person I am today. I thank my mom, dad, and brother from the bottom of my heart.

DEDICATION

To my family. I love you.

TABLE OF CONTENTS

LIST OF FIGURES

LIST OF TABLES

LIST OF ABBREVIATIONS

An	Actinide
Ln	Lanthanide
Bipy	2,2’-bipyridine
Spy	2-pyridinethiolate
py	Pyridine
THF	Tetrahydrofuran
E	S, Se, Te
PXRD	Powder X-Ray Diffraction

Parts of this thesis have been previously published as follows:

Part of Chapter 2 has been published as:

Ringgold, M.; Wu, W.; Stuber, M.; Kornienko, A. Y.; Emge, T. J.; Brennan, J. G., Monomeric thorium chalcogenolates with bipyridine and terpyridine ligands. *Dalton T* **2018,** *47* (41), 14652-14661.

Gotthelf, G.; Stuber, M. A.; Kornienko, A. Y.; Emge, T. J.; Brennan, J. G., Organosoluble tetravalent actinide di- and trifluorides. *Chem Commun (Camb)* **2018,** *54* (85), 12018-12020.

Part of Chapter 3 has been published as:

Stuber, M. A.; Kornienko, A. Y.; Emge, T. J.; Brennan, J. G., Tetrametallic Thorium Compounds with Th4E4 (E = S, Se) Cubane Cores. *Inorg Chem* **2017,** *56* (17), 10247-10256.

Chapter 1: Introduction

1.1 Introduction

A prominent aspect of inorganic coordination chemistry is concerned with the study and increased understanding of bonding characteristics of ligand s and p orbitals with main group and transition metal s, p, and d orbitals. Advances in inorganic coordination chemistry also led to new possibilities for research on rare earth 4f, and actinide 5f metals. The study of the actinides gained traction with the Manhattan Project, where chemists sought to study volatile compounds of the actinides to separate fissile isotopes for nuclear fuels and weapons.[1-3] Thorium and uranium are the two most studied actinides, owing to their natural abundance in the Earth's crust. Much of thorium and uranium chemistry is concerned with the study of aqueous species for the extraction and separation of specific isotopes. Such examples of aqueous coordination compounds include those with tributyl phosphate used in the thorium extraction, or Thorex, process.[4]

Coordination complexes provide insight into the nature of bonding in actinide compounds. Ligands can be altered at the coordinating atom, where the non-metal is typically a carbon,[5-7] pnictide,[8-12] chalcogenide,[13-16] or halide.[17-20] A series of related ligands can show differences in chemical and physical properties of coordination compounds.[1, 21-23] For example, sterically encumbered uranium complexes with similar ligands [((^{tBu}ArO)$_3$tacn)U] (^{tBu}ArOH)$_3$tacn=1,4,7-tris(3,5-di-*tert*-butyl-2-hydroxybenzyl)-1,4,7-triazacyclononane), and the adamantyl derivative [((^{Ad}ArO)$_3$tacn)U] were studied to probe a series of ligands for nitrogen- and group-transfer reactivity.[22, 24, 25] Ligands also have the ability to coordinate to the metal center by more than one atom. Such ligands with increased hapticity have been

instrumental in broadening our knowledge of actinide coordination, including the synthesis of one of the first organouranium complexes, $[U(\eta^5\text{-}C_5H_5)_3Cl]$,[26, 27] and the synthesis of uranocene, $[U(\eta^8\text{-}C_8H_8]$,[28] which helped increase our understanding of the bonding between the metal-5f and ligand orbitals. Ligands with increased denticity aid in sterically saturating the coordination sphere and stabilizing an An-R bond for reactivity studies, such as the reactivity series of $An(I)[N(CH_2CH_2NSiPr^i_3)_3]$.[29]

The study of actinide coordination complexes is driven by the desire to explore the unique chemical properties not found anywhere else on the periodic table. These properties arise from the complicated nature of the bonding orbitals. For heavy elements such as uranium and thorium, relativistic effects on the s, p, d, and f orbitals play an important role in orbital energy and bonding characteristics. Electrons in s and p orbitals increase in mass as their velocity approaches the speed of light due to relativistic quantum effects. As electron velocity increases with increasing atomic mass, orbital radii shrinks closer to the nucleus.[30] This relative contraction of the s and p orbitals greatly shields d and f orbitals of the heavier elements from the nucleus causing the latter two to undergo orbital expansion.[31] A result of relativistic orbital expansion is the comparable energies of 5f and 6d orbitals. The unfilled 5f orbital in thorium ($[Rn]6d^27s^2$) is slightly higher in energy than the 6d orbital; but as atomic number increases across the actinides and the 5f orbitals fill with unpaired electrons, the 5f orbitals fall in energy, leading to the 6d orbitals becoming higher in energy after uranium.[32, 33]

The most common oxidation state of thorium ($[Rn]6d^27s^2$) is Th^{4+}, where the 7s and 6d electrons are removed, yielding a radon noble-gas configuration. Uranium ($[Rn]5f^36d^17s^2$) has several common oxidation states, including U^{3+} ($[Rn]5f^3$), U^{4+}

($[Rn]5f^2$), U^{5+} ($[Rn]5f^1$), and U^{6+} ($[Rn]5f^0$). The low energy requirements for 5f and 6d electron conversions allow many oxidation states to occur, owing to the similar energy levels and low ionization energies of the valence electrons in the early actinides. This contrasts with the lanthanides, where the common oxidation state throughout the series is 3+. After the removal of the 6s electrons and a 4f electron, the 4f orbitals are markedly core-like in character and the energy required to remove another electron is large. There are exceptions to this, including a few instances of Ln(II) and Ln(IV). In the actinides, americium has a stable 2+ oxidation state due to the removal of $7s^2$ electrons leaving a half filled $5f^7$ configuration.

The large radial expansion of the 5f orbitals into the valence region, coupled with the overlap of available 5f and 6d orbitals can yield covalent character in actinide compounds where the valence orbitals are energetically similar to ligand frontier orbitals. This is a sharp contrast to the more ionic lanthanide series. In the lanthanides, 4f orbitals are more contracted than their 5f actinide counterparts, leading to a decreased role of the 4f orbitals in bonding with ligand-based orbitals. Covalent contributions to actinide-ligand bonding have been shown in a variety of compounds, especially in uranium complexes.[34-38] For example, photoelectron spectroscopy studies of uranocene offered insight into the overlap between uranium 5f orbitals and cyclooctatetraene frontier e_{2u} orbitals.[34] More recently, multinuclear NMR studies have been performed to aid in covalent bond character assignments; including the use of ^{77}Se and ^{125}Te coupled with quantum-chemical analyses to probe An-E bond covalencies and 5f and 6d orbital participation.[38]

Research on the nature of bonds to actinide metal centers in coordination complexes was initially performed in aqueous solutions with oxygen containing compounds. Many examples of aqueous actinide coordination complexes exist,[39-46]

as the study of the actinide-oxygen bond is relevant to extraction and processing of radioactive isotopes of various actinide metals. Actinide complexes with chalcogen (E; E = sulfur, selenium, tellurium) containing ligands are less explored than their oxygen containing counterparts. Chalcogenide ligand research has been primarily performed under non-aqueous conditions, where competing reactions with aqueous species can be mitigated. When exploring systems in non-aqueous conditions, a common approach to stabilize the actinide metal center is with the use of bulky ancillary ligands that sterically restrict access to reactivity of other potential coordinating ligands.[47-75] This aids in stabilizing the metal cation and can limit reactivity to as little as one coordination site.

By understanding the metal ligand bond in simple monomeric systems – including any steric restrictions in the coordination environment and covalent/ionic characteristics – cluster properties can be interpreted. In general, compounds without sterically demanding ligands may be precursors for cluster reactivity studies.[76] The synthesis of metal clusters is an extension of coordination chemistry where ligands may bridge two or more metal centers. Research on nanoscale clusters provides insight into how physical properties vary with cluster size, in order to determine how the properties of molecules, small clusters, and solid-state materials are erlated.[77] In contrast to main group and transition metal clusters, the field of actinide clusters is less developed.

An efficient synthesis for a monomeric starting material has precedence in the related study of lanthanide chalcogenolate compounds,[78-84] $Ln(ER)_xL_y$ (E = S, Se; R = C_6H_5, C_6F_5; L = solvent). Exploring non-aqueous cluster chemistry and the growth of clusters with ever increasing number of metal centers can be performed with the aid of less sterically demanding ligands, including aryl chalcogenolate deriatives.

The two types of ligands coordinated to the metal center are the anionic chalcogenolate ligands and solvent neutral donor ligands, typical pyridine or tetrahydrofuran (THF). Pyridine in particular is common in actinide-chalcogenido chemistry as it is a strong base. Cluster synthesis studies were performed using monomeric lanthanide-chalcogenolate compounds in the first instance of preparing the lanthanide chalcogenido-chalcogenolate cluster $Ln_8S_6(SPh)_{12}(THF)_8$ (Ln = Pr, Nd, Gd).[85] Lanthanide-chalcogenolate monomer $Ln(SPh)_3$ (Ln = Pr, Nd, Gd) was prepared via facile synthesis of Pr, Nd, or Gd with PhSSPh in THF, with subsequent addition of elemental S to yield $Ln_8S_6(SPh)_{12}(THF)_8$.[85] The eight seven-coordinate Ln(III) cations form the vertices of a cube with six S^{2-} anions cap each face of the cube. 12 SPh^- ligands bridge two Ln(III) cations along each edge of the cube. One neutral donating THF ligand is coordinated to each Ln metal cation. General features of metal chalcogenido-chalcogenolate clusters formed in this fashion are the triply or quadruply bridging chalcogenido (E^{2-}) ligands between metal centers, as well as terminal and bridging chalcogenolate (ER^-) ligands, and the coordination of neutral donor ligands that saturate the metal coordination sphere. Similar syntheses also result in clusters where EE^{2-} (E = S,Se, Te) also bridge between two or three metal anions.[86-98]

In early work on actinide chalcogenolate compounds, Jones et al. reported the synthesis of $U(SBu^n)_4$ from first reacting UCl_4 with lithium diethylamide and subsequent addition of n-butyl mercaptide.[99] Further research from Leverd *et al.* explored the thermal decomposition of three similar $(py)_3U(SBu^t)_4$ monomers upon refluxing in benzene to give the cluster $U_3S(SBu^t)_{10}$ and the accompanying side products of pyridine, 2-methylpropane-2-thiol, and 2-methylpropene (Scheme 2).[69]

Scheme 2.

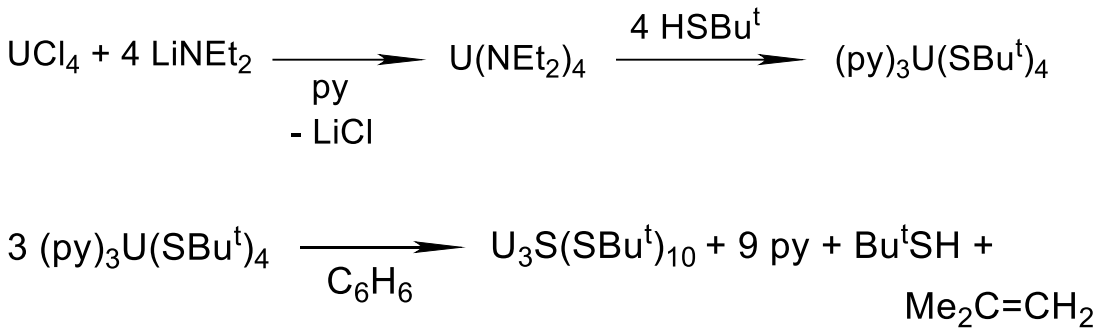

This system shows the first example of a molecular actinide cluster containing a triply bridging chalcogenido ligand, whose complicated synthesis involved the use of ligands with reactive R groups and various side products. There have subsequently been just a few examples of actinide clusters with triply bridging calcogenido ligands in the literature, including a tetrametallic U(IV) cluster $(Cp^*)_3U_3(\mu_3\text{-}S)(\mu_3\text{-}I)(\mu_2\text{-}I)_3I_3$,[100] An_4E_4 cubane clusters $py_8An_4(\mu_3\text{-}E)_4(\mu_2\text{-}EPh)_4(EPh)_4$ (An = U, E = Se;[101] An = Th, E = S, Se[102]), a double cubane cluster $[U[(\mu_3\text{-}S)_4U_3(SPS^{Me})_3(BH_4)_3]_2]$ ($[SPS^{Me}]^-$ = 1-methyl-2,6-bis(diphenylphosphine sulfide)-3,5-diphenylphosphinine anion),[103] and An_6E_8 cluster $[[U(COT)]_4[U(THF)_3]_2(\mu_3\text{-}S)_8]$.[104]

Facile synthesis of actinide chalcogenido-chalcogenolate clusters, similar to the synthesis of the lanthanide chalcogenido-chalcogenolate clusters, are rarer. Key monomeric compounds such as pyridine complexes of $U(EPh)_4$ (E = S, Se),[101] and pyridine complexes of $Th(ER)_4$ (E = S, Se; R = Ph, C_6F_5),[105] are laying the groundwork for future facile actinide cluster synthesis. The synthesis of these actinide chalcogenolates, $An(ER)_xL_y$ (An = Th, U), takes a similar approach to the lanthanides by reducing REER and oxidizing elemental An with a small amount of Hg catalyst in a neutral donating solvent at room temperature (Scheme 1).

Scheme 1.

$$An + x/2\ REER + y\ L \rightarrow An(ER)_xL_y$$

This synthesis produces An(IV), where x = 4, leading to the required addition of two moles of dichalcogenide for each actinide metal.

A facile synthesis of actinide chalcogenolate monomers that could be used to parallel lanthanide cluster synthesis would be a useful entry point for the synthesis of actinide chalcogenido-chalcogenolate clusters.[101, 106-108] An early example of this method was explored by Gaunt *et al.* where $U(SePh)_4(py)_3$, prepared via uranium metal oxidation of PhSeSePh, was subsequently reacted with elemental Se (Scheme 3).[101]

Scheme 3.

$$4\ U(SePh)_4 + 4\ Se \rightarrow U_4(\mu_3\text{-}Se)_4(\mu_2\text{-}SePh)_4(SePh)_4(py)_8 + 4\ (SePh)_2$$

In this product, four U(IV) cations and four $\mu_3\text{-}Se^{2-}$ ligands make up the vertices of a cube, four $\mu_2\text{-}SePh^-$ ligands bridge two U(IV) cations along four side faces of the cube, four $SePh^-$ ligands, and eight neutral donor pyridine ligands are bound to each U(IV) cation.

Various clusters can be prepared with a variety of starting materials. This approach to cluster synthesis has been used to prepare a series of five bimetallic thorium chalcogenido-chalcogenide compounds with halides, including $(py)_6Th_2I_4(\mu_2\text{-}E_2)_2$ (E = S, Se), $(py)_6Th_2Br_2(SC_6F_5)_2(\mu_2\text{-}S_2)_2$, and $(py)_6Th_2X_2(SC_6F_5)_2(\mu_2\text{-}Se_2)_2$ (X = Br, I).[108] This series contains the first example of $\mu_2\text{-}E_2^{2-}$ ligands bridging two thorium cations. The general approach to synthesis involves reducing I_2 and PhEEPh with elemental Th followed by the addition of elemental sulfur or selenium (Scheme 4).

Scheme 4.

$$2\ Th + 2\ I_2 + 2\ PhEEPh \rightarrow 2\ [ThI_n(EPh)_{4-n}] \rightarrow (py)_6Th_2I_4(\mu_2\text{-}E_2)_2\ (E = S, Se)$$

Various ligands can be used, such as replacing PhSeBr for I_2 and $C_6F_5SSC_6F_5$ for PhEEPh; however, the only stipulation amongst these variations is that there must always be a 2:1 ratio of oxidizing ligand starting material oxidant:metal thorium to fully oxidize all metallic thorium to Th(IV). The monomeric intermediate was not isolated, and each reaction was performed as a one-pot synthesis. Insights into facile one-pot actinide chalcogenido-chalcogenolate cluster synthesis can reveal interesting coordination preferences and bonding characteristics by varying ligand types.

This thesis describes the research into the synthesis of monomeric thorium and uranium chalcogenolates as a useful approach to the subsequent formation of chalcogenido-chalcogenolate clusters without the use of sterically bulky multidentate ancillary ligands.

Chapter 2 describes the synthesis of several novel thorium and uranium monomeric compounds and the addition of elemental selenium or silver(I) fluoride in preparing two novel thorium dimers. The influence of replacing the neutral donor pyridine ligands with bipyridine in a thorium selenolate monomer is explored, as well as using 2,2'-dipyridyl disulfide as a reactant to replace thiophenolate ligands with pyridinethiolates. The use of these monomeric actinide coordination complexes for subsequent cluster synthesis is explored.

Chapter 3 describes the synthesis and characterization of four novel thorium tetrametallic clusters with a cube-like core: $py_8Th_4E_4(EPh)_4(E'C_6F_5)_4$ (E, E' = S, Se). The facile one pot reaction affords customization of the chalcogen core and peripheral ligands. Thorium clusters with ligands containing sulfur and selenium are

synthesized with the chalcogen identity of the terminal EC_6F_5 ligands independent of the identity of the bridging E^{2-} and EPh^- ligands. Data from ^{77}Se NMR measurements suggest the tetrametallic cubane-like arrangement is maintained in pyridine solution.

Chapter 4 describes the synthesis and characterization of four novel uranium tetrametallic clusters: $py_8U_4E_4(EPh)_4(E'C_6F_5)_4$ (E, E' = S, Se). The synthesis is similar to the one-pot method for the thorium tetramers and these are the first known heterochalcogen clusters of uranium where each uranium in the cluster is bound to sulfur and selenium simultaneously. Magnetic susceptibility measurements on the series of four uranium tetramers suggest antiferromagnetic coupling between uranium atoms in the cubane-like core.

1.2 References

1. Appel, L.; Leduc, J.; Webster, C. L.; Ziller, J. W.; Evans, W. J.; Mathur, S., Synthesis of Air-Stable, Volatile Uranium(IV) and (VI) Compounds and Their Gas-Phase Conversion To Uranium Oxide Films. *Angew. Chemie.* **2015,** *127* (7), 2237-2241.
2. Berthet, J. C.; Ephritikhine, M., New advances in the chemistry of uranium amide compounds. *Coord. Chem. Rev.* **1998,** *178-180*, 83-116.
3. Tsutsui, M.; Ely, N.; Dubois, R., σ-Bonded organic derivatives of f elements. *Acc. Chem. Res.* **2002,** *9* (6), 217-222.
4. Peppard, D. F.; Mason, G. W., Some Mechanisms of Extraction of M(II), (III), (IV), and (VI) Metals by Acidic Organophosphorus Extractants. *Nuclear Science and Engineering* **1963,** *16* (4), 382-388.
5. Barnea, E.; Eisen, M., Organoactinides in catalysis. *Coord. Chem. Rev.* **2006,** *250* (7-8), 855-899.
6. Ephritikhine, M., Recent Advances in Organoactinide Chemistry As Exemplified by Cyclopentadienyl Compounds. *Organometallics.* **2013,** *32* (9), 2464-2488.
7. Seaman, L. A.; Walensky, J. R.; Wu, G.; Hayton, T. W., In Pursuit of Homoleptic Actinide Alkyl Complexes. *Inorg. Chem.* **2012,** *52* (7), 3556-3564.
8. Lewis, A. J.; Williams, U. J.; Carroll, P. J.; Schelter, E. J., Tetrakis(bis(trimethylsilyl)amido)uranium(IV): Synthesis and Reactivity. *Inorg. Chem.* **2013,** *52* (13), 7326-7328.
9. Reynolds, J. G.; Zalkin, A.; Templeton, D. H.; Edelstein, N. M., Syntheses and crystal structures of tetrakis(diphenylamido)uranium(IV) and bis(μ-oxo-tris(diphenylamido)uranium(IV) lithium diethyl etherate). *Inorg. Chem.* **2002,** *16* (5), 1090-1096.
10. Schädle, D.; Anwander, R., Rare-earth metal and actinide organoimide chemistry. *Chem. Soc. Rev.* **2019,** *48* (24), 5752-5805.
11. Siladke, N. A.; Meihaus, K. R.; Ziller, J. W.; Fang, M.; Furche, F.; Long, J. R.; Evans, W. J., Synthesis, Structure, and Magnetism of an f Element Nitrosyl Complex, $(C_5Me_4H)_3UNO$. *J. Am. Chem. Soc.* **2011,** *134* (2), 1243-1249.
12. Turner, Z., Molecular Pnictogen Activation by Rare Earth and Actinide Complexes. *Inorganics.* **2015,** *3* (4), 597-635.
13. Ephritikhine, M., Molecular actinide compounds with soft chalcogen ligands. *Coord. Chem. Rev.* **2016,** *319*, 35-62.
14. Pagano, J. K.; Arney, D. S. J.; Scott, B. L.; Morris, D. E.; Kiplinger, J. L.; Burns, C. J., A sulphur and uranium fiesta! Synthesis, structure, and characterization of neutral terminal uranium(VI) monosulphide, uranium(VI) η^2-disulphide, and uranium(IV) phosphine sulphide complexes. *Dalton Trans.* **2019,** *48* (1), 50-57.
15. Rehe, D.; Kornienko, A. Y.; Emge, T. J.; Brennan, J. G., Thorium Compounds with Bonds to Sulfur or Selenium: Synthesis, Structure, and Thermolysis. *Inorg. Chem.* **2016,** *55* (14), 6961-7.
16. Ringgold, M.; Wu, W.; Stuber, M.; Kornienko, A. Y.; Emge, T. J.; Brennan, J. G., Monomeric thorium chalcogenolates with bipyridine and terpyridine ligands. *Dalton Trans.* **2018,** *47* (41), 14652-14661.
17. Avens, L. R.; Bott, S. G.; Clark, D. L.; Sattelberger, A. P.; Watkin, J. G.; Zwick, B. D., A Convenient Entry into Trivalent Actinide Chemistry: Synthesis and Characterization of $AnI_3(THF)_4$ and $An[N(SiMe_3)_2]_3$ (An = U, Np, Pu). *Inorg. Chem.* **1994,** *33* (10), 2248-2256.

18. Berthet, J.-C.; Siffredi, G.; Thuéry, P.; Ephritikhine, M., Synthesis and crystal structure of pentavalent uranyl complexes. The remarkable stability of UO_2X (X = I, SO_3CF_3) in non-aqueous solutions. *Dalton Trans.* **2009,** (18).
19. La Pierre, H. S.; Heinemann, F. W.; Meyer, K., Well-defined molecular uranium(III) chloride complexes. *Chem. Commun.* **2014,** *50* (30), 3962-3964.
20. Van Der Sluys, W. G.; Berg, J. M.; Barnhardt, D.; Sauer, N. N., Tetrahydrofuran adducts of uranium tetrachloride. *Inorg. Chim. Acta.* **1993,** *204* (2), 251-256.
21. Barreiro, S.; Durán-Carril, M. L.; Viqueira, J.; Sousa-Pedrares, A.; García-Vázquez, J. A.; Romero, J., Structural studies and bioactivity of diorganotin(IV) complexes of pyridin-2-thionato derivatives. *J. Organomet. Chem.* **2015,** *791*, 155-162.
22. Castro-Rodríguez, I.; Nakai, H.; Meyer, K., Multiple-Bond Metathesis Mediated by Sterically Pressured Uranium Complexes. *Angew. Chemie.* **2006,** *118* (15), 2449-2452.
23. Sockwell, A. K.; Wetzler, M., Beyond Biological Chelation: Coordination of f-Block Elements by Polyhydroxamate Ligands. *Chem. Eur. J.* **2018,** *25* (10), 2380-2388.
24. Castro-Rodriguez, I.; Olsen, K.; Gantzel, P.; Meyer, K., Uranium complexes supported by an aryloxide functionalised triazacyclononane macrocycle: synthesis and characterisation of a six-coordinate U(III) species and insights into its reactivity. *Chem. Commun.* **2002,** (23), 2764-2765.
25. Castro-Rodriguez, I.; Olsen, K.; Gantzel, P.; Meyer, K., Uranium Tris-aryloxide Derivatives Supported by Triazacyclononane: Engendering a Reactive Uranium(III) Center with a Single Pocket for Reactivity. *J. Am. Chem. Soc.* **2003,** *125* (15), 4565-4571.
26. Reynolds, L. T.; Wilkinson, G., π-cyclopentadienyl compounds of uranium-IV and thorium-IV. *Journal of Inorganic and Nuclear Chemistry.* **1956,** *2* (4), 246-253.
27. Wong, C. H.; Yen, T.; Lee, T., The crystal structure of uranium chloride π-tricyclopentadienyl. *Acta Cryst.* **1965,** *18* (3), 340-345.
28. Zalkin, A.; Raymond, K. N., Structure of di-π-cyclooctatetraeneuranium (uranocene). *J. Am. Chem. Soc.* **1969,** *91* (20), 5667-5668.
29. Gardner, B. M.; Cleaves, P. A.; Kefalidis, C. E.; Fang, J.; Maron, L.; Lewis, W.; Blake, A. J.; Liddle, S. T., The role of 5f-orbital participation in unexpected inversion of the σ-bond metathesis reactivity trend of triamidoamine thorium(IV) and uranium(IV) alkyls. *Chem. Sci.* **2014,** *5* (6), 2489-2497.
30. Pitzer, K. S., Relativistic effects on chemical properties. *Acc. Chem. Res.* **2002,** *12* (8), 271-276.
31. Seth, M.; Dolg, M.; Fulde, P.; Schwerdtfeger, P., Lanthanide and Actinide Contractions: Relativistic and Shell Structure Effects. *J. Am. Chem. Soc.* **1995,** *117* (24), 6597-6598.
32. Bursten, B. E.; Rhodes, L. F.; Strittmatter, R. J., Bonding in tris(η^5-cyclopentadienyl) actinide complexes. 2. On the ground electronic configurations of "base-free" Cp_3An complexes (An = thorium, protactinium, uranium, neptunium, plutonium). *J. Am. Chem. Soc.* **1989,** *111* (8), 2756-2758.
33. Liddle, S. T., The Renaissance of Non-Aqueous Uranium Chemistry. *Angew. Chemie. Int. Ed.* **2015,** *54* (30), 8604-8641.

34. Brennan, J. G.; Green, J. C.; Redfern, C. M., Covalency in bis([8]annulene)uranium from photoelectron spectroscopy with variable photon energy. *J. Am. Chem. Soc.* **1989,** *111* (7), 2373-2377.
35. Mullane, K. C.; Hrobárik, P.; Cheisson, T.; Manor, B. C.; Carroll, P. J.; Schelter, E. J., ^{13}C NMR Shifts as an Indicator of U–C Bond Covalency in Uranium(VI) Acetylide Complexes: An Experimental and Computational Study. *Inorg. Chem.* **2019,** *58* (7), 4152-4163.
36. Réant, B. L. L.; Berryman, V. E. J.; Seed, J. A.; Basford, A. R.; Formanuik, A.; Wooles, A. J.; Kaltsoyannis, N.; Liddle, S. T.; Mills, D. P., Polarised covalent thorium(IV)– and uranium(IV)–silicon bonds. *Chem. Commun.* **2020**.
37. Roger, M.; Belkhiri, L.; Arliguie, T.; Thuéry, P.; Boucekkine, A.; Ephritikhine, M., Uranium and Lanthanide Complexes with the 2-Mercapto Benzothiazolate Ligand: Evidence for a Specific Covalent Binding Site in the Differentiation of Isostructural Lanthanide(III) and Actinide(III) Compounds. *Organometallics.* **2008,** *27* (1), 33-42.
38. Smiles, D. E.; Wu, G.; Hrobárik, P.; Hayton, T. W., Use of ^{77}Se and ^{125}Te NMR Spectroscopy to Probe Covalency of the Actinide-Chalcogen Bonding in $[Th(E_n)\{N(SiMe_3)_2\}_3]^-$ (E = Se, Te; n = 1, 2) and Their Oxo-Uranium(VI) Congeners. *J. Am. Chem. Soc.* **2016,** *138* (3), 814-825.
39. Agnall, K. W.; Beheshti, A.; Heatley, F., Some oxygen-donor complexes of cyclopentadienyl thorium(IV) halides. *Journal of the Less Common Metals.* **1978,** *61* (1), 63-69.
40. Alexander, V., Design and Synthesis of Macrocyclic Ligands and Their Complexes of Lanthanides and Actinides. *Chem. Rev.* **1995,** *95* (2), 273-342.
41. Casellato, U.; Vigato, P. A.; Vidali, M., Actinide complexes with carboxylic acids. *Coord. Chem. Rev.* **1978,** *26* (2), 85-159.
42. Clark, D. L.; Frankcom, T. M.; Miller, M. M.; Watkin, J. G., Facile solution routes to hydrocarbon-soluble Lewis base adducts of thorium tetrahalides. Synthesis, characterization, and x-ray structure of $ThBr_4(THF)_4$. *Inorg. Chem.* **1992,** *31* (9), 1628-1633.
43. Grdenić, D.; Matković, B., Co-ordination in Thorium-IV Acetylacetonate. *Nature.* **1958,** *182* (4633), 465-466.
44. Kahn, B. E.; Rieke, R. D., Carbonyl coupling reactions using transition metals, lanthanides, and actinides. *Chem. Rev.* **1988,** *88* (5), 733-745.
45. Van der Sluys, W. G.; Sattelberger, A. P., Actinide alkoxide chemistry. *Chem. Rev.* **1990,** *90* (6), 1027-1040.
46. Yoshimura, T.; Miyake, C.; Imoto, S., Some β-Diketone Chelate Complexes with Uranium(IV), Thorium(IV), and Cerium(IV). Preparation and IR Spectra. *Bulletin of the Chemical Society of Japan.* **1973,** *46* (7), 2096-2101.
47. Andrez, J.; Pecaut, J.; Scopelliti, R.; Kefalidis, C. E.; Maron, L.; Rosenzweig, M. W.; Meyere, K.; Mazzanti, M., Synthesis and reactivity of a terminal uranium(IV) sulfide supported by siloxide ligands. *Chem. Sci.* **2016,** *7* (9), 5846-5856.
48. Arliguie, T.; Thuery, P.; Fourmigue, M.; Ephritikhine, M., Reduction of dithiocarbonates as a novel route to dithiolene compounds of uranium. Crystal structure of the first bimetallic dithiolene complex of an f-element. *Organometallics.* **2003,** *22* (14), 3000-3003.

49. Arliguie, T.; Thuery, P.; Le Floch, P.; Mezailles, N.; Ephritikhine, M., A homoleptic SPS-based complex and a double-cubane-type sulfur cluster of an actinide element. *Polyhedron.* **2009,** *28* (8), 1578-1582.
50. Arnold, P. L.; Stevens, C. J.; Bell, N. L.; Lord, R. M.; Goldberg, J. M.; Nichol, G. S.; Love, J. B., Multi-electron reduction of sulfur and carbon disulfide using binuclear uranium(III) borohydride complexes. *Chem. Sci.* **2017,** *8* (5), 3609-3617.
51. Avens, L. R.; Barnhart, D. M.; Burns, C. J.; Mckee, S. D.; Smith, W. H., Oxidation Chemistry of a Uranium(III) Aryloxide. *Inorg. Chem.* **1994,** *33* (19), 4245-4254.
52. Brennan, J. G.; Andersen, R. A.; Zalkin, A., Chemistry of Trivalent Uranium Metallocenes - Electron-Transfer Reactions - Synthesis and Characterization of $[(MeC_5H_4)_3U]_2E$ (E = S, Se, Te) and the Crystal Structures of $[(MeC_5H_4)_3U]_2S$ and $(MeC_5H_4)_3UOPPh_3$. *Inorg. Chem.* **1986,** *25* (11), 1761-1765.
53. Brown, J. L.; Wu, G.; Hayton, T. W., Chalcogen Atom Transfer to Uranium(III): Synthesis and Characterization of $[(R_2N)_3U]_2(\mu\text{-}E)$ and $[(R_2N)_3U]_2(\mu\text{-}\eta^2\text{:}\eta^2\text{-}S_2)$ (R = $SiMe_3$; E = S, Se, Te). *Organometallics.* **2013,** *32* (5), 1193-1198.
54. Camp, C.; Antunes, M. A.; Garcia, G.; Ciofini, I.; Santos, I. C.; Pecaut, J.; Almeida, M.; Marcalo, J.; Mazzanti, M., Two-electron versus one-electron reduction of chalcogens by uranium(III): synthesis of a terminal U(V) persulfide complex. *Chem. Sci.* **2014,** *5* (2), 841-846.
55. Evans, W. J.; Miller, K. A.; Hillman, W. R.; Ziller, J. W., Two-electron reductive reactivity of trivalent uranium tetraphenylborate complexes of $(C_5Me_5)^{1-}$ and $(C_5Me_4H)^{1-}$. *J. Organomet. Chem.* **2007,** *692* (17), 3649-3654.
56. Evans, W. J.; Miller, K. A.; Kozimor, S. A.; Ziller, J. W.; DiPasquale, A. G.; Rheingold, A. L., Actinide hydride complexes as multielectron reductants: Analogous reduction chemistry from $[(C_5Me_5)_2UH]_2$, $[(C_5Me_5)_2UH_2]_2$, and $[(C_5Me_5)_2ThH_2]_2$. *Organometallics.* **2007,** *26* (14), 3568-3576.
57. Evans, W. J.; Miller, K. A.; Ziller, J. W.; DiPasquale, A. G.; Heroux, K. J.; Rheingold, A. L., Formation of $(C_5Me_5)_2U(EPh)Me$, $(C_5Me_5)_2U(EPh)_2$, and $(C_5Me_5)_2U(\eta^2\text{-}TeC_6H_4)$ from $(C_5Me_5)_2UMe_2$ and PhEEPh (E = S, Se, Te). *Organometallics.* **2007,** *26* (17), 4287-4293.
58. Evans, W. J.; Montalvo, E.; Ziller, J. W.; DiPasquale, A. G.; Rheingold, A. L., Uranium Metallocene Complexes of the 1,3,4,6,7,8-Hexahydro-*2H*-pyrimido[1,2-*a*]pyrimidinato Ligand, $(hpp)^-$. *Inorg. Chem.* **2010,** *49* (1), 222-228.
59. Evans, W. J.; Takase, M. K.; Ziller, J. W.; DiPasquale, A. G.; Rheingold, A. L., Reductive Reactivity of the Tetravalent Uranium Complex $[\eta^5\text{-}C_5Me_5)(\eta^8\text{-}C_8H_8)U]_2(\mu\text{-}\eta^3\text{:}\eta^3\text{-}C_8H_8)$. *Organometallics.* **2009,** *28* (1), 236-243.
60. Evans, W. J.; Walensky, J. R.; Ziller, J. W., Reaction Chemistry of the U^{3+} Metallocene Amidinate $(C_5Me_5)_2[^iPrNC(Me)N^iPr]U$ Including the Isolation of a Uranium Complex of a Monodentate Acetate. *Inorg. Chem.* **2010,** *49* (4), 1743-1749.
61. Franke, S. M.; Rosenzweig, M. W.; Heinemann, F. W.; Meyer, K., Reactivity of uranium(III) with H_2E (E = S, Se, Te): synthesis of a series of mononuclear and dinuclear uranium(IV) hydrochalcogenido complexes. *Chem. Sci.* **2015,** *6* (1), 275-282.
62. Gardner, B. M.; King, D. M.; Tuna, F.; Wooles, A. J.; Chilton, N. F.; Liddle, S. T., Assessing crystal field and magnetic interactions in diuranium-μ-chalcogenide triamidoamine complexes with U(IV)-E-U(IV) cores (E = S, Se, Te): implications for determining the presence or absence of actinide-actinide magnetic exchange. *Chem. Sci.* **2017,** *8* (9), 6207-6217.

63. Graves, C. R.; Scott, B. L.; Morris, D. E.; Kiplinger, J. L., Facile access to pentavalent uranium organometallics: One-electron oxidation of Uranium(IV) imido complexes with copper(I) salts. *J. Am. Chem. Soc.* **2007,** *129* (39), 11914-11915.
64. Graves, C. R.; Scott, B. L.; Morris, D. E.; Kiplinger, J. L., Selenate and tellurate complexes of pentavalent uranium. *Chem. Commun.* **2009,** (7), 776-778.
65. Karmazin, L.; Mazzanti, M.; Pecaut, J., Unique crown thioether complexes of f elements: the crystal structure of U(III) and La(III) complexes of 1,4,7-trithiacyclononane. *Chem. Commun.* **2002,** (6), 654-655.
66. Lam, O. P.; Heinemann, F. W.; Meyer, K., Activation of elemental S, Se and Te with uranium(III): bridging U-E-U (E = S, Se) and diamond-core complexes U-E_2-U (E = O, S, Se, Te). *Chem. Sci.* **2011,** *2* (8), 1538-1547.
67. Leverd, P. C.; Arliguie, T.; Lance, M.; Nierlich, M.; Vigner, J.; Ephritikhine, M., Monocyclooctatetraene Uranium Thiolate Complexes - Crystal-Structure of [(U(η-C_8H_8)(μ-SPr^i)$_2$)$_2$]. *J. Chem. Soc., Dalton Trans.* **1994,** (4), 501-504.
68. Leverd, P. C.; Ephritikhine, M.; Lance, M.; Vigner, J.; Nierlich, M., Triscyclopentadienyl uranium thiolates and selenolates. *J. Organomet. Chem.* **1996,** *507* (1-2), 229-237.
69. Leverd, P. C.; Lance, M.; Vigner, J.; Nierlich, M.; Ephritikhine, M., Synthesis and Reactions of Uranium(IV) Tetrathiolate Complexes. *J. Chem. Soc. Dalton* **1995,** (2), 237-244.
70. Rosenzweig, M. W.; Hummer, J.; Scheurer, A.; Lamsfus, C. A.; Heinemann, F. W.; Maron, L.; Mazzanti, M.; Meyer, K., A complete series of uranium(IV) complexes with terminal hydrochalcogenido (EH) and chalcogenido (E) ligands E = O, S, Se, Te. *Dalton Trans.* **2019,** *48* (29), 10853-10864.
71. Santos, I. G.; Abram, U., Synthesis and structures of dioxouranium complexes with 2-pyridineformamide thiosemicarbazones. *Inorg. Chem. Commun.* **2004,** *7* (3), 440-442.
72. Shinomoto, R.; Zalkin, A.; Edelstein, N. M., Preparation and Crystal-Structures of Tetrakis-(Methyltrihydroborato)Uranium(IV)Bis(Tetrahydrofuranate) and Tetrakis(Methyltrihydroborato)-Uranium(IV)Tetrahydrothiophenate. *Inorg. Chim. Acta.* **1987,** *139* (1-2), 91-95.
73. Sitran, S.; Fregona, D.; Casellato, U.; Vigato, P. A.; Graziani, R.; Faraglia, G., Dioxouranium(VI) Complexes with Pentadentate Bases Containing Acetal Groups. *Inorg. Chim. Acta.* **1987,** *132* (2), 279-288.
74. Thomson, R. K.; Graves, C. R.; Scott, B. L.; Kiplinger, J. L., Synthesis and Molecular Structure of (C_5Me_5)$_2$U(O^tBu)(SePh): A Mixed-Ligand Alkoxide-Selenide Uranium(IV) Metallocene Complex Resulting from tert-Butoxy-Trimethylsilane Elimination. *J. Chem. Crystallogr.* **2011,** *41* (8), 1241-1244.
75. Zalkin, A.; Brennan, J. G., A Trivalent-Uranium Thioether Coordination Compound. *Acta. Crystallogr. C.* **1985,** *41* (Sep), 1295-1297.
76. Korobkov, I.; Gambarotta, S., Ligand Metalation in the Reactivity of a Tetravalent Uranium Amides. *Inorg. Chem.* **2010,** *49* (7), 3409-3418.
77. Pinkard, A.; Champsaur, A. M.; Roy, X., Molecular Clusters: Nanoscale Building Blocks for Solid-State Materials. *Acc. Chem. Res.* **2018,** *51* (4), 919-929.
78. Banerjee, S.; Emge, T. J.; Brennan, J. G., Heterometallic Ln/Hg Compounds with Fluorinated Thiolate Ligands. *Inorg. Chem.* **2004,** *43* (20), 6307-6312.
79. Freedman, D.; Kornienko, A.; Emge, T. J.; Brennan, J. G., Divalent Samarium Compounds with Heavier Chalcogenolate (EPh; E = Se, Te) Ligands. *Inorg. Chem.* **2000,** *39* (10), 2168-2171.

80. Khasnis, D. V.; Brewer, M.; Lee, J.; Emge, T. J.; Brennan, J. G., Rare Earth Phenyltellurolates: 1D Coordination Polymers. *J. Am. Chem. Soc.* **1994,** *116* (16), 7129-7133.
81. Kornienko, A.; Freedman, D.; Emge, T. J.; Brennan, J. G., Heteroleptic Lanthanide Compounds with Chalcogenolate Ligands: Reduction of PhNNPh/PhEEPh (E = Se or Te) Mixtures with Ln (Ln = Ho, Er, Tm, Yb). Thermolysis Can Give LnN or LnE. *Inorg. Chem.* **2001,** *40* (1), 140-145.
82. Krogh-Jespersen, K.; Romanelli, M. D.; Melman, J. H.; Emge, T. J.; Brennan, J. G., Covalent Bonding and the Trans Influence in Lanthanide Compounds. *Inorg. Chem.* **2010,** *49* (2), 552-560.
83. Lee, J.; Freedman, D.; Melman, J. H.; Brewer, M.; Sun, L.; Emge, T. J.; Long, F. H.; Brennan, J. G., Trivalent Lanthanide Chalcogenolates: $Ln(SePh)_3$, $Ln_2(EPh)_6$, $Ln_4(SPh)_{12}$, and $[Ln(EPh)_3]_n$ (E = S, Se). How Metal, Chalcogen, and Solvent Influence Structure. *Inorg. Chem.* **1998,** *37* (10), 2512-2519.
84. Melman, J. H.; Rohde, C.; Emge, T. J.; Brennan, J. G., Trivalent Lanthanide Compounds with Fluorinated Thiolate Ligands: Ln−F Dative Interactions Vary with Ln and Solvent. *Inorg. Chem.* **2002,** *41* (1), 28-33.
85. Melman, J. H.; Emge, T. J., Cubic lanthanide sulfido clusters: $Ln_8S_6(SPh)_{12}(THF)_8$ (Ln = Pr, Nd, Gd). *Chem. Commun.* **1997,** (23), 2269-2270.
86. Banerjee, S.; Sheckelton, J.; Emge, T. J.; Brennan, J. G., Heterometallic Ln/Hg Tellurido Clusters. *Inorg. Chem.* **2010,** *49* (4), 1728-1732.
87. Fitzgerald, M.; Emge, T. J.; Brennan, J. G., Chalcogen-Rich Lanthanide Clusters with Fluorinated Thiolate Ligands. *Inorg. Chem.* **2002,** *41* (13), 3528-3532.
88. Freedman, D.; Emge, T. J.; Brennan, J. G., $(THF)_8Ln_8E_6(EPh)_{12}$ Cluster Reactivity: Systematic Control of Ln, E, EPh, and Neutral Donor Ligands. *Inorg. Chem.* **1999,** *38* (20), 4400-4404.
89. Freedman, D.; Emge, T. J.; Brennan, J. G., Chalcogen-Rich Lanthanide Clusters: Compounds with Te^{2-}, $(TeTe)^{2-}$, TePh, TeTePh, $(TeTeTe(Ph)TeTe)^{5-}$, and $[(TeTe)_4TePh]^{9-}$ Ligands; Single Source Precursors to Solid-State Lanthanide Tellurides. *Inorg. Chem.* **2002,** *41* (3), 492-500.
90. Freedman, D.; Sayan, S.; Emge, T. J.; Croft, M.; Brennan, J. G., Heterovalent Clusters: $Ln_4Se(SePh)_8$ (Ln_4= Sm_4, Yb_4, Sm_2Yb_2, Nd_2Yb_2). *J. Am. Chem. Soc.* **1999,** *121* (50), 11713-11719.
91. Huebner, L.; Kornienko, A.; Emge, T. J.; Brennan, J. G., Lanthanide Clusters with Internal Ln: Fragmentation and the Formation of Dimers with Bridging Se^{2-} and Se_2^{2-}Ligands. *Inorg. Chem.* **2005,** *44* (14), 5118-5122.
92. Kornienko, A.; Banerjee, S.; Kumar, G. A.; Riman, R. E.; Emge, T. J.; Brennan, J. G., Heterometallic Chalcogenido Clusters Containing Lanthanides and Main Group Metals: Emissive Precursors to Ternary Solid-State Compounds. *J. Am. Chem. Soc.* **2005,** *127* (40), 14008-14014.
93. Kornienko, A.; Emge, T. J.; Kumar, G. A.; Riman, R. E.; Brennan, J. G., Lanthanide Clusters with Internal Ln Ions: Highly Emissive Molecules with Solid-State Cores. *J. Am. Chem. Soc.* **2005,** *127* (10), 3501-3505.
94. Kornienko, A.; Huebner, L.; Freedman, D.; Emge, T. J.; Brennan, J. G., Lanthanide−Transition Metal Chalcogenido Cluster Materials. *Inorg. Chem.* **2003,** *42* (25), 8476-8480.
95. Kornienko, A.; Moore, B. F.; Kumar, G. A.; Tan, M.-C.; Riman, R. E.; Brik, M. G.; Emge, T. J.; Brennan, J. G., Highly NIR-Emissive Lanthanide Polyselenides. *Inorg. Chem.* **2011,** *50* (18), 9184-9190.

96. Kornienko, A. Y.; Emge, T. J.; Brennan, J. G., Chalcogen-Rich Lanthanide Clusters: Cluster Reactivity and the Influence of Ancillary Ligands on Structure. *J. Am. Chem. Soc.* **2001,** *123* (48), 11933-11939.
97. Melman, J. H.; Fitzgerald, M.; Freedman, D.; Emge, T. J.; Brennan, J. G., Chalcogen-Rich Lanthanide Clusters from Lanthanide Halide Starting Materials: A New Approach to the Low-Temperature Synthesis of LnS_x Solids from Molecular Precursors. *J. Am. Chem. Soc.* **1999,** *121* (43), 10247-10248.
98. Moore, B. F.; Kumar, G. A.; Tan, M.-C.; Kohl, J.; Riman, R. E.; Brik, M. G.; Emge, T. J.; Brennan, J. G., Lanthanide Clusters with Chalcogen Encapsulated Ln: NIR Emission from Nanoscale $NdSe_x$. *J. Am. Chem. Soc.* **2011,** *133* (2), 373-378.
99. Jones, R. G.; Karmas, G.; Martin, G. A.; Gilman, H., Organic Compounds of Uranium. II. Uranium(IV) Amides, Alkoxides and Mercaptides. *J. Am. Chem. Soc.* **1956,** *78* (17), 4285-4286.
100. Clark, D. L.; Gordon, J. C.; Huffman, J. G.; Watkin, J. G.; Zwick, B. D., Preparation of mono-pentamethylcyclopentadienyl uranium(IV) sulfido clusters through oxidation of $(\eta\text{-}C_5Me_5)UI_2(THF)_3$ - X-ray structural characterization of $(\eta\text{-}C_5Me_5)_3U_3(\mu_3\text{-}I)(\mu_3\text{-}S)(\mu_2\text{-}I)_3I_3$. *New Journal of Chemistry* **1995,** *19* (5-6), 495-502.
101. Gaunt, A. J.; Scott, B. L.; Neu, M. P., U(IV) chalcogenolates synthesized via oxidation of uranium metal by dichalcogenides. *Inorg. Chem.* **2006,** *45* (18), 7401-7407.
102. Ringgold, M.; Rehe, D.; Hrobarik, P.; Kornienko, A. Y.; Emge, T. J.; Brennan, J. G., Thorium Cubanes-Synthesis, Solid-State and Solution Structures, Thermolysis, and Chalcogen Exchange Reactions. *Inorg. Chem.* **2018,** *57* (12), 7129-7141.
103. Arliguie, T.; Thuéry, P.; Floch, P. L.; Mézailles, N.; Ephritikhine, M., A homoleptic SPS-based complex and a double-cubane-type sulfur cluster of an actinide element. *Polyhedron.* **2009,** *28* (8), 1578-1582.
104. Arliguie, T.; Blug, M.; Le Floch, P.; Mezailles, N.; Thuery, P.; Ephritikhine, M., Organouranium complexes with phosphinine-based SPS pincer ligands. Variations with the substituent at the phosphorus atom. *Organometallics.* **2008,** *27* (16), 4158-4165.
105. Rehe, D.; Kornienko, A. Y.; Emge, T. J.; Brennan, J. G., Thorium Compounds with Bonds to Sulfur or Selenium: Synthesis, Structure, and Thermolysis. *Inorg Chem.* **2016,** *55* (14), 6961-6967.
106. Ringgold, M.; Rehe, D.; Hrobárik, P.; Kornienko, A. Y.; Emge, T. J.; Brennan, J. G., Thorium Cubanes–Synthesis, Solid-State and Solution Structures, Thermolysis, and Chalcogen Exchange Reactions. *Inorg. Chem.* **2018,** *57* (12), 7129-7141.
107. Stuber, M. A.; Kornienko, A. Y.; Emge, T. J.; Brennan, J. G., Tetrametallic Thorium Compounds with Th4E4 (E = S, Se) Cubane Cores. *Inorg. Chem.* **2017,** *56* (17), 10247-10256.
108. Wu, W.; Rehe, D.; Hrobárik, P.; Kornienko, A. Y.; Emge, T. J.; Brennan, J. G., Molecular Thorium Compounds with Dichalcogenide Ligands: Synthesis, Structure, ^{77}Se NMR Study, and Thermolysis. *Inorg. Chem.* **2018,** *57* (23), 14821-14833.

Chapter 2: Actinide Complexes with Bidentate Ligands and Exploration of Cluster Synthesis with Selenium and Fluoride

2.1 Introduction

Understanding the complicated bonding characteristics in actinide (An) compounds remains as a great fundamental interest in inorganic chemistry due to the unique nature of the valence f-orbitals, partial shielding of the valence orbitals by filled s and p orbitals, and the overlap between the energetically similar 5f and 6d orbitals. Through the synthesis of novel actinide complexes and clusters, we can explore the unique chemical properties of the actinides and define the relationships amongst the physical properties[1-26] of molecular, cluster, and solid-state actinide materials[27, 28]

Monomeric coordination compounds of the actinides such as the pyridine complexes of $Th(ER)_4$ (E = S, Se; R = Ph, C_6F_5)[29] are an entryway into the study of actinide coordination chemistry, where various ligands can be altered to probe An-L bonding. Actinide clusters are the next step in exploring the reactivity of monomeric coordination compounds; however, they are commonly synthesized with sterically bulky ancillary ligands in order to stabilize the coordination environment around the actinide center.[30-52] Actinide cluster chemistry is more limited with chalcogen (E = S, Se) containing ligands, including An-ER,[29, 53-84] An-μ_3E^{2-},[60, 67, 78, 85-87] and An-(E-E).[81, 88-94]

Neutral donor ligands can also be used to probe bonding in actinide compounds, and they also impart additional complex stability because of the chelate

effect. Metal complexes are more stable with bidentate ligands compared to similar monodentate ligands. A bidentate ligand that binds to a metal cation from one coordinating atom will allow the second subsequent association to continue as a faster, more kinetically favored step due to the close proximity of the second atom of the bound ligand to the metal cation. One of the most widely used chelating ligands in coordination chemistry, 2,2'-bipyridine (bipy),[95, 96] has been used to stabilize actinide ions in a range of compound classes.[69-71, 97-108]

Another bidentate ligand related to pyridine is pyridine-2-thiolate (Spy) (Figure 2.1), which contains a sulfur based negative charge and exhibits interesting range of binding properties including monodentate binding,[109, 110] bidentate chelating, and bridging two metal centers (i.e. one metal through S and the other through N).[111]

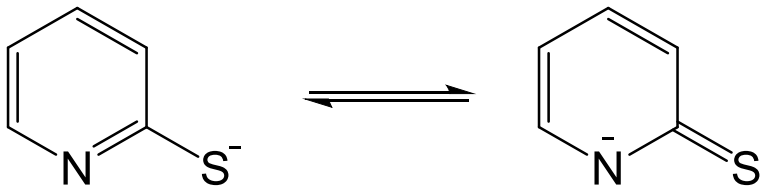

Figure 2.1 Resonance structures of pyridine-2-thiolate (Spy), showing binding modes through the S and N atoms.

The use of Spy is well documented in transition metal chemistry;[112-132] with applications ranging from catalysis,[120, 124, 129] and in vitro cancer inhibitory studies,[126] to modeling the active sites of several enzymes.[117, 118, 128] Research on lanthanide compounds of Spy is limited,[133-139] and the actinide series is represented by only a small number of uranium pyridinethiolate compounds,[58, 60, 140-142] with no reports of related thorium compounds.

2.2 Results and discussion

2.2.1 Bipyridine Complex of Thorium Selenolate

Thorium metal reduces $C_6F_5SeSeC_6F_5$ to cleave the Se-Se bond and form a Th(IV) selenolate compound that subsequently reacts with bipy to form a bis-bipy Th(IV) selenolate chelate compound $(bipy)_2Th(SeC_6F_5)_4$ (Figure 2.1). The synthetic approach starts with the series of Th(IV) chalcogenolates, $(py)_xTh(ER)_4$ (E = S, Se; R = Ph, C_6F_5),[29] with the subsequent displacement of py by bipy. This allows for the study of Th(IV) chalcogenolate structure as the neutral donor ligand changes

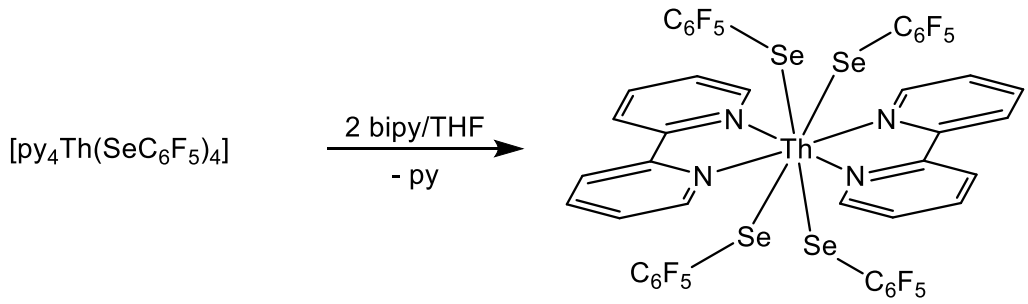

Figure 2.2 Synthesis of $(bipy)_2Th(SC_6F_5)_4$ (**1**).

Table 2.1 Summary of Crystallographic Details for **1**.

	$(bipy)_2Th(SeC_6F5)_4 \bullet 2THF$
Empirical Formula	$C_{52}H_{32}F_{20}N_4O_2Se_4Th$
Fw	1672.69
Crystal system	monoclinic
Space group	C2/c
a (Å)	26.340(1)
b (Å)	12.750(1)
c (Å)	17.396(1)
β (deg)	114.296(1)
V ($Å^3$)	5324.7(4)
Z	4
D_{calc} (Mg/cm^3)	2.087
T (K)	100(2)
abs coeff (mm^{-1})	5.652
$R(int)/N_{unique}$	0.0357/8110
$R(F)^a$ [$I > 2\sigma(I)$]	0.0271
$R_w(F^2)^b$ [$I>2\sigma(I)$]	0.0605

Definitions: [a] $R(F) = \Sigma||F_o| - |F_c||/\Sigma|F_o|$; [b] $R_w(F^2) = [\Sigma[w(F_o^2 - F_c^2)^2]/\Sigma[w(F_o^2)^2]]^{1/2}$

Figure 2.2 shows the POVRAY diagram of $(bipy)_2Th(SC_6F_5)_4$ (**1**). The crystallized product was characterized by low-temperature single-crystal X-ray diffraction, details given in (Table 2.1). Purity of the sample was confirmed by elemental analysis and phase purity was confirmed by powder X-ray diffraction (PXRD).

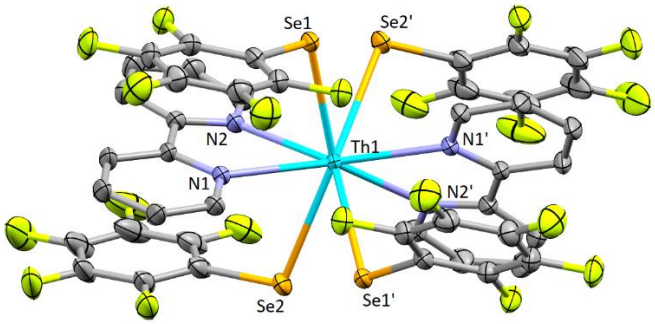

Figure 2.3 Thermal ellipsoid diagram of $(bipy)_2Th(SC_6F_5)_4$ (**1**), with orange Se, light green F, light blue Th, purple N, grey C, H atoms removed for clarity, and ellipsoids at the 50% probability level.

In **1**, two bidentate bipy ligands and four $SeC_6F_5^-$ form an eight coordinate Th(IV) selenolate complex. Bond geometries are consistent with prior literature, including the pyridine derivatives $(py)_xTh(ER)_4$ (E = S, Se; R = Ph, C_6F_5),[29] and the series of $(bipy)_2Th(ER)_4$ (E = S, Se; R = Ph, C_6F_5):[71] $(bipy)_2Th(SPh)_4$ and $(bipy)_2Th(SePh)_4$ were synthesized by Marissa Ringgold, and $(bipy)_2Th(SC_6F_5)_4$ was synthesized by Wen Wu.[71] Th-Se distances for **1** (2.970-3.016 Å) are consistent with the range of previously reported Th-Se(C_6F_5) bond lengths (2.9519(7)-3.0183(7) Å) in the pyridine derivative $py_4Th(SeC_6F_5)_4$.[29] The range of Th-Se bond lengths is comparable to the bipy derivative $(bipy)_2Th(SePh)_4$ (2.954-3.015 Å),[71] and slightly longer than those found in the pyridine derivative $py_3Th(SePh)_4$ (2.9039(6)-2.9465 Å)[29] due to increased stabilization of the negative charge throughout the fluorinated ring, withdrawing charge density away from the Th-Se bond. The $py_3Th(SePh)_4$ monomer is seven coordinate, while the bipy derivative and similar $(bipy)_2Th(SeC_6F_5)_4$ (**1**) are eight-coordinate, as bipy preferentially binds to the Th(IV) cation over py in solution. Seven coordinate mixed py-bipy complexes are not seen.

Bonds from thorium to a nitrogen atom are comparable between the pyridine and bipy Th(IV) chalcogenolates as well. Th-N(bipy) distances in **1** (2.613-2.618 Å) are consistent with the range of Th-N(bipy) distances in the non-fluorinated derivative, $(bipy)_2Th(SePh)_4$ (2.620-2.653 Å),[71] and are slightly shorter than the Th-N(py) distances in $py_3Th(SePh)_4$ (2.626(4)-2.657(4) Å)[29] and $py_4Th(SeC_6F_5)_4$ (2.635(4)-2.685(4) Å),[29] due to stronger σ-donor characteristics of bidentate bipyridine compared to monodentate pyridine.

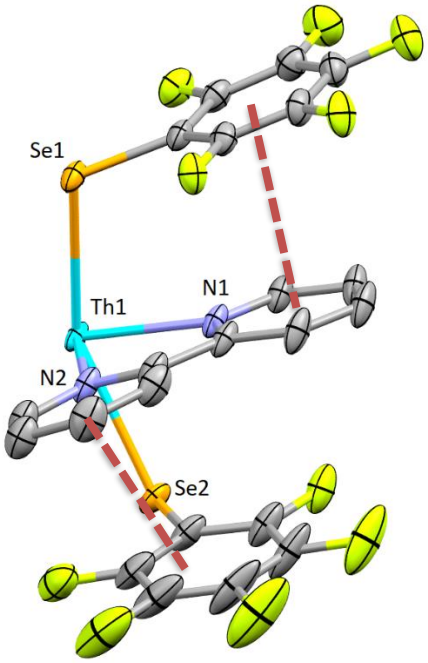

Figure 2.4 Thermal ellipsoid diagram of the asymmetric unit of $(bipy)_2Th(SC_6F_5)_4$ (**1**), with orange Se, light green F, light blue Th, purple N, grey C, H atoms removed for clarity, and ellipsoids at the 50% probability level. This shows the face-to-face stacking interactions between bipy and fluorinated phenyl ligands, indicated with red dashed lines.

Each $SeC_6F_5^-$ ligand is positioned in such a way that two instances of intramolecular double π…π stacking are observed in the complex. This SC_6F_5…bipy…SC_6F_5 arrangement occurs in a stepwise manner, with the fluorinated phenyl ring on Se1 stacking with the pyridine ring at N1 on bipy with a distance of

3.573 Å and the fluorinated phenyl ring on Se2 stacking with the pyridine ring at N2 on bipy with a distance of 3.528 Å (Figure 2.3). This is similar to the face-to-face stacking of 2,2'-bipyridine in the solid state at a distance of 3.518 Å,[95] and longer than π…π stacking in graphite with a distance of 3.35 Å.[143]

2.2.2 Actinide Pyridinethiolates

Thorium and uranium metals are oxidized by pySSpy in a solution of pyridine for compounds **2** and **3** to yield soluble monomeric An(IV) tetrachalogenolates – $pyAn(Spy)_4$ [An = Th(**2**), U(**3**)]. Like the synthesis of previous Ln and An chalcogenolate compounds with REER (E = S, Se; R = Ph, C_6F_5), elemental Hg is used as a catalyst to reductively cleave pySSpy to quickly form Spy^- to oxidize Th or U metals in only a few days (Figure 2.4).

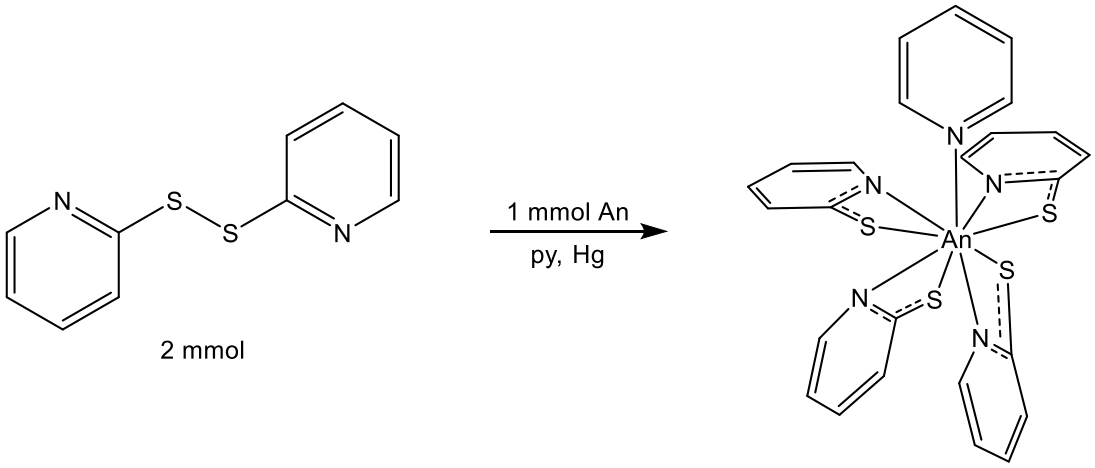

Figure 2.5 Synthesis of $pyAn(Spy)_4$ (An = Th (**2**), and U (**3**)).

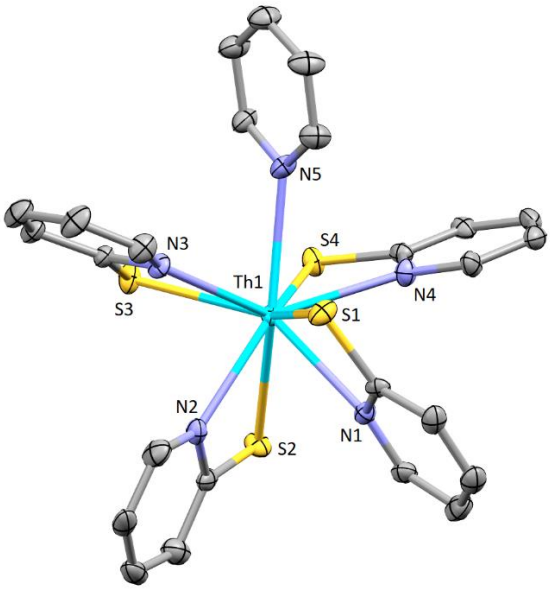

Figure 2.6 Thermal ellipsoid diagram of pyTh(Spy)$_4$ (**2**), with yellow S, light blue Th, purple N, grey C, H atoms removed for clarity, and ellipsoids at the 50% probability level.

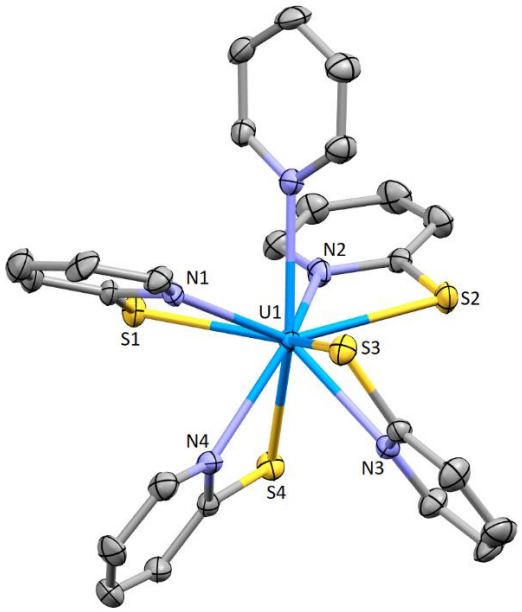

Figure 2.7 Thermal ellipsoid diagram of pyU(Spy)$_4$ (**3**), with yellow S, blue U, purple N, grey C, H atoms removed for clarity, and ellipsoids at the 50% probability level.

Table 2.2 Summary of Crystallographic Details for **2** – **5**.

compound	**2**	**3**	**4**	**5**
empirical formula	$C_{27.50}H_{23.50}N_{5.50}S_4Th$	$C_{25}H_{21}N_5S_4U$	$C_{50}H_{48.35}I_{2.35}N_{10}S_{1.66}Se_4Th_2$	$C_{22.50}H_{20.50}I_2N_{4.50}S_2U$
fw	791.30	757.74	1920.68	909.88
space group (No.)	$P2_1$ (4)	$P2_12_12_1$ (19)	P-1 (2)	$Pca2_1$ (29)
a (Å)	9.5982(9)	9.5683(14)	9.6725(9)	16.8836(15)
b (Å)	16.4959(15)	15.339(2)	11.8540(11)	9.1867(8)
c (Å)	18.3890(17)	18.093(3)	13.0886(12)	34.221(3)
α (deg)	90	90	82.3912(16)	90
β (deg)	101.2169(14)	90	78.5115(16)	90
γ (deg)	90	90	76.4887(16)	90
V ($Å^3$)	2855.9(5)	2655.6(7)	1424.1(2)	5307.8(8)
Z	4	4	1	8
D(calcd) (Mg/m^3)	1.840	1.895	2.240	2.277
temperature (°K)	120(2)	293(2)	120(2)	120(2)
λ (Å)	0.71073	0.71073	0.71073	0.71073
abs coeff (mm^{-1})	5.542	6.451	9.149	8.619
$R(F)^a$ [$I > 2\sigma(I)$]	0.0371	0.0350	0.0401	0.0888
$R_w(F^2)^b$ [$I > 2\sigma(I)$]	0.0869	0.0668	0.0970	0.0933

Definitions: ^{a} $R(F) = \Sigma||F_o| - |F_c||/\Sigma|F_o|$; ^{b} $R_w(F^2) = [\Sigma[w(F_o^2 - F_c^2)^2]/\Sigma[w(F_o^2)^2]]^{1/2}$

The POVRAY diagrams in Figures 2.5-2.6 show the molecular structures of $pyTh(Spy)_4$ (**2**) and $pyU(Spy)_4$ (**3**). Purity of the samples were confirmed by elemental analysis and phase purity was confirmed by powder X-ray diffraction (PXRD). The crystallized products were characterized by low-temperature single-crystal X-ray diffraction, details given in Table 2.2. Compounds **2** and **3** crystallize in the $P2_1$ and $P2_12_12_1$ unit cells, respectively; each with four molecules per unit cell.

The use of elemental chalcogen in the synthesis of multimetallic clusters is used to form chalcogenido bridging ligands. Elemental Se is added in-situ to a solution of "$Th(SePh)_2(Spy)I$", where thorium metal was oxidized by a mixture of pySSpy, PhSeSePh, and I_2 in pyridine. The Se is reduced to $(Se_2)^{2-}$ and oxidation of $SePh^-$ to give PhSeSePh leads to the formation of $(py)_4Th_2(Se_2)_2I_2(Spy)_2$ (**4**) (Figure 2.7).

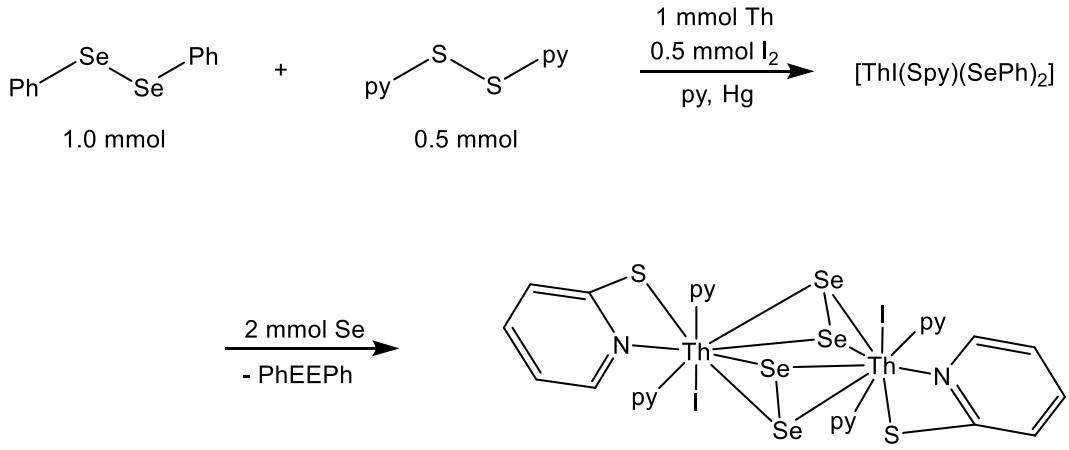

Figure 2.8 Synthesis of $py_4Th_2I_2(Spy)_2(Se_2)_2$ (**4**).

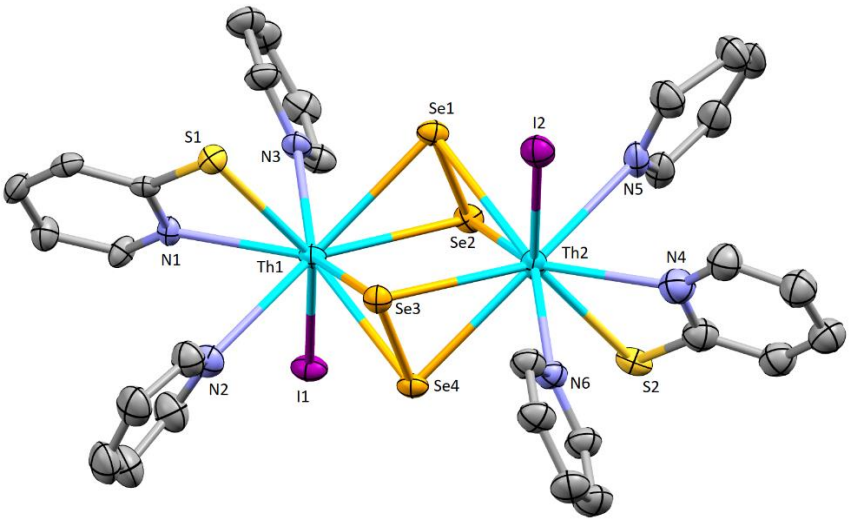

Figure 2.9 Thermal ellipsoid diagram of $(py)_4Th_2I_2(Spy)_2(Se_2)_2$ (**4**), with yellow S, orange Se, dark pink I, light blue Th, purple N, grey C, H atoms removed for clarity, and ellipsoids at the 50% probability level.

Figure 2.8 shows the POVRAY diagram of the molecular structure of $(py)_4Th_2I_2(Spy)_2(Se_2)_2$ (**4**). Purity of the samples were confirmed by elemental analysis, and phase purity of the sample was analyzed via powder X-ray diffraction (PXRD) which showed a small impurity, possibly due to the slight disorder about one of the iodide ligands. The recrystallized products were characterized by low-temperature single-crystal X-ray diffraction, details given in Table 2.2.

In an attempt to form a bimetallic uranium compound similar to **4** (Figure 2.7), uranium metal was oxidized by a mixture of pySSpy, PhSeSePh, and I_2 in pyridine and subsequent in-situ addition of elemental Se. However, $py_2UI_2(Spy)_2$ (**5**) is produced from this synthetic method. A higher yield syntheses of **5** was performed via Figure 2.9.

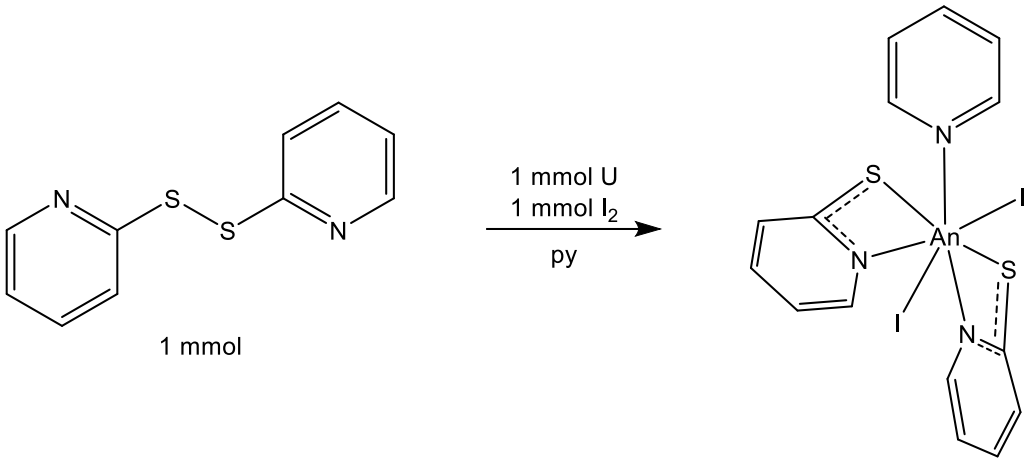

Figure 2.10 Synthesis of $py_2UI_2(Spy)_2$ (**5**).

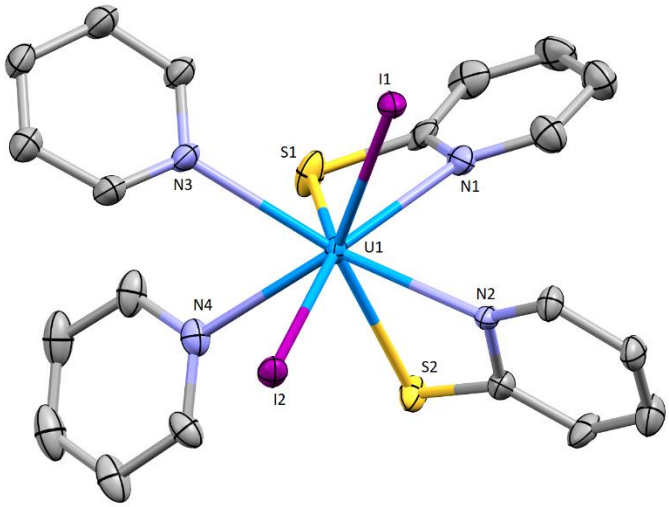

Figure 2.11 Thermal ellipsoid diagram of $py_2UI_2(Spy)_2$ (**5**), with yellow S, dark pink I, blue U, purple N, grey C, H atoms removed for clarity, and ellipsoids at the 50% probability level.

Figure 2.10 shows a POVRAY diagram of the molecular structure of $py_2UI_2(Spy)_2$ (**5**). The recrystallized product was characterized by low-temperature single-crystal X-ray diffraction, details given in Table 2.2. Purity of the sample was confirmed by elemental analysis and phase purity was confirmed by PXRD.

Four new compounds containing Spy^- ligands have been synthesized in one-pot reactions with minimal reactive steps. Compounds **2** and **4** are the first examples of thorium compounds with Spy^- ligands. Compounds **2** and **3** are isostructural monomers with a thorium and uranium metal-center, respectively, with each monomer being nine-coordinate: bonds to N and S in the four bidentate Spy ligands, and the N atom of the single pyridine neutral donor ligand. Compound **4** is a thorium dimer containing a central Th-(μ_2-E_2)$_2$-Th core, with each nine coordinate thorium metal center also containing one bidentate Spy ligand (bound via the S ad N atoms), one iodide ligand, and two pyridine ligands. Compound **5** is an eight-coordinate uranium monomer containing two bidentate Spy ligands, two iodide ligands, and two pyridine ligands.

Related compounds in the literature are limited. While no thorium compounds with Spy exist elsewhere, there are few examples of uranium compounds; including the isomorphous THF adduct (THF)(USC_5H_4)$_4$ that crystalizes in the same $P2_12_12_1$ space group as **3**,[60] and an oxo-bridged tetranuclear compound $(HNEt_3)_2[(UO_2)_4(O)_2(SC_5NH_4)_6]\bullet Me_2CO$,[141] which is produced from the reaction of $UO_2(NO_3)_2\bullet 6H_2O$ with an excess of pyridine-2-thiol and triethylamine in the presence of atmospheric oxygen.[141]

Table 2.3 Selected Distances (Å), and Angles (°) for **2** – **5**.

Bond/Angle	**2**	**3**	**4**	**5**
An-N(py)	2.704(7)	2.651(6)	2.72-2.76(2)	2.612(10), 2.662(11)
An-S	2.874-2.897(2)	2.809-2.852(2)	2.856-2.865(9)	2.729(3), 2.773(3)
An-N(Spy)	2.570-2.619(5)	2.503-2.550(5)	2.583(14), 2.599(9)	2.552(1), 2.521(10)
An-I			3.1478(14), 3.1547(18)	3.0432-3.0742(10)
An-Se			2.993-3.029(3)	
Se-Se			2.358(3), 2.351(3)	
S-An-N(Spy)	56.4-57.3(2)	57.5-58.6(1)	58.1(3), 58.1(5)	58.4(2), 59.6(2)
S-C-N(Spy)	114.9-115.4(6)	113.6-115.3(5)	118(1), 118(2)	114(1), 113.4(9)
An-S-C	83.4-84.2(3)	82.0-83.7(2)	82.6(5), 82.2(7)	84.2(5), 85.5(4)
S-An-I			141.0(1), 140.7(2)	111.92(8), 151.25(8), 138.84(8), 93.27(8)
I-An-I				88.13(3)
E-An-I (acute angle)			78.21-81.33(9)	
E-An-I (obtuse angle)			123.4-126.7(1)	

Bond geometries for each of the four compounds are consistent with prior literature, with bond length and angle values reflecting the size of the atomic and ionic components. Relevant bond lengths and angles shown in Table 2.3. All four compounds contain at least one pyridine bound to An(IV), all consistent with previously reported An-N(py) bond lengths.[29, 71, 78, 81, 87] Th-N(py) distances for **2** (2.704(7) Å) and **4** (2.72(2)-2.76(2) Å) are consistent with the wide range of previously reported Th-N(py) bond lengths (2.626(4)-2.718(5) Å) in monomeric

$(py)_xTh(ER)_4$ (x = 3,4; E = S, Se; R = Ph, C_6F_5),[29] and are longer than the reported Th-N(bipy) bond lengths (2.613-2.618 Å) in $(bipy)_2Th(SeC_6F_5)_4$ (**1**). U-N(py) distances for **3** (2.651(6) Å) and **5** (2.612(10), 2.662(11) Å) are consistent with previously reported U-N(py) bond lengths (2.563(5)-2.629(5) Å) in monomeric $U(SPh)_4(py)_3$.[60] The An-N(Spy) bonds in **2** (2.570(7)-2.619(5) Å), **3** (2.503(5)-2.550(5) Å), **4** (2.583(14), 2.599(9) Å), and **5** (2.552(1), 2.521(10) Å) are consistently shorter than the bonds to pyridine and bipyridine. This arises due to a resonance effect shortening bonds to S and N on Spy, coupled with the more electronegative S relative to N in bipy.

Th-S(Spy) bond lengths in **2** (2.874(2)-2.897(2) Å) and **4** (2.856(6)-2.865(9) Å) are slightly longer than in monodentate Th-S(Ph) bond lengths (2.8111(11)-2.8481(6) Å) in monomeric $(py)_xTh(SR)_4$ (x = 3,4; R = Ph, C_6F_5),[29] due to the nine-coordinate environment of **2** and **4** having greater ligand-ligand repulsions, and the ability for pyridine-2-thiolate to disperse electron density between nitrogen and sulfur. This yields a shorter M-N bond than if the nitrogen was a neutral donor, and a longer M-S bond as electron density moves away from the negatively charged sulfur atom. All U-S(Spy) bond lengths in **3** (2.809(2)-2.852(2) Å) are consistent with previously reported U-S(Spy) bond lengths (2.8222(8)-2.8380(8) Å) in $U(Spy)_4(THF)$.[60] The two U-S(Spy) bond lengths **5** (2.729(3), 2.773(3) Å) are comparable to U-S bonds in monodentate sulfur ligands – i.e. U-S(Ph) bond lengths (2.7169(17)-2.7639(17) Å) in $U(SPh)_4(py)_3$.[60]

Bond lengths to Th-I in **4** (3.1478(14), 3.1547(18) Å) are consistent with Th-I bond lengths (3.174(1)-3.216(1) Å) in similar dimers $(py)_6Th_2I_4E_4$ (E= S, Se) and $(py)_6Th_2I_2(SC_6F_5)_2Se_4$.[81] U-I bonds (3.0433(1)-3.0744(1) Å) in **5** are consistent with U-I bonds (2.9558(4)-3.0438(4) Å) in $(py)_3UI_4$.[144]

Successful synthesis of the dimeric thorium $(py)_4Th_2I_2(Spy)_2(Se_2)_2$ (**4**) was achieved by reducing elemental Se to the $(Se_2)^{2-}$ ligand. Th-Se bond lengths in **4** (2.993(3)-3.029(3) Å) are comparable to those in the literature,[29, 69-71, 78, 81, 83, 84, 87] including Th-Se bond lengths (2.971(1)-3.024(1) Å) from the series of $(Se_2)_2$ bridged dimeric thorium clusters by Wu, et al,[81] and similar Th-Se bond lengths (2.871(1), 2.880(1) Å) in $[\eta^5\text{-}1,2,4\text{-}(Me_3C)_3C_5H_2]_2Th(SePh)_2$.[83]

2.2.3 Bimetallic Thorium Fluoride Compound

As with the incorporation of E to yield clusters with bridging E^{2-} or EE^{2-}, F^- can be employed to synthesize multimetallic clusters from monomeric chalcogenolate compounds. This has precedence in the study of lanthanides with reaction of monomeric $Ln(SePh)_3$ and NH_4F to yield a large fluoride bridged cluster $(py)_{24}Ln_{28}F_{68}(SePh)_{16}$.[145] The study of actinide clusters with incorporated bridging fluoride clusters is less explored, with compounds relying on sterically bulky Cp related ligands.[70, 146]

The ligand based metathesis reaction of a Th(IV) chalcogenolate with silver(I) fluoride in pyridine gives a bimetallic Th(IV) complex with both bridging and terminal fluoride ligands. The use of AgF explores the facile synthesis of actinide fluoride compounds with minimal reactive steps. The metathesis reaction occurs with the exchange of SPh with Ag for F on thorium (Figure 2.11).

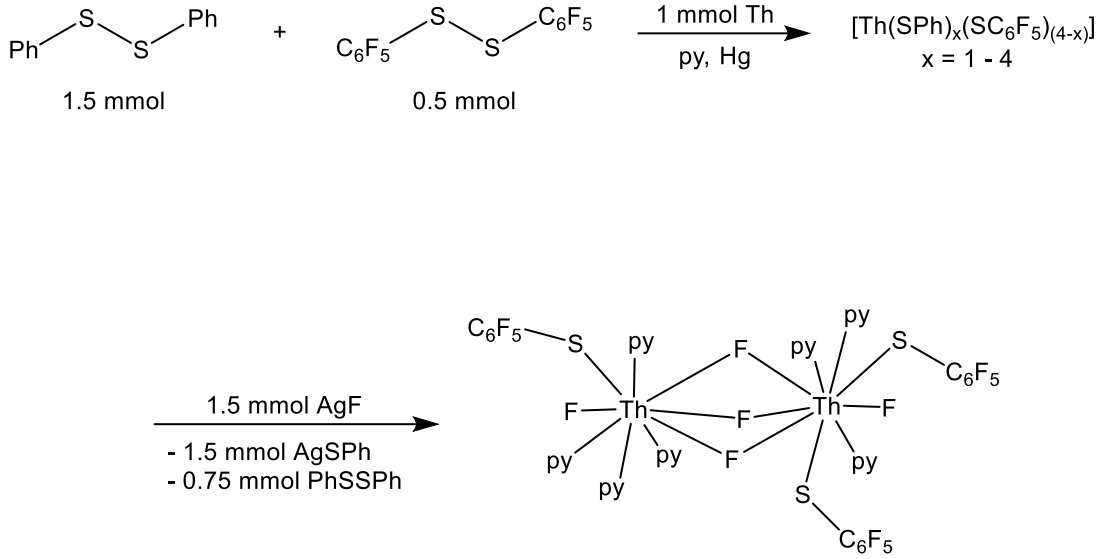

Figure 2.12 Synthesis of $py_7Th_2F_5(SC_6F_5)_3$ (**6**).

Table 2.4 Summary of Crystallographic Details for **6**.

	$py_7Th_2F_5(SC_6F_5)_3 \bullet 2py$
empirical formula	$C_{63}H_{45}F_{20}N_9S_3Th_2$
fw	1868.34
space group (No.)	P-1 (2)
a (Å)	1101776(10)
b (Å)	12.1625(11)
c (Å)	25.368(2)
α (deg)	81.4051(15)
β (deg)	86.7035(15)
γ (deg)	74.0481(15)
V ($Å^3$)	3278.2(5)
Z	2
D(calcd) (Mg/m^3)	1.893
temperature (°K)	120(2)
λ (Å)	0.71073
abs coeff (mm^{-1})	4.732
R(F)[a] [I > 2 σ(I)]	0.0360
$R_W(F^2)$[b] [I > 2 σ(I)]	0.0438

Definitions: [a] $R(F) = \Sigma||F_o| - |F_c||/\Sigma|F_o|$; [b] $R_w(F^2) = [\Sigma[w(F_o^2 - F_c^2)^2]/\Sigma[w(F_o^2)^2]]^{1/2}$

Figure 2.12 shows a POVRAY diagram of $py_7Th_2F_5(SC_6F_5)_3$ (**6**). The crystallized product was characterized by spectroscopic methods and low-temperature single-crystal X-ray diffraction, details given in Table 2.4. Purity of the bulk phase was analyzed by PXRD.

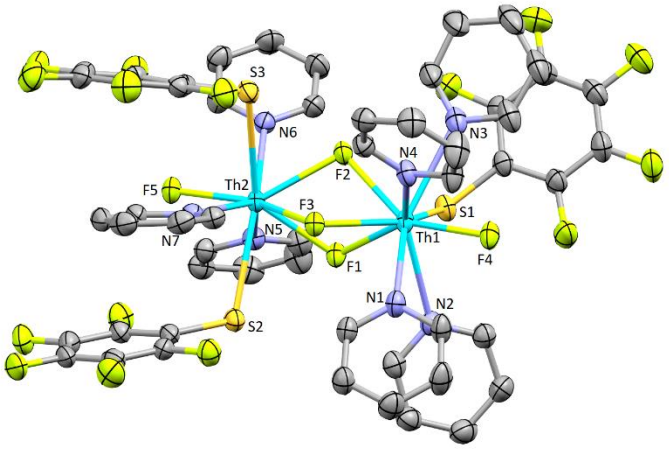

Figure 2.13 Thermal ellipsoid diagram of $py_7Th_2F_5(SC_6F_5)_3$ (**6**), with yellow S, light green F, light blue Th, purple N, grey C, H atoms removed for clarity, and ellipsoids at the 50% probability level.

Table 2.5 Selected Distances (Å), and Angles (°) for **6**.

Bond/Angle	$py_7Th_2F_5(SC_6F_5)_3 \bullet 2py$
Th-(η-F)	2.165(2), 2.155(2)
Th-(μ_2-F)	2.354-2.407(2)
Th-N	2.639-2.722(4)
Th-S	2.9206-2.9669(11)
Th-Th	3.7473(3)
Th-(μ_2-F)-Th	103.77-104.12(9)
Th-Th-(η-F)	176.58(7), 176.98(7)
Th-S-C	110.50-111.88(14)

Bimetallic **6** has two nine coordinate Th(IV) cations, bridged by three fluoride ligands. The terminally bound ligands are asymmetrically distributed across the two Th(IV) coordination centers [Th(1): 4 F, 1 S(C_6F_5), 4 N(py); Th(2): 4 F, 2 S(C_6F_5), 3 N(py)]. The Th-(μ_2-F)$_3$-Th core shows the same fluoride bridging motif as the organometallic dimer [η^5-1,3-(Me_3C)$_2$$C_5H_3$]$_2$Th(F)($\mu$-F)$_3$Th[$\eta^5$-1,3-($Me_3C$)$_2$$C_5H_3$](F)(bipy);[69] ligand redistributions were presumed to have been halted by sterically bulky substituted cyclopentadienyl ligands that prevent formation of ThF_4.[69] The terminally bound fluoride ligands in the organometallic thorium dimer are angled at ~98° to the bimetallic Th-Th axis,[69] while the terminally bound fluoride ligands on **6** are angled at ~177° and are nearly in line with the bimetallic Th-Th axis of the Th-(μ_2-F)$_3$-Th core, allowing repulsions to be mitigated amongst bridging and terminal fluorides in **6** in the presence of less sterically restricting $SC_6F_5^-$ ligands.

Bond geometries are consistent with prior literature, with bonds and angles shown in Table 2.5. Seven Th-N(py) bonds (2.639(4)-2.722(4) Å) present in complex **6** are consistent with previously reported Th-N(py) bond lengths (2.634(4)-2.718(5) Å) in monomeric py$_3$Th(SC_6F_5)$_4$.[29] Compound **6** contains three Th-S(C_6F_5) bonds (2.9206(11)-2.9669(11) Å) which are slightly longer than Th-S(C_6F_5) bond lengths (2.8111(11)-2.8253(10) Å) in monomeric py$_3$Th(SC_6F_5)$_4$.[29] Two nine-coordinate Th(IV) cations in compound **6** leads to a slight increase in bond length relative to seven-coordinate py$_3$Th(SC_6F_5)$_4$.

Bond lengths between thorium and fluoride ligands differ between bridging μ^2-F and terminal F. The terminal Th-F bonds in **6** (2.155(2) and 2.165(2) Å) are consistent with terminal Th-F bonds (2.138(3) and 2.188(2) Å) in the organometallic dimer [η^5-1,3-(Me_3C)$_2$$C_5H_3$]$_2$Th(F)($\mu$-F)$_3$Th[$\eta^5$-1,3-($Me_3C$)$_2$$C_5H_3$](F)(bipy).[69] The Th-($\mu_2$-F) bonds (2.354(2)-2.407(2) Å) in the bimetallic core of **6** are longer than the

terminal fluorides, and are comparable to the Th-(μ_2-F) bonds (2.318(2)-2.478(2) Å).[69] Bonds between thorium and the bridging fluorides are longer than their terminal counterparts due to repulsions from the three proximal electronegative fluorides, and as good π donors, their electron density spread between two metal cation centers.

Each $SC_6F_5^-$ ligand is positioned in such a way that there are two different π…π stacking motifs within each molecule. The fluorinated phenyl ring on S1 is stacking with the pyridine ring at N3 with a distance of 3.530 Å, while the phenyl rings at S2 and S3 sandwich the pyridine ring at N7 with distances of 3.706 Å and (3.441 Å) respectively.

2.3 Conclusion

Several actinide chalcogenolates were synthesized by the reduction of REER (E = S, Se; R = Ph, C_6F_5, py) by metallic thorium or uranium, in exploring the coordination of these compounds with bidentate neutral donor ligand, 2,2'-bipyridine, and comparing these with bidentate pyridinethiolates. Coordination complexes containing pyridinethiolates were then used as novel starting materials for preparing actinide-chalcogen polymetallic products. The use of bidentate ligands changed product identity, where bipy stabilizes eight-coordinate geometries, and the pyridinethiolates can exhibit nine-coordinate geometries in monomeric and dimeric compounds. Cluster synthesis was also explored using ligand based redox reactions in which SPh anions initially bound to thorium reduce elemental Se to form $(py)_4Th_2(Se_2)_2I_2(Spy)_2$. Metathesis reactions of an in situ prepared thorium thiolate and AgF was also explored to give the novel bimetallic fluoride/chalcogenolate compound $py_7Th_2F_5(SC_6F_5)_3$.

2.4 References

1. Banerjee, S.; Huebner, L.; Romanelli, M. D.; Kumar, G. A.; Riman, R. E.; Emge, T. J.; Brennan, J. G., Oxoselenido clusters of the lanthanides: Rational introduction of oxo ligands and near-IR emission from Nd(III). *J. Am. Chem. Soc.* **2005,** *127* (45), 15900-15906.
2. Banerjee, S.; Kumar, G. A.; Riman, R. E.; Emge, T. J.; Brennan, J. G., Oxoclusters of the lanthanides begin to resemble solid-state materials at very small cluster sizes: Structure and NIR emission from Nd(III). *J. Am. Chem. Soc.* **2007,** *129* (18), 5926-5931.
3. Beltran, T. F.; Delaude, L., Recent Advances in Small Clusters and Polymetallic Assemblies Based on Transition Metals and Dithiocarboxylate Zwitterions Derived from N-Heterocyclic Carbenes. *J. Clust. Sci.* **2017,** *28* (2), 667-678.
4. Bootharaju, M. S.; Kozlov, S. M.; Cao, Z.; Harb, M.; Maity, N.; Shkurenko, A.; Parida, M. R.; Hedhili, M. N.; Eddaoudi, M.; Mohammed, O. F.; Bakr, O. M.; Cavallo, L.; Basset, J. M., Doping-Induced Anisotropic Self-Assembly of Silver Icosahedra in $[Pt_2Ag_{23}Cl_7(PPh_3)_{10}]$ Nanoclusters. *J. Am. Chem. Soc.* **2017,** *139* (3), 1053-1056.
5. Chen, X. H.; Wu, K. C.; Snijders, J. G.; Lin, C. S., Electronic structures and nonlinear optical properties of trinuclear transition metal clusters M-(μ-S)-M' (M = Mo, W; M ' = Cu, Ag, Au). *Inorg. Chem.* **2003,** *42* (2), 532-540.
6. Geach, J.; Walters, C. J.; James, B.; Caviness, K. E.; Hefferlin, R. A., Global molecular identification from graphs. Main-group triatomic molecules. *Croat. Chem. Acta.* **2002,** *75* (2), 383-400.
7. Guirado-Lopez, R. A.; Dorantes-Davila, J.; Pastor, G. M., Orbital magnetism in transition-metal clusters: From Hund's rules to bulk quenching. *Phys. Rev. Lett.* **2003,** *90* (22).
8. Karashimada, R.; Iki, N., Thiacalixarene assembled heterotrinuclear lanthanide clusters comprising Tb-III and Yb-III enable f-f communication to enhance Yb-III-centred luminescence. *Chem. Commun.* **2016,** *52* (15), 3139-3142.
9. Kornienko, A.; Banerjee, S.; Kumar, G. A.; Riman, R. E.; Emge, T. J.; Brennan, J. G., Heterometallic chalcogenido clusters containing lanthanides and main group metals: Emissive precursors to ternary solid-state compounds. *J. Am. Chem. Soc.* **2005,** *127* (40), 14008-14014.
10. Li, Z.; Li, X. X.; Yang, T.; Cai, Z. W.; Zheng, S. T., Four-Shell Polyoxometalates Featuring High-Nuclearity Ln_{26} Clusters: Structural Transformations of Nanoclusters into Frameworks Triggered by Transition-Metal Ions. *Angew. Chemie. Int. Ed.* **2017,** *56* (10), 2664-2669.
11. Lv, X. H.; Yang, S. L.; Li, Y. X.; Zhang, C. X.; Wang, Q. L., Syntheses, structures and magnetic properties of four-spin Mn-Imino nitroxide radical complexes. *J. Mol. Struct.* **2017,** *1133*, 211-216.
12. Masternak, J.; Zienkiewicz-Machnik, M.; Kowalik, M.; Jablonska-Wawrzycka, A.; Rogala, P.; Adach, A.; Barszcz, B., Recent advances in coordination chemistry of metal complexes based on nitrogen heteroaromatic alcohols. Synthesis, structures and potential applications. *Coord. Chem. Rev.* **2016,** *327*, 242-270.
13. Moore, B. F.; Kumar, G. A.; Tan, M. C.; Kohl, J.; Riman, R. E.; Brik, M. G.; Emge, T. J.; Brennan, J. G., Lanthanide Clusters with Chalcogen Encapsulated

Ln: NIR Emission from Nanoscale $NdSe_x$. *J. Am. Chem. Soc.* **2011,** *133* (2), 373-378.
14. Peng, J. B.; Kong, X. J.; Zhang, Q. C.; Orendac, M.; Prokleska, J.; Ren, Y. P.; Long, L. S.; Zheng, Z. P.; Zheng, L. S., Beauty, Symmetry, and Magnetocaloric Effect-Four-Shell Keplerates with 104 Lanthanide Atoms. *J. Am. Chem. Soc.* **2014,** *136* (52), 17938-17941.
15. Rivera, M.; Martinez-Vado, F. I.; Mendoza-Huizar, L. H.; Amelines-Sarria, O.; Betancourt, I., Morphological and local magnetic properties of cobalt clusters electrodeposited onto indium tin oxide substrates. *J Mater Sci: Mater Electron.* **2017,** *28* (13), 9245-9251.
16. Schipper, D. E.; Ikhlef, D.; Khalal, S.; Saillard, J. Y.; Whitmire, K. H., New Main-Group-Element-Rich nido-Octahedral Cluster System: Synthesis and Characterization of $[Et_4N][Fe_2(CO)_6(\mu_3\text{-}As)\{\mu_3\text{-}EFe(CO)_4\}_2]$. *Inorg. Chem.* **2016,** *55* (13), 6679-6684.
17. Shaw, R.; Laye, R. H.; Jones, L. F.; Low, D. M.; Talbot-Eeckelaers, C.; Wei, Q.; Milios, C. J.; Teat, S.; Helliwell, M.; Raftery, J.; Evangelisti, M.; Affronte, M.; Collison, D.; Brechin, E. K.; McInnes, E. J. L., 1,2,3-Triazolate-bridged tetradecametallic transition metal clusters $[M_{14}(L)_6O_6(OMe)_{18}X_6]$ ($M = Fe^{III}$, Cr^{III} and $V^{III/IV}$) and related compounds: Ground-state spins ranging from S=0 to S=25 and spin-enhanced magnetocaloric effect. *Inorg. Chem.* **2007,** *46* (12), 4968-4978.
18. Tian, H.; Qiao, X.; Xie, C. Z.; Ouyang, Y.; Xu, J. Y., Synthesis, characterization, and magnetochemical properties of two Mn_4 clusters derived from 2-pyridinecarboxaldehyde Schiff base ligands. *J. Coord. Chem.* **2017,** *70* (7), 1207-1220.
19. Wang, W.; Fullmer, L. B.; Bandeira, N. A. G.; Goberna-Ferron, S.; Zakharov, L. N.; Bo, C.; Keszler, D. A.; Nyman, M., Crystallizing Elusive Chromium Polycations. *Chem 1.* **2016,** *1* (6), 887-901.
20. Wang, Y. Y.; Ma, Y. Q.; Liu, R.; Yang, L. L.; Tian, G. R.; Sheng, N., Tetranuclear Complexes with $\{M_4O_4\}$ ($M = Co^{II}$, Ni^{II}) Cubane-Like Core: Synthesis, Crystal Structure, and Magnetic Properties. *Z. Anorg. Allg. Chem.* **2016,** *642* (7), 546-550.
21. Wu, J. F.; Li, X. L.; Zhao, L.; Guo, M.; Tang, J. K., Enhancement of Magnetocaloric Effect through Fixation of Carbon Dioxide: Molecular Assembly from Ln_4 to Ln_4 Cluster Pairs. *Inorg. Chem.* **2017,** *56* (7), 4104-4111.
22. Wu, M. Y.; Jiang, F. L.; Kong, X. J.; Yuan, D. Q.; Long, L. S.; Al-Thabaiti, S. A.; Hong, M. C., Two polymeric 36-metal pure lanthanide nanosize clusters. *Chem. Sci.* **2013,** *4* (8), 3104-3109.
23. Xiong, J.; Ding, H. Y.; Meng, Y. S.; Gao, C.; Zhang, X. J.; Meng, Z. S.; Zhang, Y. Q.; Shi, W.; Wang, B. W.; Gao, S., Hydroxide-bridged five-coordinate Dy^{III} single-molecule magnet exhibiting the record thermal relaxation barrier of magnetization among lanthanide-only dimers. *Chem. Sci.* **2017,** *8* (2), 1288-1294.
24. Zhang, H. F.; Zhang, J.; Liu, R.; Li, Y. H.; Liu, W.; Li, W., Five Disk-Shaped $\{M_7^{II}\}$ (M = Mn, Fe, Co, Cu, Zn) Clusters and One Capsule-Like $\{Cu^{II6}Na^{I2}\}$ Cluster Assembled from the Same Schiff Base Ligand. *Eur. J. Inorg. Chem.* **2016,** (26), 4134-4143.
25. Zhou, L. L.; Ding, L.; Wei, K. Y.; Sun, Y. Q.; Chen, Y. P., Novel Lanthanide Cluster Polymers Based on Cubane-like $[Ln_4(OH)_4]^{8+}$ Clusters and Sulfate Anions. *Chinese. J. Struc. Chem.* **2016,** *35* (3), 375-382.

26. Zhou, Y.; Zheng, X. Y.; Cai, J.; Hong, Z. F.; Yan, Z. H.; Kong, X. J.; Ren, Y. P.; Long, L. S.; Zheng, L. S., Three Giant Lanthanide Clusters Ln_{37} (Ln = Gd, Tb, and Eu) Featuring A Double-Cage Structure. *Inorg. Chem.* **2017,** *56* (4), 2037-2041.
27. Mesbah, A.; Prakash, J.; Ibers, J. A., Overview of the crystal chemistry of the actinide chalcogenides: incorporation of the alkaline-earth elements. *Dalton Trans.* **2016,** *45* (41), 16067-16080.
28. Simon, A., Discrete and Condensed Clusters - a Link between Molecular and Solid-State Chemistry. *Pure. Appl. Chem.* **1995,** *67* (2), 311-312.
29. Rehe, D.; Kornienko, A. Y.; Emge, T. J.; Brennan, J. G., Thorium Compounds with Bonds to Sulfur or Selenium: Synthesis, Structure, and Thermolysis. *Inorg. Chem.* **2016,** *55* (14), 6961-7.
30. Arliguie, T.; Belkhiri, L.; Bouaoud, S. E.; Thuery, P.; Villiers, C.; Boucekkine, A.; Ephritikhine, M., Lanthanide(III) and Actinide(III) Complexes $[M(BH_4)_2(THF)_5][BPh_4]$ and $[M(BH_4)_2(18\text{-crown-}6)][BPh_4]$ (M = Nd, Ce, U): Synthesis, Crystal Structure, and Density Functional Theory Investigation of the Covalent Contribution to Metal-Borohydride Bonding. *Inorg. Chem.* **2009,** *48* (1), 221-230.
31. Berthet, J. C.; Thuery, P.; Ephritikhine, M., Unprecedented reduction of the uranyl ion $[UO_2]^{2+}$ into a polyoxo uranium(IV) cluster: Synthesis and crystal structure of the first f-element oxide with a $M_6(\mu_3\text{-}O)_8$ core. *Chem. Commun.* **2005,** (27), 3415-3417.
32. Berthet, J. C.; Thuery, P.; Ephritikhine, M., Formation of Uranium(IV) Oxide Clusters from Uranocene $[U(\eta^8\text{-}C_8H_8)_2]$ and Uranyl $[UO_2X_2]$ Compounds. *Inorg. Chem.* **2010,** *49* (17), 8173-8177.
33. Chatelain, L.; Scopelliti, R.; Mazzanti, M., Synthesis and Structure of Nitride-Bridged Uranium(III) Complexes. *J. Am. Chem. Soc.* **2016,** *138* (6), 1784-1787.
34. Di Pietro, P.; Kerridge, A., Assessing covalency in equatorial U-N bonds: density based measures of bonding in BTP and isoamethyrin complexes of uranyl. *Phys. Chem. Chem. Phys.* **2016,** *18* (25), 16830-9.
35. Falaise, C.; Nyman, M., The Key Role of U_{28} in the Aqueous Self-Assembly of Uranyl Peroxide Nanocages. *Chem. Eur. J.* **2016,** *22* (41), 14678-14687.
36. Falaise, C.; Volkringer, C.; Loiseau, T., Mixed Formate-Dicarboxylate Coordination Polymers with Tetravalent Uranium: Occurrence of Tetranuclear $\{U_4O_4\}$ and Hexanuclear $\{U_6O_4(OH)_4\}$ Motifs. *Cryst. Growth. Des.* **2013,** *13* (7), 3225-3231.
37. Gourier, D.; Caurant, D.; Arliguie, T.; Ephritikhine, M., EPR and angle-selected ENDOR study of 5f-ligand interactions in the $[U(\eta^7\text{-}C_7H_7)_2]^-$ anion, an f^1 analogue of uranocene. *J. Am. Chem. Soc.* **1998,** *120* (24), 6084-6092.
38. Huang, Q. R.; Kingham, J. R.; Kaltsoyannis, N., The strength of actinide-element bonds from the quantum theory of atoms-in-molecules. *Dalton Trans.* **2015,** *44* (6), 2554-2566.
39. Knope, K. E.; Vasiliu, M.; Dixon, D. A.; Soderholm, L., Thorium(IV)-Selenate Clusters Containing an Octanuclear Th(IV) Hydroxide/Oxide Core. *Inorg. Chem.* **2012,** *51* (7), 4239-4249.
40. Knope, K. E.; Wilson, R. E.; Vasiliu, M.; Dixon, D. A.; Soderholm, L., Thorium(IV) Molecular Clusters with a Hexanuclear Th Core. *Inorg. Chem.* **2011,** *50* (19), 9696-9704.

41. Kozimor, S. A.; Yang, P.; Batista, E. R.; Boland, K. S.; Burns, C. J.; Clark, D. L.; Conradson, S. D.; Martin, R. L.; Wilkerson, M. P.; Wolfsberg, L. E., Trends in Covalency for d- and f-Element Metallocene Dichlorides Identified Using Chlorine K-Edge X-ray Absorption Spectroscopy and Time-Dependent Density Functional Theory. *J. Am. Chem. Soc.* **2009,** *131* (34), 12125-12136.
42. Minasian, S. G.; Krinsky, J. L.; Williams, V. A.; Arnold, J., A heterobimetallic complex with an unsupported Uranium(III)-Aluminum(I) bond: $(CpSiMe_3)_3U\text{-}AlCp^*$ ($Cp^* = C_5Me_5$). *J. Am. Chem. Soc.* **2008,** *130* (31), 10086-10090.
43. Oelkers, B.; Butovskii, M. V.; Kempe, R., f-Element-Metal Bonding and the Use of the Bond Polarity To Build Molecular Intermetalloids. *Chem. Eur. J.* **2012,** *18* (43), 13566-13579.
44. Oliveri, A. F.; Pilgrim, C. D.; Qiu, J.; Colla, C. A.; Burns, P. C.; Casey, W. H., Dynamic Phosphonic Bridges in Aqueous Uranyl Clusters. *Eur. J. Inorg. Chem.* **2016,** (6), 797-801.
45. Parry, J.; Carmona, E.; Coles, S.; Hursthouse, M., Synthesis and Single-Crystal X-Ray-Diffraction Study on the First Isolable Carbonyl Complex of an Actinide, $(C_5Me_4H)_3U(CO)$. *J. Am. Chem. Soc.* **1995,** *117* (9), 2649-2650.
46. Qiu, J.; Ling, J.; Jouffret, L.; Thomas, R.; Szymanowski, J. E. S.; Burns, P. C., Water-soluble multi-cage super tetrahedral uranyl peroxide phosphate clusters. *Chem. Sci.* **2014,** *5* (1), 303-310.
47. Sigmon, G. E.; Szymanowski, J. E. S.; Carter, K. P.; Cahill, C. L.; Burns, P. C., Hybrid Lanthanide-Actinide Peroxide Cage Clusters. *Inorg. Chem.* **2016,** *55* (6), 2682-2684.
48. Travia, N. E.; Scott, B. L.; Kiplinger, J. L., A Rare Tetranuclear Thorium(IV) μ_4-Oxo Cluster and Dinuclear Thorium(IV) Complex Assembled by Carbon-Oxygen Bond Activation of 1,2-Dimethoxyethane (DME). *Chem. Eur. J.* **2014,** *20* (51), 16846-16852.
49. Woidy, P.; Kraus, F., $[Th_{10}(\mu\text{-}F_{16})(\mu_3\text{-}O_4)(\mu_4\text{-}O_4)(NH_3)_{32}](NO_3)_8$ 19.6 NH_3 - the Largest Thorium Complex from Solution known to Date. *Z. Anorg. Allg. Chem.* **2014,** *640* (8-9), 1547-1550.
50. Xiao, C. L.; Wang, C. Z.; Mei, L.; Zhang, X. R.; Wall, N.; Zhao, Y. L.; Chai, Z. F.; Shi, W. Q., Europium, uranyl, and thorium-phenanthroline amide complexes in acetonitrile solution: an ESI-MS and DFT combined investigation. *Dalton Trans.* **2015,** *44* (32), 14376-14387.
51. Zhang, Y. J.; Karatchevtseva, I.; Kadi, F.; Lu, K.; Yoon, B.; Price, J. R.; Li, F.; Lumpkin, G. R., Synthesis, spectroscopic characterization and crystal structures of thorium(IV) mononuclear lactato and hexanuclear formato complexes. *Polyhedron.* **2015,** *87*, 377-382.
52. Zhang, Y. J.; Bhadbhade, M.; Price, J. R.; Karatchevtseva, I.; Kong, L. G.; Scales, N.; Lumpkin, G. R.; Li, F., Uranyl peroxide clusters stabilized by dicarboxylate ligands: A pentagonal ring and a dimer with extensive uranyl-cation interactions. *Polyhedron.* **2015,** *92*, 99-104.
53. Clark, D. L.; Miller, M. M.; Watkin, J. G., Synthesis, Characterization, and X-Ray Structure of the Uranium Thiolate Complex $U(S\text{-}2,6\text{-}Me_2C_6H_3)[N(SiMe_3)_2]_3$. *Inorg. Chem.* **1993,** *32* (5), 772-774.
54. Diaconescu, P. L.; Arnold, P. L.; Baker, T. A.; Mindiola, D. J.; Cummins, C. C., Arene-bridged diuranium complexes: Inverted sandwiches supported by delta backbonding. *J. Am. Chem. Soc.* **2000,** *122* (25), 6108-6109.

55. Evans, W. J.; Miller, K. A.; Hillman, W. R.; Ziller, J. W., Two-electron reductive reactivity of trivalent uranium tetraphenylborate complexes of $(C_5Me_5)^{1-}$ and $(C_5Me_4H)^{1-}$. *J. Organomet. Chem.* **2007,** *692* (17), 3649-3654.
56. Evans, W. J.; Miller, K. A.; Kozimor, S. A.; Ziller, J. W.; DiPasquale, A. G.; Rheingold, A. L., Actinide hydride complexes as multielectron reductants: Analogous reduction chemistry from $[(C_5Me_5)_2UH]_2$, $[(C_5Me_5)_2UH_2]_2$, and $[(C_5Me_5)_2ThH_2]_2$. *Organometallics.* **2007,** *26* (14), 3568-3576.
57. Evans, W. J.; Miller, K. A.; Ziller, J. W.; DiPasquale, A. G.; Heroux, K. J.; Rheingold, A. L., Formation of $(C_5Me_5)_2U(EPh)Me$, $(C_5Me_5)_2U(EPh)_2$, and $(C_5Me_5)_2U(\eta^2\text{-}TeC_6H_4)$ from $(C_5Me_5)_2UMe_2$ and PhEEPh (E = S, Se, Te). *Organometallics.* **2007,** *26* (17), 4287-4293.
58. Evans, W. J.; Walensky, J. R.; Ziller, J. W., Reaction Chemistry of the U^{3+} Metallocene Amidinate $(C_5Me_5)_2[^iPrNC(Me)N^iPr]U$ Including the Isolation of a Uranium Complex of a Monodentate Acetate. *Inorg. Chem.* **2010,** *49* (4), 1743-1749.
59. Franke, S. M.; Rosenzweig, M. W.; Heinemann, F. W.; Meyer, K., Reactivity of uranium(III) with H_2E (E = S, Se, Te): synthesis of a series of mononuclear and dinuclear uranium(IV) hydrochalcogenido complexes. *Chem. Sci.* **2015,** *6* (1), 275-282.
60. Gaunt, A. J.; Scott, B. L.; Neu, M. P., U(IV) chalcogenolates synthesized via oxidation of uranium metal by dichalcogenides. *Inorg. Chem.* **2006,** *45* (18), 7401-7407.
61. Gotthelf, G.; Stuber, M. A.; Kornienko, A. Y.; Emge, T. J.; Brennan, J. G., Organosoluble tetravalent actinide di- and trifluorides. *Chem. Commun.* **2018,** *54* (85), 12018-12020.
62. Graves, C. R.; Scott, B. L.; Morris, D. E.; Kiplinger, J. L., Facile access to pentavalent uranium organometallics: One-electron oxidation of Uranium(IV) imido complexes with copper(I) salts. *J. Am. Chem. Soc.* **2007,** *129* (39), 11914-11915.
63. Graves, C. R.; Scott, B. L.; Morris, D. E.; Kiplinger, J. L., Selenate and tellurate complexes of pentavalent uranium. *Chem. Commun.* **2009,** (7), 776-778.
64. Karmazin, L.; Mazzanti, M.; Pecaut, J., Unique crown thioether complexes of f elements: the crystal structure of U(III) and La(III) complexes of 1,4,7-trithiacyclononane. *Chem. Commun.* **2002,** (6), 654-655.
65. Leverd, P. C.; Ephritikhine, M.; Lance, M.; Vigner, J.; Nierlich, M., Triscyclopentadienyl uranium thiolates and selenolates. *J. Organomet. Chem.* **1996,** *507* (1-2), 229-237.
66. Leverd, P. C.; Lance, M.; Nierlich, M.; Vigner, J.; Ephritikhine, M., Synthesis and Crystal-Structure of Homoleptic Uranium Hexathiolates - $[NEt_2H_2]_2[U(SPh)_6]$ and $[(Ph_3P)Cu(\mu\text{-}SPh)_3\text{-}U(\mu\text{-}SPh)_3Cu(PPh_3)]$. *J. Chem. Soc., Dalton Trans.* **1994,** (24), 3563-3567.
67. Leverd, P. C.; Lance, M.; Vigner, J.; Nierlich, M.; Ephritikhine, M., Synthesis and Reactions of Uranium(IV) Tetrathiolate Complexes. *J. Chem. Soc., Dalton Trans.* **1995,** (2), 237-244.
68. Lin, Z. R.; Brock, C. P.; Marks, T. J., Synthesis, Structural Characterization, and Properties of the Organothorium Alkylthiolate Complex $[(CH_3)_5C_5]_2Th(SCH_2CH_2CH_3)_2$. *Inorg. Chim. Acta.* **1988,** *141* (1), 145-149.
69. Ren, W. S.; Song, H. B.; Zi, G. F.; Walter, M. D., A bipyridyl thorium metallocene: synthesis, structure and reactivity. *Dalton Trans.* **2012,** *41* (19), 5965-5973.

70. Ren, W. S.; Zi, G. F.; Walter, M. D., Synthesis, Structure, and Reactivity of a Thorium Metallocene Containing a 2,2 '-Bipyridyl Ligand. *Organometallics.* **2012,** *31* (2), 672-679.
71. Ringgold, M.; Wu, W.; Stuber, M.; Kornienko, A. Y.; Emge, T. J.; Brennan, J. G., Monomeric thorium chalcogenolates with bipyridine and terpyridine ligands. *Dalton Trans.* **2018,** *47* (41), 14652-14661.
72. Rosenzweig, M. W.; Hummer, J.; Scheurer, A.; Lamsfus, C. A.; Heinemann, F. W.; Maron, L.; Mazzanti, M.; Meyer, K., A complete series of uranium(IV) complexes with terminal hydrochalcogenido (EH) and chalcogenido (E) ligands E = O, S, Se, Te. *Dalton Trans.* **2019,** *48* (29), 10853-10864.
73. Santos, I. G.; Abram, U., Synthesis and structures of dioxouranium complexes with 2-pyridineformamide thiosemicarbazones. *Inorg. Chem. Commun.* **2004,** *7* (3), 440-442.
74. Sitran, S.; Fregona, D.; Casellato, U.; Vigato, P. A.; Graziani, R.; Faraglia, G., Dioxouranium(VI) Complexes with Pentadentate Bases Containing Acetal Groups. *Inorg. Chim. Acta.* **1987,** *132* (2), 279-288.
75. Smiles, D. E.; Wu, G.; Kaltsoyannis, N.; Hayton, T. W., Thorium-ligand multiple bonds via reductive deprotection of a trityl group. *Chem. Sci.* **2015,** *6* (7), 3891-3899.
76. Spencer, L. P.; Yang, P.; Scott, B. L.; Batista, E. R.; Boncella, J. M., Oxidative Addition to U(V)-U(V) Dimers: Facile Routes to Uranium(VI) Bis(imido) Complexes. *Inorg. Chem.* **2009,** *48* (24), 11615-11623.
77. Spencer, L. P.; Yang, P.; Scott, B. L.; Batista, E. R.; Boncella, J. M., Uranium(VI) Bis(imido) Chalcogenate Complexes: Synthesis and Density Functional Theory Analysis. *Inorg. Chem.* **2009,** *48* (6), 2693-2700.
78. Stuber, M. A.; Kornienko, A. Y.; Emge, T. J.; Brennan, J. G., Tetrametallic Thorium Compounds with Th_4E_4 (E = S, Se) Cubane Cores. *Inorg. Chem.* **2017,** *56* (17), 10247-10256.
79. Thomson, R. K.; Graves, C. R.; Scott, B. L.; Kiplinger, J. L., Synthesis and Molecular Structure of $(C_5Me_5)_2U(O^tBu)(SePh)$: A Mixed-Ligand Alkoxide-Selenide Uranium(IV) Metallocene Complex Resulting from tert-Butoxy-Trimethylsilane Elimination. *J. Chem. Crystallogr.* **2011,** *41* (8), 1241-1244.
80. Tomson, N. C.; Anderson, N. H.; Tondreau, A. M.; Scott, B. L.; Boncella, J. M., Oxidation of uranium(IV) mixed imido-amido complexes with PhEEPh and to generate uranium(VI) bis(imido) dichalcogenolates, $U(NR)_2(EPh)_2(L)_2$. *Dalton Trans.* **2019,** *48* (29), 10865-10873.
81. Wu, W.; Rehe, D.; Hrobarik, P.; Kornienko, A. Y.; Emge, T. J.; Brennan, J. G., Molecular Thorium Compounds with Dichalcogenide Ligands: Synthesis, Structure, ^{77}Se NMR Study, and Thermolysis. *Inorg. Chem.* **2018,** *57* (23), 14821-14833.
82. Zalkin, A.; Brennan, J. G., A Trivalent-Uranium Thioether Coordination Compound. *Acta. Crystallogr. C.* **1985,** *41* (Sep), 1295-1297.
83. Zhang, C.; Hou, G.; Zi, G.; Walter, M. D., A base-free terminal thorium phosphinidene metallocene and its reactivity toward selected organic molecules. *Dalton Trans.* **2019,** *48* (7), 2377-2387.
84. Zhou, E. W.; Ren, W. S.; Hou, G. H.; Zi, G. F.; Fang, D. C.; Walter, M. D., Small Molecule Activation Mediated by a Thorium Terminal Imido Metallocene. *Organometallics.* **2015,** *34* (14), 3637-3647.
85. Arliguie, T.; Blug, M.; Le Floch, P.; Mezailles, N.; Thuery, P.; Ephritikhine, M., Organouranium complexes with phosphinine-based SPS pincer

ligands. Variations with the substituent at the phosphorus atom. *Organometallics.* **2008,** *27* (16), 4158-4165.
86. Arliguie, T.; Thuéry, P.; Floch, P. L.; Mézailles, N.; Ephritikhine, M., A homoleptic SPS-based complex and a double-cubane-type sulfur cluster of an actinide element. *Polyhedron.* **2009,** *28* (8), 1578-1582.
87. Ringgold, M.; Rehe, D.; Hrobarik, P.; Kornienko, A. Y.; Emge, T. J.; Brennan, J. G., Thorium Cubanes-Synthesis, Solid-State and Solution Structures, Thermolysis, and Chalcogen Exchange Reactions. *Inorg. Chem.* **2018,** *57* (12), 7129-7141.
88. Andrez, J.; Pecaut, J.; Scopelliti, R.; Kefalidis, C. E.; Maron, L.; Rosenzweig, M. W.; Meyere, K.; Mazzanti, M., Synthesis and reactivity of a terminal uranium(IV) sulfide supported by siloxide ligands. *Chem. Sci.* **2016,** *7* (9), 5846-5856.
89. Arnold, P. L.; Puig-Urrea, L.; Wells, J. A. L.; Yuan, D.; Cruickshank, F. L.; Young, R. D., Applications of boroxide ligands in supporting small molecule activation by U(III) and U(IV) complexes. *Dalton Trans.* **2019,** *48* (15), 4894-4905.
90. Arnold, P. L.; Stevens, C. J.; Bell, N. L.; Lord, R. M.; Goldberg, J. M.; Nichol, G. S.; Love, J. B., Multi-electron reduction of sulfur and carbon disulfide using binuclear uranium(III) borohydride complexes. *Chem. Sci.* **2017,** *8* (5), 3609-3617.
91. Brown, J. L.; Wu, G.; Hayton, T. W., Chalcogen Atom Transfer to Uranium(III): Synthesis and Characterization of $[(R_2N)_3U]_2(\mu\text{-}E)$ and $[(R_2N)_3U]_2(\mu\text{-}\eta^2\text{:}\eta^2\text{-}S_2)$ (R = $SiMe_3$; E = S, Se, Te). *Organometallics.* **2013,** *32* (5), 1193-1198.
92. Camp, C.; Antunes, M. A.; Garcia, G.; Ciofini, I.; Santos, I. C.; Pecaut, J.; Almeida, M.; Marcalo, J.; Mazzanti, M., Two-electron versus one-electron reduction of chalcogens by uranium(III): synthesis of a terminal U(V) persulfide complex. *Chem. Sci.* **2014,** *5* (2), 841-846.
93. Franke, S. M.; Heinemann, F. W.; Meyer, K., Reactivity of uranium(IV) bridged chalcogenido complexes U(IV)-E-U(IV) (E = S, Se) with elemental sulfur and selenium: synthesis of polychalcogenido-bridged uranium complexes. *Chem. Sci.* **2014,** *5* (3), 942-950.
94. Gardner, B. M.; King, D. M.; Tuna, F.; Wooles, A. J.; Chilton, N. F.; Liddle, S. T., Assessing crystal field and magnetic interactions in diuranium-μ-chalcogenide triamidoamine complexes with U(IV)-E-U(IV) cores (E = S, Se, Te): implications for determining the presence or absence of actinide-actinide magnetic exchange. *Chem. Sci.* **2017,** *8* (9), 6207-6217.
95. Constable; Housecroft, The Early Years of 2,2'-Bipyridine—A Ligand in Its Own Lifetime. *Molecules.* **2019,** *24* (21).
96. Kaes, C.; Katz, A.; Hosseini, M. W., Bipyridine: The Most Widely Used Ligand. A Review of Molecules Comprising at Least Two 2,2'-Bipyridine Units. *Chem. Rev.* **2000,** *100* (10), 3553-3590.
97. Antunes, M. A.; Pereira, L. C. J.; Santos, I. C.; Mazzanti, M.; Marçalo, J.; Almeida, M., $[U(Tp^{Me2})_2(bipy)]^+$: A Cationic Uranium(III) Complex with Single-Molecule-Magnet Behavior. *Inorg. Chem.* **2011,** *50* (20), 9915-9917.
98. Arnaudet, L.; Bougon, R.; Buu, B.; Lance, M.; Nierlich, M.; Vigner, J., Interaction between Uranium(V) and -(VI) Fluorides and Nitrogen Bases. Characterization and Crystal Structures of the Dimorphic Adduct UF_5(bipy) (bipy = 2,2'-Bipyridyl). *Inorg. Chem.* **1994,** *33* (20), 4510-4516.
99. Berthet, J.-C.; Thuéry, P.; Ephritikhine, M., Thorocene adducts of the neutral 2,2′-bipyridine and its radical anion. Synthesis and crystal structures of [Th(η^8-

$C_8H_8)_2(\kappa^2$-bipy)] and [Th(μ-η^8:η^5-$C_8H_8)_2(\kappa^2$-bipy)K$(py)_2]_\infty$. *Comptes. Rendus. Chimie.* **2014,** *17* (6), 526-533.
100. Diaconescu, P. L.; Cummins, C. C., Radical anionic versus neutral 2,2′-bipyridyl coordination in uranium complexes supported by amide and ketimide ligands. *Dalton Trans.* **2015,** *44* (6), 2676-2683.
101. Duval, P. B.; Burns, C. J.; Clark, D. L.; Morris, D. E.; Scott, B. L.; Thompson, J. D.; Werkema, E. L.; Jia, L.; Andersen, R. A., Synthesis and Structural Characterization of the First Uranium Cluster Containing an Isopolyoxometalate Core. *Angew. Chemie. Int. Ed.* **2001,** *40* (18), 3357-3361.
102. Fortier, S.; Veleta, J.; Pialat, A.; Le Roy, J.; Ghiassi, K. B.; Olmstead, M. M.; Metta-Magaña, A.; Murugesu, M.; Villagrán, D., [U$(bipy)_4$]: A Mistaken Case of U^0? *Chem. Eur. J.* **2016,** *22* (6), 1931-1936.
103. Haiges, R.; Vasiliu, M.; Dixon, D. A.; Christe, K. O., The Uranium(VI) Oxoazides [$UO_2(N_3)_2\cdot CH_3CN$], [$(bipy)_2(UO_2)_2(N_3)_4$], [$(bipy)UO_2(N_3)_3]^-$, [$UO_2(N_3)_4]^{2-}$, and [$(UO_2)_2(N_3)_8]^{4-}$. *Chem. Eur. J.* **2017,** *23* (3), 652-664.
104. Maria, L.; Domingos, Â.; Galvão, A.; Ascenso, J.; Santos, I., The Role of Neutral Coligands on the Stabilization of Mono-Tp^{iPr2}U(III) Complexes. *Inorg. Chem.* **2004,** *43* (20), 6426-6434.
105. Mehdoui, T.; Berthet, J.-C.; Thuéry, P.; Salmon, L.; Rivière, E.; Ephritikhine, M., Lanthanide(III)/Actinide(III) Differentiation in the Cerium and Uranium Complexes [M$(C_5Me_5)_2(L)]^{0,+}$ (L=2,2′-Bipyridine, 2,2′:6′,2″-Terpyridine): Structural, Magnetic, and Reactivity Studies. *Chem. Eur. J.* **2005,** *11* (23), 6994-7006.
106. Rivière, C.; Nierlich, M.; Ephritikhine, M.; Madic, C., Complexation Studies of Iodides of Trivalent Uranium and Lanthanides (Ce and Nd) with 2,2‘-Bipyridine in Anhydrous Pyridine Solutions. *Inorg. Chem.* **2001,** *40* (17), 4428-4435.
107. Wiley, R. O.; Von Dreele, R. B.; Brown, T. M., Synthesis, characterization, and molecular structure of tetraethylammonium pentakis(isothiocyanato)bis(2,2'-bipyridine)uranate(IV). *Inorg. Chem.* **1980,** *19* (11), 3351-3356.
108. Yang, P.; Zhou, E.; Fang, B.; Hou, G.; Zi, G.; Walter, M. D., Preparation of (η^5-$C_5Me_5)_2$Th(bipy) and Its Reactivity toward Small Molecules. *Organometallics.* **2016,** *35* (12), 2129-2139.
109. Raper, E. S., Complexes of heterocyclic thionates .1. Complexes of monodentate and chelating ligands. *Coord. Chem. Rev.* **1996,** *153*, 199-255.
110. Raper, E. S., Complexes of heterocyclic thionates .2. complexes of bridging ligands. *Coord. Chem. Rev.* **1997,** *165*, 475-567.
111. Umakoshi, K.; Sasaki, Y., Quadruply Bridged Dinuclear Complexes of Platinum, Palladium, and Nickel. *Advances in Inorganic Chemistry*. 1993; pp 187-239.
112. Arnaiz, F. J.; Aguado, R.; Pedrosa, M. R.; Maestro, M. A., Dioxomolybdenum(VI) thionates: molecular structure of dioxobis(pyridine-2-thiolate-N,S)molybdenum(VI). *Polyhedron.* **2004,** *23* (4), 537-543.
113. Becker, E.; Mereiter, K.; Schmid, R.; Kirchner, K., Facile S-S bond activation of alkyl and aryl disuffides by [$RuCp(CH_3CN)_3]^+$: Formation of dinuclear Ru(III)-Ru(III) complexes with bridging thiolate ligands. *Organometallics.* **2004,** *23* (12), 2876-2883.
114. Begum, N.; Kabir, S. E.; Hossain, G. M. G.; Rahman, A. F. M. M.; Rosenberg, E., Investigations of pyridine-2-thiol as a ligand: Synthesis and X-ray structures of the mixed Mo-Mn dinuclear complex $CpMoMn(CO)_3(\mu$-$CO)(\mu$-η^2-pyS)(μ-η^1-pyS), the electron-deficient trimolybdenum cluster $CP_3Mo_3(\mu$-$CO)_2(\mu$-

S)(μ_3-S)(μ-η^2-NC_5H_4), and the mononuclear $CpMo(CO)_2$(μ-η^2-pyS). *Organometallics.* **2005,** *24* (2), 266-271.
115. Castillo, A.; Barea, G.; Esteruelas, M. A.; Lahoz, F. J.; Lledos, A.; Maseras, F.; Modrego, J.; Onate, E.; Oro, L. A.; Ruiz, N.; Sola, E., Thermally activated site exchange and quantum exchange coupling processes in unsymmetrical trihydride osmium compounds. *Inorg. Chem.* **1999,** *38* (8), 1814-1824.
116. Chadwick, S.; Englich, U.; Senge, M. O.; Noll, B. C.; Ruhlandt-Senge, K., Novel structural principles in magnesium thiolate chemistry: Monomers, trimers, and the first magnesiate thiolate. *Organometallics.* **1998,** *17* (14), 3077-3086.
117. Chen, D. F.; Scopelliti, R.; Hu, X. L., Synthesis and Reactivity of Iron Acyl Complexes Modeling the Active Site of [Fe]-Hydrogenase. *J. Am. Chem. Soc.* **2010,** *132* (3), 928-929.
118. Halder, P.; Ghorai, S.; Banerjee, S.; Mondal, B.; Rana, A., Iron(II) complexes of 2-mercaptopyridine as rubredoxin site analogues. *Dalton Trans.* **2017,** *46* (40), 13739-13744.
119. Hamaguchi, T.; Doud, M. D.; Hilgar, J.; Rinehart, J. D.; Kubiak, C. P., Competing ferro- and antiferromagnetic interactions in a hexagonal bipyramidal nickel thiolate cluster. *Dalton Trans.* **2016,** *45* (6), 2374-2377.
120. Han, Z. J.; Shen, L. X.; Brennessel, W. W.; Holland, P. L.; Eisenberg, R., Nickel Pyridinethiolate Complexes as Catalysts for the Light-Driven Production of Hydrogen from Aqueous Solutions in Noble-Metal-Free Systems. *J. Am. Chem. Soc.* **2013,** *135* (39), 14659-14669.
121. Jung, O. S.; Lee, Y. A.; Kim, Y. T.; Chae, H. K., An organometallic mercaptopyridine complex with unusual bond shift fluxionality: metal-mediated tautomerism of (pentamethylcyclopentadienyl)bis(pyridine-2-thiolato)rhodium(III). *Inorg. Chim. Acta.* **2000,** *299* (1), 100-103.
122. Kitano, K.; Tanaka, R.; Kimura, T.; Tsuda, T.; Shimizu, S.; Takagi, H.; Nishioka, T.; Shiomi, D.; Ichimura, A.; Kinoshita, I.; Isobe, K.; Ooi, S., Lantern-type dinuclear Cr(III)Pt(II) and V(IV)Pt(II) complexes bridged by pyridine-2-thiolate. Synthesis and characterization. *J. Chem. Soc., Dalton Trans.* **2000,** (6), 995-1000.
123. Lobana, T. S.; Paul, S.; Castineiras, A., Pyridine-2-thione derivatives of silver(I) and mercury(II): crystal structures of dimeric [bis(diphenylphosphino)methane][(1-oxopyridine-2-thionato)silver(I), [2-(benzylsulfanyl)pyridine 1-oxide]dichloromercury(II) and phenyl(pyridine-2-thionato)mercury(II). *J. Chem. Soc., Dalton Trans.* **1999,** (11), 1819-1824.
124. Nakayama, Y.; Miyamoto, K.; Ueyama, N.; Nakamura, A., Synthesis, structure and catalytic activity of a seven-coordinate titanium(IV) tris(pyridine-2-thiolate) complex. *Chem. Lett.* **1999,** (5), 391-392.
125. Seino, H.; Yoshikawa, T.; Hidai, M.; Mizobe, Y., Preparation of mononuclear and dinuclear Rh hydrotris(pyrazolyl)borato complexes containing arenethiolato ligands and conversion of the mononuclear complexes into dinuclear Rh-Rh and Rh-Ir complexes with bridging arenethiolato ligands. *Dalton Trans.* **2004,** (21), 3593-3600.
126. Shpakovsky, D. B.; Banti, C. N.; Beaulieu-Houle, G.; Kourkoumelis, N.; Manoli, M.; Manos, M. J.; Tasiopoulos, A. J.; Hadjikakou, S. K.; Milaeva, E. R.; Charalabopoulos, K.; Bakas, T.; Butler, I. S.; Hadjiliadis, N., Synthesis, structural characterization and in vitro inhibitory studies against human breast cancer of the bis-(2,6-di-tert-butylphenol)tin(IV) dichloride and its complexes. *Dalton Trans.* **2012,** *41* (48), 14568-14582.

127. Sie, W. S.; Jian, J. Y.; Su, T. C.; Lee, G. H.; Lee, H. M.; Shiu, K. B., Synthesis, structures, and properties of iridium(III) bis-cyclometallated complexes containing three-atom chelates. *J. Organomet. Chem.* **2008,** *693* (8-9), 1510-1517.
128. Sousa Pedrares, A.; Teng, W.; Ruhlandt-Senge, K., Syntheses and structures of magnesium pyridine thiolates--model compounds for magnesium binding in photosystem I. *Chemistry.* **2003,** *9* (9), 2019-24.
129. Takashima, Y.; Nakayama, Y.; Hashiguchi, M.; Hosoda, T.; Yasuda, H.; Hirao, T.; Harada, A., Syntheses of group 4 transition metal complexes bearing 2-pyridinethiolate ligands and their catalytic activities for ethylene polymerization. *Polymer.* **2006,** *47* (16), 5762-5774.
130. Umakoshi, K.; Misasa, N.; Ohtsu, C.; Kojima, T.; Sokolov, M.; Wakeshima, M.; Hinatsu, Y.; Onishi, M., Unusual magnetic properties of the edge-sharing bioctahedral dirhenium(IV) complex of pyridine2-thiolate. *Angew. Chem. Int. Ed.* **2005,** *44* (5), 720-724.
131. Wang, H.; Guo, X. Q.; Zhong, R.; Lin, Y. J.; Zhang, P. C.; Hou, X. F., Reactions of half-sandwich rhodium(III) and iridium(III) compounds with pyridinethiolate ligands: Mono-, di-, and tri-nuclear complexes. *J. Organomet. Chem.* **2009,** *694* (20), 3362-3368.
132. Zhang, P. C.; Wang, H.; Liu, S.; Guo, X. Q.; Hou, X. F., Reactions of 2-pyridinethiolate cobalt(III) complexes with pyridinethiolate or benzenethiolate ligands. *J. Organomet. Chem.* **2008,** *693* (17), 2903-2906.
133. Berardini, M.; Brennan, J., Europium Pyridinethiolates - Synthesis, Structure, and Thermolysis. *Inorg. Chem.* **1995,** *34* (24), 6179-6185.
134. Berardini, M.; Lee, J. S.; Freedman, D.; Lee, J.; Emge, T. J.; Brennan, J. G., Early-and late-lanthanide pyridinethiolates: Synthesis, redox stability, and structure. *Inorg. Chem.* **1997,** *36* (25), 5772-5776.
135. Lee, J. S.; Emge, T. J.; Brennan, J. G., Heterometallic lanthanide - Group 14 metal chalcogenolates. *Inorg. Chem.* **1997,** *36* (22), 5064-5068.
136. Lopes, I.; Hillier, A. C.; Liu, S. Y.; Domingos, A.; Ascenso, J.; Galvao, A.; Sella, A.; Marques, N., Solid-state structure and solution behavior of eight-coordinate Sm(III) poly(pyrazolyl)-borate compounds. *Inorg. Chem.* **2001,** *40* (6), 1116-1125.
137. Mashima, K.; Shibahara, T.; Nakayama, Y.; Nakamura, A., Synthesis and Characterization of Cationic Pyridine-2-Thiolate Complexes of Lanthanoid(Iii) - Crystal-Structures of Pentagonal Bipyramidal $[Ln(SC_5H_4N)_2(hmpa)_3]I$ (Ln=Sm, Yb, Hmpa=Hexamethylphosphoric Triamide). *J. Organomet. Chem.* **1995,** *501* (1-2), 263-269.
138. Mashima, K.; Shibahara, T.; Nakayama, Y.; Nakamura, A., Mononuclear η^8-cyclooctatetraenyl(thiolato)samarium(III) complexes $(\eta^8\text{-}C_8H_8)Sm(SR)(hmpa)_2$ (R = 2,4,6-triisopropylphenyl and 2-pyridyl; HMPA = hexamethylphosphoric triamide) derived from metallic samarium, diaryl disulfide, and 1,3,5,7-cyclooctatetraene in the presence of HMPA. *J. Organomet. Chem.* **1998,** *559* (1-2), 197-201.
139. Mironova, O. A.; Sukhikh, T. S.; Konchenko, S. N.; Pushkarevsky, N. A., Synthesis, structural and IR spectral studies of lanthanide (Nd, Sm) phenyl- and 2-pyridylthiolates supported by bulky 2,6-diisopropylphenyl substituted beta-diketiminate ligand. *Polyhedron.* **2019,** *159*, 337-344.
140. Antunes, M. A.; Dias, M.; Monteiro, B.; Domingos, A.; Santos, I. C.; Marques, N., Synthesis and reactivity of uranium(IV) amide complexes supported by a triamidotriazacyclononane ligand. *Dalton Trans.* **2006,** (27), 3368-3374.

141. Rose, D.; Chang, Y. D.; Chen, Q.; Zubieta, J., Reactions of Uranyl Thiolate Complexes with Molecular-Oxygen - Syntheses and Crystal and Molecular-Structures of the Uranyl Thiolate Peroxo Species $(HNEt_3)_2[(UO_2)_2(O_2)(SC_4N_2H_3)_4]$ and $(HNEt_3)[H(UO_2)_2(O_2)(SC_4N_2H_2Me)_4]\cdot Me_2CO\cdot 0.5Et_3N$ and of the Uranyl Thiolate Oxo Cluster $(HNEt_3)_2[(UO_2)_4(O)_2(SC_5NH_4)_6]\cdot Me_2CO$. *Inorg. Chem.* **1994,** *33* (23), 5167-5168.
142. Rose, D. J.; Chen, Q.; Zubieta, J., Synthesis and characterization of uranyl thiolate complexes. Crystal and molecular structures of $[Me_4N][UO_2(NO_3)_2(C_5H_4NS)]$ and $[C_{16}H_{25}N_2S_2Si_2][UO_2(NO_3)_2(C_8H_{12}NSSi)]$. *Inorg. Chim. Acta.* **1998,** *268* (1), 163-167.
143. Delhaes, P., *Graphite and Precursors*. First Edition ed.; Taylor & Francis: London, 2000; p 312 pages.
144. Berthet, J.-C.; Thuéry, P.; Ephritikhine, M., New Efficient Synthesis of $[UI_4(MeCN)_4]$. X-ray Crystal Structures of $[UI_2(MeCN)_7][UI_6]$, $[UI_4(py)_3]$, and $[U(dmf)_9]I_4$. *Inorg. Chem.* **2005,** *44* (4), 1142-1146.
145. Romanelli, M.; Kumar, G. A.; Emge, T. J.; Riman, R. E.; Brennan, J. G., Intense Near-IR Emission from Nanoscale Lanthanoid Fluoride Clusters. *Angew. Chemie. Int. Ed.* **2008,** *47* (32), 6049-6051.
146. Dorn, H.; Murphy, E. F.; Shah, S. A. A.; Roesky, H. W., Organometallic fluorides of the lanthanide and actinide elements. *Journal of Fluorine Chemistry* **1997,** *86* (2), 121-125.

Chapter 3: Tetrametallic Thorium Compounds with Th_4E_4 (E = S, Se) Cubane Cores

3.1 Introduction

Cluster chemistry allows for the study of size dependent properties of compounds with varying numbers of metal cations, which allows us to link the physical properties of molecules with those of solid-state compounds.[1, 2] Clusters with covalent main group[3-14] and transition metal ions[4, 15-21] have been used to probe structure-property relationships,[22-27] and related lanthanide cluster chemistry[28-40] has been gaining traction over the past two decades. However, the study of analogous actinide cluster chemistry is less developed compared to the synthesis of transition metal and rare-earth metal clusters. This is expected to be particularly challenging, given the complicated nature of the bonding in actinide compounds.

Throughout its history, actinide cluster chemistry[41-49] has been dominated by the structural and reactivity studies of oxygen containing anions in uranium clusters,[50-58] including the study of compounds with uranyl functionalities,[59-63] and many tetrameric and higher hydroxide- or oxide-bridging actinide (including uranyl oxido) compounds.[52, 64-80] Meanwhile, oxide clusters of thorium are less explored.[53, 56, 57] Actinide cluster chemistry with less electronegative anions[81-87] is even more limited. There exists a handful of uranium clusters with chalcogenido (E^{2-}; E = S, Se) anions,[88-90] including a uranium selenido cubane, $(py)_8U_4Se_4(SePh)_8$,[91] and sulfido double cubane, $[U((\mu_3\text{-}S)_4U_3(SPS^{Me})_3(BH_4)_3)_2]$.[92] Altogether, there are a number of dimers,[81, 93-98] 3 trimers,[88, 89, 99] one tetramer,[91] one hexamer,[100] and a heptomer,[101] all with U(IV) connected by E^{2-}.

The M_4E_4 cubane framework is a recurring structural motif in inorganic chemistry that incorporates a wide range of metals from every part of the periodic chart bridged by various anions.[102-110] These cubane structures are involved in a wide range of important processes,[111] from the active site of photosynthesis[112, 113] and as catalysts[114-116] in water splitting,[117] to low temperature CVD synthesis of novel solid-state phases.[118, 119] Analogous f-block metal cubanes are relatively scarce,[39, 120-131] with a number of compounds built with hydroxide frameworks.[132-136] There are even reports of lanthanide clusters with less electronegative ligand systems,[121, 125, 137-139] and the two previously mentioned uranium structures with cubane motifs.[91, 92] Outlined in this chapter is the description of the first exploration of thorium cubane compounds with stabilizing terminal fluorinated ligands.[140]

Incorporation of fluorinated ligands[141-146] into multimetallic rare earth and actinide clusters is intended to increase product solubility which can potentially lead to the synthesis of larger clusters, or to facilitate spectroscopic studies in solution. In the study of lanthanide clusters, heteroleptic EPh/EC_6F_5 (E = S, Se) ligand combinations have been used to synthesize hydrocarbon soluble polymetallic products with E^{2-} and EC_6F_5 ligands.[147] EPh ligands bound to electropositive metals will reduce elemental E to form E^{2-} that bridge the metal cations, as the accompanying oxidation of EPh yields PhEEPh as a side product to the accompanying cluster. Due to inductive stabilization of the negative charge on the fluorinated phenyl ring, similar activity is not observed with EC_6F_5 ligands, as they remain terminally bound to the metal cation. This difference in reactivity can be used to generate polynuclear metal chalcogenide compounds with ancillary EC_6F_5. Fluorinated EC_6F_5 ligands are utilized to explore the stabilization of heterochalogen clusters of the actinides where each actinide cation is bound to sulfur and selenium.

Few heterochalcogen coordination complexes are known,[148-150] with this work employing fluorinated chalcogenolate ligands to synthesize the first known heterochalcogen actinide clusters,[140] informing subsequent actinide heterochalcogen cluster studies.[151, 152]

This chapter outlines the synthesis and characterization of a series of thorium cubanes that have both EPh and EC_6F_5 ligands. The impact of ring fluorination on chalcogen-metal binding affinity is evident, and solution NMR experiments indicate that the well-defined solid-state structures are maintained in solution.

3.2 Results and discussion

Thorium metal is oxidized by a mixture of PhEEPh and $C_6F_5E'E'C_6F_5$ (E, E'= S, Se) in pyridine to give soluble monomeric Th(IV) tetrachalcogenolates "$Th(EPh)_x(E'C6F5)_{4-x}$". With a 3:1 EPh:$E'C_6F_5$ ratio, addition of elemental E to these in-situ prepared solutions of "$Th(EPh)_x(E'C_6F_5)_{4-x}$" leads to ligand based redox reactions in either pyridine or pyridine/toluene mixtures (Figure 3.1).

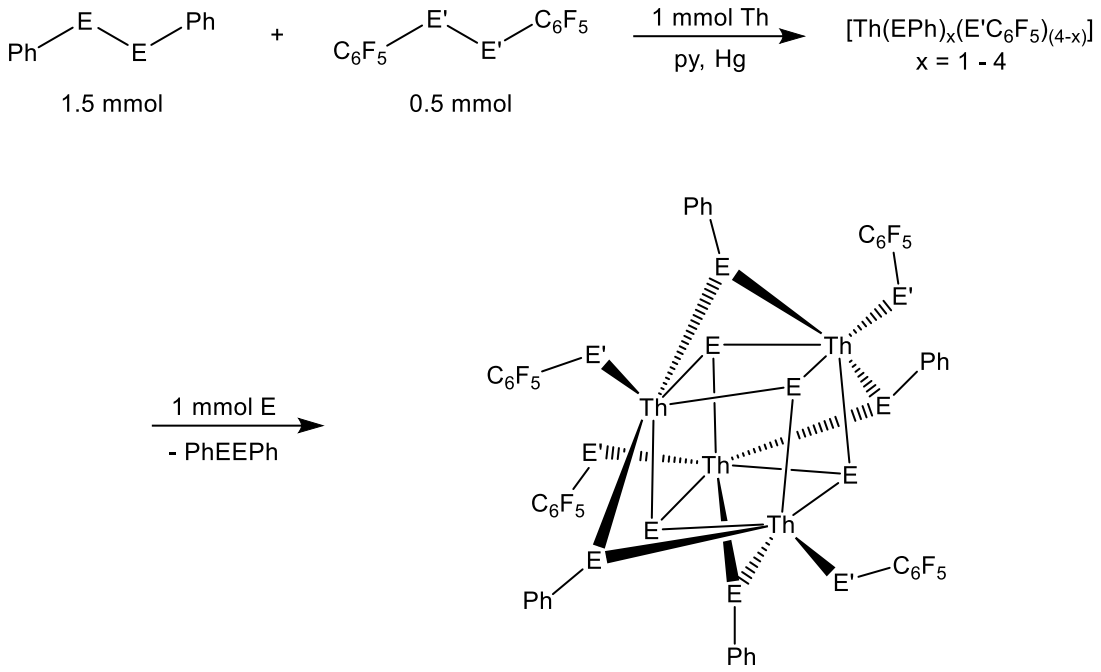

Figure 3.1 Synthesis of the series of $(py)_8Th_4(\mu_3\text{-}E)_4(\mu_2\text{-}EPh)_4(E'C_6F_5)_4$ (E, E' = S, Se) with py removed for clarity.

Elemental E is reduced to E^{2-} as EPh^- is oxidized to PhEEPh, with $E'C_6F_5$ remaining negatively charged, leading to the isolation of $(py)_8Th_4E_4(EPh)_4(E'C_6F_5)_4$ (Reaction 1). Trace elemental Hg acts as a catalyst reducing the time required for all Th to be consumed. While these ligand based redox reactions were initially targeted to give cubanes with all possible combinations of S, Se at the E, EPh, and $E'C_6F_5$ ligand sites, it is only when E = E(Ph) that ordered compounds were consistently isolated. Reactions where elemental E ≠ E(Ph) either revealed mixed ratios of S and Se in each of the four (μ_3-E^{2-}) sites, or no reaction upon addition of elemental E to intermediate "$Th(SPh)_x(SC_6F_5)_{4-x}$". In the case where elemental Se was added to intermediate "$Th(SPh)_x(SC_6F_5)_{4-x}$", the elemental Se stayed as a darker precipitate after stirring and without color change, as elemental Se is a poor oxidant compared to S.[153] In the case where elemental S is added to intermediate "$Th(SePh)_x(SeC6F5)_{4-x}$", ligand based redox reaction occurred where elemental S is reduced to S^{2-}. Alkyl

migration yields a source of Se^{2-} from $Se(Ph)^{-}$, and reveals a variable ratio of S:Se in the four (μ_3-E^{2-}) sites of the cubane core.

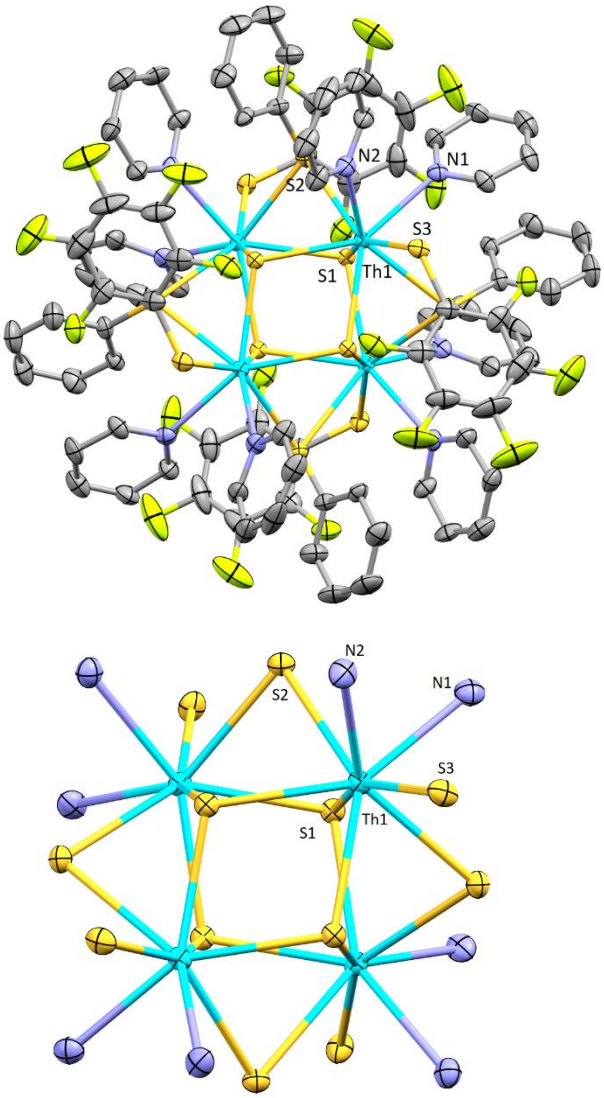

Figure 3.2 (Top) Thermal ellipsoid diagram of $py_8Th_4S_4(\mu_2\text{-}SPh)_4(SC_6F_5)_4$ (**7**), with light green F, yellow S, light blue Th, purple N, gray C, H atoms removed for clarity, and ellipsoids at the 50% probability level. The view is of the top region of the cubane core. (Bottom) Diagram of the cubane core region of **7** in the same orientation as the top figure.

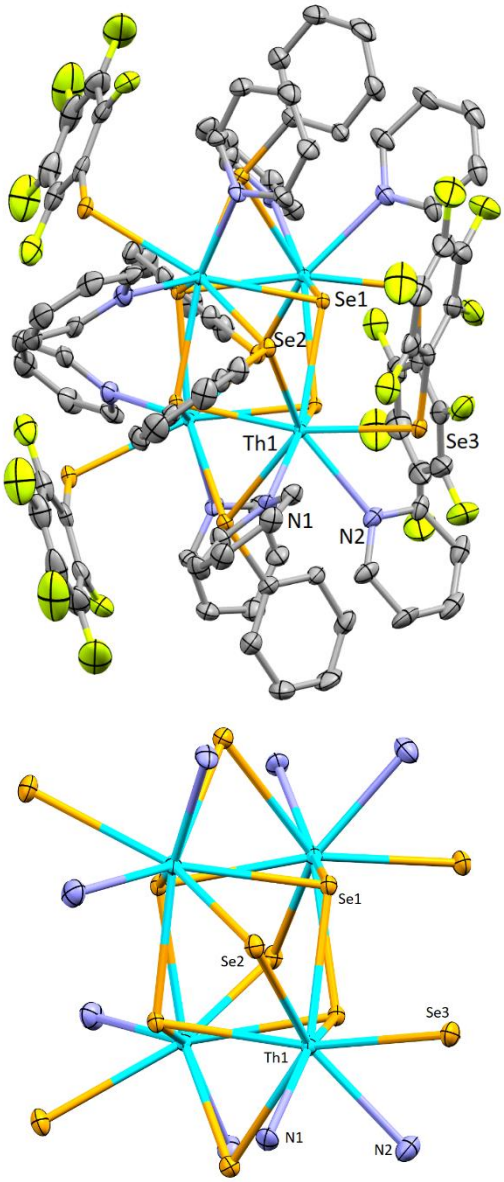

Figure 3.3 (Top) Thermal ellipsoid diagram of $py_8Th_4Se_4(\mu_2\text{-}SePh)_4(SeC_6F_5)_4$ (**8**), with light green F, orange Se, light blue Th, purple N, gray C, H atoms removed for clarity, and ellipsoids at the 50% probability level. The view is of the side of the cubane core. (Bottom) Diagram of the cubane core region of **8** in the same orientation as the top figure.

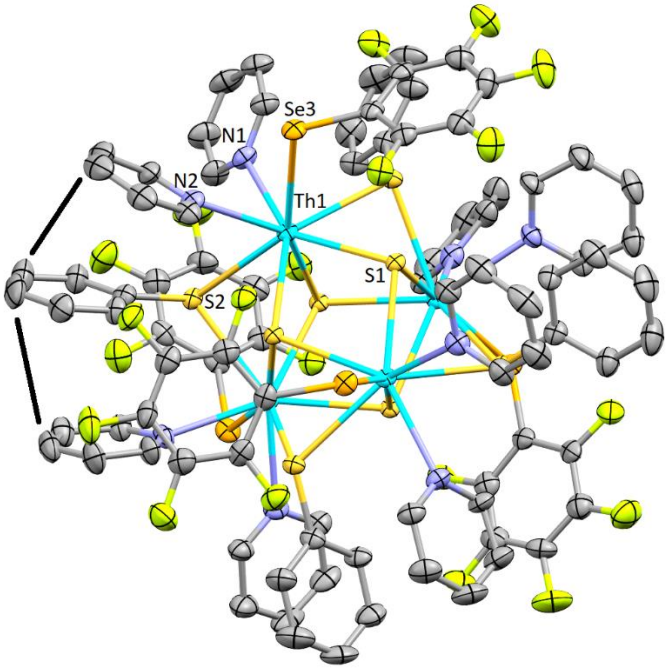

Figure 3.4 Thermal ellipsoid diagram of $py_8Th_4S_4(\mu_2\text{-}SPh)_4(SeC_6F_5)_4$ (**9**), with light green F, yellow S, orange Se, light blue Th, purple N, gray C, H atoms removed for clarity, and ellipsoids at the 50% probability level. Black lines indicate possible π…π interactions between nearest neighboring pyridine and phenyl groups for **7** – **10.**

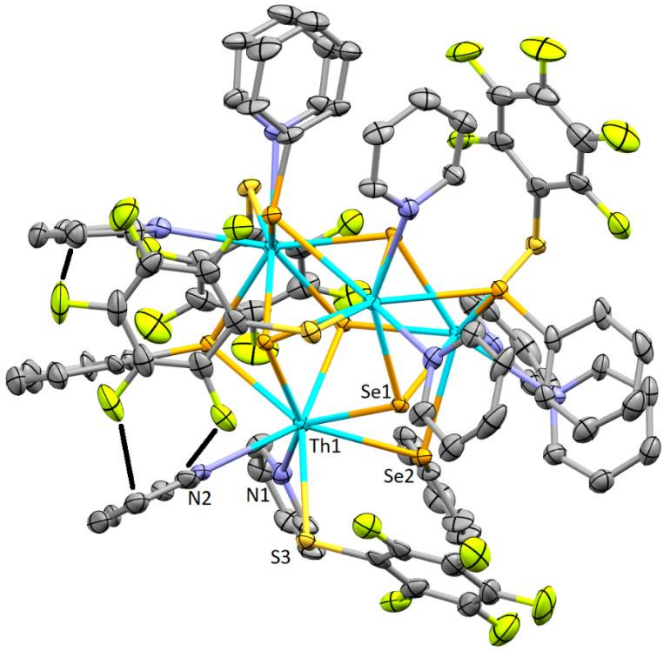

Figure 3.5 Thermal ellipsoid diagram of $py_8Th_4S_4(\mu_2\text{-}SPh)_4(SeC_6F_5)_4$ (**10**), with light green F, yellow S, orange Se, light blue Th, purple N, gray C, H atoms removed for clarity, and ellipsoids at the 50% probability level. The pyridine and fluorinated phenyl groups most likely to engage in H-bonding interactions between adjacent C(H) and F atoms (broken lines) for **7**-**10**.

Table 3.1 Summary of Crystallographic Details for **7** – **10**.

compound	**7**	**8**	**9**	**10**
empirical formula	C_{98} H_{70} $F_{20}N_{10}S_{12}Th_4$	C_{98} H_{70} $F_{20}N_{10}Se_{12}Th_4$	C_{98} H_{70} $F_{20}N_{10}$ S_8 Se_4Th_4	C_{98} H_{70} $F_{20}N_{10}$ S_4 Se_8Th_4
fw	3080.52	3643.32	3268.12	3455.72
space group (No.)	I-4 (82)	I-4 (82)	I-4 (82)	I-4 (82)
a (Å)	20.059(1)	20.376(8)	20.248(1)	20.366(2)
V (Å^3)	5040.2(6)	5209.6(10)	5128.3(6)	5211.6(13)
Z	2	2	2	2
D(calcd) (g/cm^{-3})	2.030	2.323	2.116	2.202
temperature (°K)	120(2)	100(2)	120(2)	120(2)
λ (Å)	0.71073	0.71073	0.71073	0.71073
abs coeff (mm^{-1})	6.221	9.971	7.452	8.650
R(F)[a] [I > 2 σ(I)]	0.0316	0.0357	0.0298	0.0353
$R_w(F^2)$[b] [I > 2 σ(I)]	0.0673	0.0705	0.0680	0.0708

Definitions: [a] $R(F) = \Sigma||F_o| - |F_c||/\Sigma|F_o|$; [b] $R_w(F^2) = [\Sigma[w(F_o^2 - F_c^2)^2]/\Sigma[w(F_o^2)^2]]^{1/2}$

Figures 3.2-3.5 show the POVRAY diagrams of the molecular structures of **7** - **10** from a variety of orientations, with relevant bond lengths and angles given in Table 3.2. The individual cluster molecules in **7** – **10** have a site symmetry of is S_4, with a central Th_4E_{12} core region [$Th_4(\mu_3\text{-}E)_4(\mu_2\text{-}E)_4(E')_4$] surrounded by 16 aromatic rings from EPh, E'C_6F_5, and pyridine, yielding four different types of ligands in the series of compounds. The shape of the "cubane" portion $Th_4(\mu_3\text{-}E)_4$ of the core is not perfectly cubic, with elongated (e.g., "diamond" shaped, as in Figure 3.2 bottom) top and bottom Th_2E_2 facets and four regular (e.g., more "square" shaped, Figure 3.3 bottom) side Th_2E_2 facets. An isomorphous uranium cubane, $(py)_8U_4Se_4(SePh)_8$, has been described and exhibits the same core motif as **7** - **10**.[91] The elongated top and

bottom facets of the cubane have diagonal Th…Th distances of ~4.6 Å, as summarized in Table 3.2 for **7** - **10**. The square-shaped sides have closer Th…Th distances to each other of about 4.0 Å. The three Th-μ_3E bonds are also inequivalent, with shorter legs to the sides (2.775(2) Å in **7**, 2.782(1) Å in **9** for Th-S and 2.902(1) Å in **8**, 2.909(1) Å in **10** for Th-Se) compared to the top (2.832(2), 2.838(2) Å in **7**; 2.838(1), 2.850(1) Å in **9** for Th-S and 2.950(1), 2.977(1) Å in **8**; 2.960(1), 2.971(1) Å in **10** for Th-Se), suggesting some relief of strain in the top/bottom Th_2E_2 facets.

Table 3.2 Selected Distances (Å), and Angles (°) for **7** – **10**.

Bond/Angle	**7** (E,E'=S, S)	**8** (E,E'=Se, Se)	**9** (E,E'=S, Se)	**10** (E,E'=Se, S)
Th-N	2.644(6), 2.696(7)	2.641(8), 2.694(8)	2.647(6), 2.705(6)	2.670(9), 2.708(9)
Th-μ_3E *(side)*	2.775(2)	2.902(1)	2.782(1)	2.909(1)
Th-μ_3E *(top)*	2.832(2), 2.838(2)	2.950(1), 2.977(1)	2.838(1), 2.850(1)	2.960(1), 2.971(1)
Th-E'(C_6F_5)	2.904(2)	3.020(1)	3.030(1)*	2.899(2)
Th-E(Ph)	2.973(2), 2.982(2)	3.080(1), 3.088(1)	2.977(2), 2.985(2)	3.081(1), 3.096(1)
Th…Th *(side)*	4.024(<1)	4.154(<1)	4.017(<1)	4.173(<1)
Th…Th *(top)*	4.543(<1)	4.748(<1)	4.573(<1)	4.758(<1)
E'-C(E'C_6F_5)	1.738(8)	1.892(11)	1.886(11)*	1.767(12)
E-C(EPh)	1.780(8)	1.919(10)	1.776(7)	1.936(11)
Th- μ_3E-Th *(side)*	91.57(5), 91.71(5)	89.91(3), 90.46(2)	91.00(4), 91.25(4)	90.42(3), 90.62(3)
Th- μ_3E-Th *(top)*	107.45(6)	106.47(3)	107.04(5)	106.71(3)
Th-E(Ph)-Th *(side)*	85.01(5)	84.68(3)	84.71(4)	84.99(3)
Th-E'-C(E'C_6F_5)	110.4(3)	108.1(3)	108(2)*	110.3(3)
Th-E-C(EPh)	116.5(3), 119.2(3)	115.4(3), 117.3(3)	116.4(2), 119.6(2)	115.0(3), 116.4(3)

* Average of two parts for minor SeC_6F_5 site disorder in compound **3**.

All bond distances in Table 3.2 are consistent with values reflecting the sizes of the atomic/ionic components, and with several examples of similar structures found in the Cambridge Structural Database.[154] The range of Th-N bond lengths here (2.641(8) – 2.708(9) Å), is consistent with previously reported Th-N(pyridine) bond lengths, i.e. 2.624(3) – 2.718(5) Å for monomeric $(py)_xTh(ER)_4$,[155] (x = 3,4; E = S, Se; R = Ph, C_6F_5) and 2.662(8), 2.696(8) Å in cis-$(py)_2Th(OC_6H_3Me_2\text{-}2,6)_4$.[156]

Bonds between thorium and E(R) are also consistent with the literature. The bridging Th-S(Ph) distances in compounds **7** (2.973(2), 2.982(2) Å) and **9** (2.977(2), 2.985(2) Å) are longer than the terminal Th-S distances in monomeric $(py)_4Th(SPh)_4$,[155] (2.8451(6) and 2.8481(6) Å), due to electron density from $S(Ph)^-$ spread between the two thorium cation metal centers. In compounds **8** and **10** the Th-μ_2Se(Ph) bond lengths are 3.080(1), 3.088(1) Å and 3.081(1), 3.096(1) Å respectively, and due to an increase in ligand repulsions in eight-coordinate sites in the thorium tetramers, they are slightly longer than the Th-Se distances in the monomeric selenolate derivative $(py)_3Th(SePh)_4$[155] which range from 2.9039(6) to 2.9465(6) Å, the 2.938(8) Å terminal Th-Se bond in [η^5-1,2,4-$(Me_3C)_3C_5H_2$]$Th(SePh)_3$(bipy),[157] the 2.918(1) Å bond in [[η^5-1,2,4-$(Me_3C)_3C_5H_2$]$Th(SePh)]_2$[μ-N(p-tolyl)]$_2$[158] or the 2.9317(5) Å bond in $(MeC(N^iPr)_2)_3ThSeCH_2SiMe_3$.[159]

As for bonds to the terminally bound fluorinated ligands, in clusters **7** and **10** the Th-S(C_6F_5) bond lengths are 2.9040(2) Å and 2.899(2) Å respectively, which are significantly longer than the 2.8111(11), 2.8252(10) and 2.8253(10) Å distances in seven coordinate $(py)_3Th_4(SC_6F_5)_4$.[155] The terminal Th-Se(C_6F_5) bond lengths in **8** (3.020(1) Å) and **9** (3.030(1) Å) are also slightly longer than the 2.9519(7), 2.9961(7), 3.0137(7), and 3.0183(7) Å distances in monomeric $(py)_4Th(SeC_6F_5)_4$.[155]

Compounds with comparable bonds between Th(IV) and μ_3-E^{2-} have no precedent – the solid-state literature contains only examples of doubly bridging E^{2-} bound to Th(IV). Nevertheless, in compounds **7** and **9**, the range of Th-μ^3sulfido bond lengths comprising the side Th_2E_2 facets (see Figure 3.3 bottom) at 2.775(2) – 2.782(1) Å, is comparable to the 2.7759(3) Å distance reported for Th-μ_2-S in the layered solid-state structure of $Ba_2Th(S_2)_2S_2$.[160] In clusters **8** and **10**, the range of Th-μ_3-Se bond distances in the elongated top Th_2E_2 facets (Figure 3.2 bottom) is 2.950(1) – 2.971(1) Å, is comparable to the 2.9522(1) Å Th-μ_2-Se value in solid-state $Ba_3ThSe_3(Se_2)_2$.[161] The Th-μ_3E distances in **7** (2.775(1)-2.838(2) Å) and **9** (2.782(1)-2.850(1) Å) are shorter than those in **8** (2.902(1)-2.977(1) Å) and **10** (2.9091(1)-2.971(1)) Å), consistent with the larger ionic radii of Se^{2-} (1.98 Å) versus S^{2-} (1.84Å).[162, 163]

Table 3.3 Selected Distances (Å) for **7** – **10**.

π...π Contact	**7**	**8**	**9**	**10**
py…EPh	3.09(1), 3.28(1)	3.10(1), 3.28(2)	3.10(1), 3.30(1)	3.13(2), 3.29(2)
py-EPh dihedral	8.8(6)	9.4(1)	9.6(5)	6.7(7)
EPh…py'	3.12(1), 3.63(1)	3.16(2), 3.56(2)	3.15(1), 3.65(1)	3.14(2), 3.56(2)
EPh…py' dihedral	16.8(4)	13.9(1)	18.2(4)	13.8(1)
H…F-C	**7**	**8**	**9**	**10**
F(1)…H(17)	2.52	2.54	2.55*	2.51
F(1)…H(15)	2.72	2.71	2.68*	2.78
F(1)…H(14)	2.78	2.69	2.78*	2.70
F(2)…H(26)/H(27)	2.53/2.59	2.71/2.61	2.70/2.59*	3.09/2.83
F(3)…H(14)	2.62	2.64	2.60*	2.70
F(4)…H(16)	2.31	2.26	2.26*	2.35
F(4)…H(19)	2.72	2.82	2.93*	2.79
F(5)…H(18)	2.51	2.62	2.50*	2.64

* Average of two parts for minor SeC_6F_5 site disorder in compound **3**.

In regards to the solid-state structures of similar isomorphous actinide cubanes, the uranium cubane $(py)_8U_4Se_4(SePh)_8$ was found to crystallize in the monoclinic space group C2/c,[91] while the series of thorium cubanes were found to crystallize in various monoclinic unit cells and higher symmetry orthorhombic and tetragonal unit cells.[151] Fluorinated arenes appear to play a significant and consistent role in determining the solid-state structure of **7 - 10** which all crystallize in the same tetragonal I-4 unit cell.

In compounds **7** – **10**, π … π interactions are present, but not involving stacking motifs between molecules in each unit cell, nor involving fluorinated ligands. Typically, ring fluorination often involves favoring lattices that exhibit extensive π… π stacking interactions between molecules in the unit cell, however in the present case, only intramolecular π … π interactions occur, with C_6F_5 in **7 - 10** perpendicular to the neighboring non-fluorinated rings. Within the tetramer, the arrangement of ligands on the closest pair of Th atoms (e.g., Th…Th on the "side", as in Figure 3.3 bottom) is defined by a stack of three adjacent overlapping ligands that appear to engage in close π … π interactions, namely py(N1)…μ_2-EPh and μ_2-EPh…py(N2), as shown in Figure 3.4. The closest inter-planar C…C distances for this triplet of rings (e.g., py…Ph…py) are shown in Table 3.3. The terminal E'C_6F_5 ligand does not appear to engage in π … π interactions but caps the area directly above and perpendicular to the adjacent μ_2-EPh ligand sandwiched between py. All five of the F atoms in C_6F_5 are within 3 Å of the H atoms of nearby py groups sandwiching Ph. The closest of these presumably weak F…H hydrogen-bond interactions are shown in Figure 3.5, including close contact to the disordered py of solvation (Table 3.3). The sum of van der Waals radii of both hydrogen and fluorine

is 2.67 Å,[164] with H…F distances up to about 3.0 Å of note due to weak H…F interactions and concurrent crystal packing.

Compound **9** contains an instance of observed rotational disorder within the region occupied by the SeC_6F_5 ligand, where the compound has a significant mismatch of size for E versus E' atoms (E = S; E' = Se). In contrast, for compound **10**, where E = Se and E' = S, such disorder does not exist. This is apparently consistent with an E'C_6F_5 ligand closer to the core region due to the shorter Th-S bond in **10** versus the longer Th-Se bond in **9** (Table 3.2). With X-ray diffraction data for many samples with this cubane structure, we have never found less than complete occupancy of E'C_6F_5 at the terminal ligand site, and complete occupancy of EPh at the μ_2 bridging site, when the fluorinated ligand was used. Thus, whether the cause is a better match of larger site to larger ligand or a lack of flexibility of the bridging ligand, the E'C_6F_5 is nevertheless a unique terminal ligand site for this series of compounds.

Table 3.4 ^{77}Se NMR Summary. NC_5D_5 solvent used.

Compound	Se^{2-}	μ-SePh	SePh	SeC_6F_5
$Th_4Se_4(\mu SePh)_4(SeC_6F_5)_4$ (**8**)	915	480		369
$Th_4Se_4(\mu SePh)_4(SC_6F_5)_4$ (**10**)	904	479		
$Th(SeC_6F_5)_4$[155]				400
$Th(SePh)_4$[155]			659	
PhSeSePh[165]		456		
$C_6F_5SeSeC_6F_5$				377

Diamagnetic Th provides an opportunity to probe the solution structure of these cubanes. While solid-state structures are consistent throughout the series, alternative structures in solution are always possible, given that larger clusters prepared in weakly basic THF solutions have been shown to fragment in strong

donor solvents such as pyridine.[166] To probe solution structure, ^{77}Se NMR spectroscopy was used because this nucleus has a favorable chemical shift dispersion, and the results were informative even though data from relevant thorium selenolate complexes are limited: ^{77}Se NMR resonances have been measured for $(py)_3Th(SePh)_4$ (659 ppm),[155] $(py)_4Th(SeC_6F5)_4$ (400 ppm),[155] and $(MeC(N^iPr)_2)_3ThSeCH_2SiMe_3$ (221 ppm),[159] the latter having a thorium coordination environment comprised of considerably more electronegative elements and a remarkably acute Th-Se-C angle (81°) that makes comparison with the present work difficult. Cubane **9** was too insoluble to give meaningful data, while **8** and **10** were adequately soluble, and spectra consistent with the tetrametallic structure being maintained in solution (Table 3.4). Cubane **8** has three ^{77}Se resonances: 915 assigned to the bridging μ_3-Se^{2-}, 480 assigned to the bridging μ_2-SePh, and 369 assigned to the terminal (η-SeC_6F_5). Cubane **10** has two ^{77}Se resonances: 904 assigned to the bridging μ_3-Se^{2-}, and 479 assigned to the bridging μ_2-SePh. These peaks can be assigned by comparison with other clusters and molecular chalcogenolates. The peak for **8** at 915 ppm and the peak for **10** at 904 ppm can be attributed to the Se^{2-}, consistent with recently published 992 ppm for $[K(18\text{-crown-6})][Th(Se)(NR_2)_3]$.[87] Similar peaks are absent in the spectra of **7** and **9** with bridging μ_3-S^{2-}, as well as spectra of the two molecular chalcogenolates $(py)_3Th(SePh)_4$ and $(py)_4Th(SeC_6F_5)_4$. The terminal fluorinated selenolate can be assigned to the ^{77}Se resonance at 369 ppm in **8**, given similar the resonance at 400 ppm in molecular $Th(SeC_6F_5)_4$, and noticeably similar to the resonance at 377 ppm for $C_6F_5SeSeC_6F_5$. Finally, resonances for the SePh ligand at 480 ppm in **8** and 479 ppm in **10** are noticeably similar to the resonance at 456 ppm for PhSeSePh, and shifted significantly from the resonance at 659 ppm in $Th(SePh)_4$, where the SePh are all terminally bound. Thus,

bridging μ_2-SePh resonances in **8** and **10** are consistent with SePh ligands bridging metal centers, and data is consistent with the solid-state structures prevailing in solution.

3.3 Conclusion

A group of $(py)_8Th_4E_4(\mu^2\text{-}EPh)_4(E'C_6F_5)_4$ cubane clusters (E = S, Se; E' = S, Se) were prepared for various combinations of E, E' = S, Se, using ligand based redox reactions in which EPh anions reduce elemental E. All four compounds are isostructural, with a number of H…F interactions noted in the solid-state structures. There is a consistent and unique pattern of EPh versus $E'C_6F_5$ ligand positions and dihedrals on going from **7 - 10**, resulting in nearly the same packing arrangement for these $(py)_8Th_4E_4(\mu_2\text{-}EPh)_4(E'C_6F_5)_4$ compounds, regardless of whether E or E' are S or Se. Fluorinated ligands always bind terminally, while the EPh ligands always bridge metal centers. Solution state ^{77}Se NMR measurements suggest that the tetrametallic formulation is retained in pyridine solution.

3.4 References

1. Mesbah, A.; Prakash, J.; Ibers, J. A., Overview of the crystal chemistry of the actinide chalcogenides: incorporation of the alkaline-earth elements. *Dalton Trans.* **2016,** *45* (41), 16067-16080.
2. Simon, A., Discrete and Condensed Clusters - a Link between Molecular and Solid-State Chemistry. *Pure. Appl. Chem.* **1995,** *67* (2), 311-312.
3. Alivisatos, A. P., Perspectives on the physical chemistry of semiconductor nanocrystals. *J. Phys. Chem.* **1996,** *100* (31), 13226-13239.
4. Choi, C. L.; Alivisatos, A. P., From Artificial Atoms to Nanocrystal Molecules: Preparation and Properties of More Complex Nanostructures. *Annu. Rev. Phys. Chem.* **2010,** *61*, 369-389.
5. Corrigan, J. F.; Brown, M. J.; Degroot, M. W.; Tran, D. T. T.; Wallbank, A. I., Main group and transition metal-selenolate complexes: Rings to clusters. *Phosphorus Sulfur Silicon Relat. Elem.* **2001,** *168*, 99-104.
6. Geach, J.; Walters, C. J.; James, B.; Caviness, K. E.; Hefferlin, R. A., Global molecular identification from graphs. Main-group triatomic molecules. *Croat. Chem. Acta.* **2002,** *75* (2), 383-400.
7. Gorrell, I. B., Alkali and alkaline-earth metals *Ann. Rep. Prog. Chem., Sect. A: Inorg. Chem.* **2005,** *101*, 20-33.
8. Halcrow, M. A., Pyrazoles and pyrazolides-flexible synthons in self-assembly. *Dalton Trans.* **2009,** (12), 2059-2073.
9. Hohlein, S.; Konig-Haagen, A.; Bruggemann, D., Thermophysical Characterization of $MgCl_2 \cdot 6H_2O$, Xylitol and Erythritol as Phase Change Materials (PCM) for Latent Heat Thermal Energy Storage (LHTES). *Materials.* **2017,** *10* (4).
10. Hu, C. L.; Mao, J. G., First-principles study of electronic structures and nonlinear optical properties of $AMoO_3(IO_3)$ (A = Li, Rb and Cs) crystals. *J. Phys. Condens. Mat.* **2010,** *22* (15).
11. Jiang, L. M.; Li, Y. Y.; Xing, J.; Wu, J. G.; Chen, Q.; Liu, H.; Xiao, D. Q.; Zhu, J. G., Phase structure and enhanced piezoelectric properties in $(1-x)(K_{0.48}Na_{0.52})(Nb_{0.95}Sb_{0.05})O_3-x(Bi_{0.5}Na_{0.42}Li_{0.08})_{0.9}Sr_{0.1}ZrO_3$ lead-free piezoelectric ceramics. *Ceram. Int.* **2017,** *43* (2), 2100-2106.
12. Khan, M. M. M.; Ghosh, S.; Hogarth, G.; Tocher, D. A.; Richmond, M. G.; Kabir, S. E.; Roesky, H. W., Mixed main group transition metal clusters: Reactions of $[Ru_3(CO)_{10}(\mu\text{-dppm})]$ with Ph_3SnH. *J. Organomet. Chem.* **2017,** *840*, 47-55.
13. Kiremire, E. M. R., The main group elements, fragments, compounds and clusters obey the 4n rule and form 4n series: they are close relatives to transition metal counterparts via the 14n linkage *Int. J. Chem.* **2016,** *8* (2), 94 -109.
14. Weller, A. S.; Shang, M. Y.; Fehlner, T. P., Synthesis and characterization of the nine-atom, rhena- and tungsta-boranes $(Cp^*Re)_2B_7H_7$ and $(Cp^*W)_2B_7H_9$, $Cp^* = \eta^5\text{-}C_5Me_5$. Molecular mimics of hypoelectronic main-group clusters in Zintl phases. *Chem. Commun.* **1998,** (17), 1787-1788.
15. Beltran, T. F.; Delaude, L., Recent Advances in Small Clusters and Polymetallic Assemblies Based on Transition Metals and Dithiocarboxylate Zwitterions Derived from N-Heterocyclic Carbenes. *J. Clust. Sci.* **2017,** *28* (2), 667-678.
16. Jiang, C. M.; Baker, L. R.; Lucas, J. M.; Vura-Weis, J.; Alivisatos, A. P.; Leone, S. R., Characterization of Photo-Induced Charge Transfer and Hot Carrier Relaxation Pathways in Spinel Cobalt Oxide (Co_3O_4). *J. Phys. Chem. C.* **2014,** *118* (39), 22774-22784.

17. Li, B. L.; Wang, J. P.; Zou, H. L.; Garaj, S.; Lim, C. T.; Xie, J. P.; Li, N. B.; Leong, D. T., Low-Dimensional Transition Metal Dichalcogenide Nanostructures Based Sensors. *Adv. Funct. Mater.* **2016,** *26* (39), 7034-7056.
18. Masternak, J.; Zienkiewicz-Machnik, M.; Kowalik, M.; Jablonska-Wawrzycka, A.; Rogala, P.; Adach, A.; Barszcz, B., Recent advances in coordination chemistry of metal complexes based on nitrogen heteroaromatic alcohols. Synthesis, structures and potential applications. *Coord. Chem. Rev.* **2016,** *327*, 242-270.
19. Singh, S.; Pramanik, P.; Sangaraju, S.; Mallick, A.; Giebeler, L.; Thota, S., Size-dependent structural, magnetic, and optical properties of $MnCo_2O_4$ nanocrystallites. *J. Appl. Phys.* **2017,** *121* (19).
20. Wang, Y. Y.; Ma, Y. Q.; Liu, R.; Yang, L. L.; Tian, G. R.; Sheng, N., Tetranuclear Complexes with $\{M_4O_4\}$ ($M = Co^{II}$, Ni^{II}) Cubane-Like Core: Synthesis, Crystal Structure, and Magnetic Properties. *Z. Anorg. Allg. Chem.* **2016,** *642* (7), 546-550.
21. Zhang, H. F.; Zhang, J.; Liu, R.; Li, Y. H.; Liu, W.; Li, W., Five Disk-Shaped $\{M_7^{II}\}$ (M = Mn, Fe, Co, Cu, Zn) Clusters and One Capsule-Like $\{Cu^{II6}Na^{I2}\}$ Cluster Assembled from the Same Schiff Base Ligand. *Eur. J. Inorg. Chem.* **2016,** (26), 4134-4143.
22. Bootharaju, M. S.; Kozlov, S. M.; Cao, Z.; Harb, M.; Maity, N.; Shkurenko, A.; Parida, M. R.; Hedhili, M. N.; Eddaoudi, M.; Mohammed, O. F.; Bakr, O. M.; Cavallo, L.; Basset, J. M., Doping-Induced Anisotropic Self-Assembly of Silver Icosahedra in $[Pt_2Ag_{23}Cl_7(PPh_3)_{10}]$ Nanoclusters. *J. Am. Chem. Soc.* **2017,** *139* (3), 1053-1056.
23. Chen, X. H.; Wu, K. C.; Snijders, J. G.; Lin, C. S., Electronic structures and nonlinear optical properties of trinuclear transition metal clusters M-(μ-S)-M' (M = Mo, W; M ' = Cu, Ag, Au). *Inorg. Chem.* **2003,** *42* (2), 532-540.
24. Guirado-Lopez, R. A.; Dorantes-Davila, J.; Pastor, G. M., Orbital magnetism in transition-metal clusters: From Hund's rules to bulk quenching. *Phys. Rev. Lett.* **2003,** *90* (22).
25. Rivera, M.; Martinez-Vado, F. I.; Mendoza-Huizar, L. H.; Amelines-Sarria, O.; Betancourt, I., Morphological and local magnetic properties of cobalt clusters electrodeposited onto indium tin oxide substrates. *J Mater Sci: Mater Electron.* **2017,** *28* (13), 9245-9251.
26. Shaw, R.; Laye, R. H.; Jones, L. F.; Low, D. M.; Talbot-Eeckelaers, C.; Wei, Q.; Milios, C. J.; Teat, S.; Helliwell, M.; Raftery, J.; Evangelisti, M.; Affronte, M.; Collison, D.; Brechin, E. K.; McInnes, E. J. L., 1,2,3-Triazolate-bridged tetradecametallic transition metal clusters $[M_{14}(L)_6O_6(OMe)_{18}X_6]$ ($M = Fe^{III}$, Cr^{III} and $V^{III/IV}$) and related compounds: Ground-state spins ranging from S=0 to S=25 and spin-enhanced magnetocaloric effect. *Inorg. Chem.* **2007,** *46* (12), 4968-4978.
27. Tian, H.; Qiao, X.; Xie, C. Z.; Ouyang, Y.; Xu, J. Y., Synthesis, characterization, and magnetochemical properties of two Mn_4 clusters derived from 2-pyridinecarboxaldehyde Schiff base ligands. *J. Coord. Chem.* **2017,** *70* (7), 1207-1220.
28. Banerjee, S.; Huebner, L.; Romanelli, M. D.; Kumar, G. A.; Riman, R. E.; Emge, T. J.; Brennan, J. G., Oxoselenido clusters of the lanthanides: Rational introduction of oxo ligands and near-IR emission from Nd(III). *J. Am. Chem. Soc.* **2005,** *127* (45), 15900-15906.

29. Banerjee, S.; Kumar, G. A.; Riman, R. E.; Emge, T. J.; Brennan, J. G., Oxoclusters of the lanthanides begin to resemble solid-state materials at very small cluster sizes: Structure and NIR emission from Nd(III). *J. Am. Chem. Soc.* **2007,** *129* (18), 5926-5931.
30. Karashimada, R.; Iki, N., Thiacalixarene assembled heterotrinuclear lanthanide clusters comprising Tb-III and Yb-III enable f-f communication to enhance Yb-III-centred luminescence. *Chem. Commun.* **2016,** *52* (15), 3139-3142.
31. Kornienko, A.; Banerjee, S.; Kumar, G. A.; Riman, R. E.; Emge, T. J.; Brennan, J. G., Heterometallic chalcogenido clusters containing lanthanides and main group metals: Emissive precursors to ternary solid-state compounds. *J. Am. Chem. Soc.* **2005,** *127* (40), 14008-14014.
32. Li, Z.; Li, X. X.; Yang, T.; Cai, Z. W.; Zheng, S. T., Four-Shell Polyoxometalates Featuring High-Nuclearity Ln_{26} Clusters: Structural Transformations of Nanoclusters into Frameworks Triggered by Transition-Metal Ions. *Angew. Chem. Int. Ed.* **2017,** *56* (10), 2664-2669.
33. Lv, X. H.; Yang, S. L.; Li, Y. X.; Zhang, C. X.; Wang, Q. L., Syntheses, structures and magnetic properties of four-spin Mn-Imino nitroxide radical complexes. *J. Mol. Struct.* **2017,** *1133*, 211-216.
34. Moore, B. F.; Kumar, G. A.; Tan, M. C.; Kohl, J.; Riman, R. E.; Brik, M. G.; Emge, T. J.; Brennan, J. G., Lanthanide Clusters with Chalcogen Encapsulated Ln: NIR Emission from Nanoscale $NdSe_x$. *J. Am. Chem. Soc.* **2011,** *133* (2), 373-378.
35. Peng, J. B.; Kong, X. J.; Zhang, Q. C.; Orendac, M.; Prokleska, J.; Ren, Y. P.; Long, L. S.; Zheng, Z. P.; Zheng, L. S., Beauty, Symmetry, and Magnetocaloric Effect-Four-Shell Keplerates with 104 Lanthanide Atoms. *J. Am. Chem. Soc.* **2014,** *136* (52), 17938-17941.
36. Wu, J. F.; Li, X. L.; Zhao, L.; Guo, M.; Tang, J. K., Enhancement of Magnetocaloric Effect through Fixation of Carbon Dioxide: Molecular Assembly from Ln_4 to Ln_4 Cluster Pairs. *Inorg. Chem.* **2017,** *56* (7), 4104-4111.
37. Wu, M. Y.; Jiang, F. L.; Kong, X. J.; Yuan, D. Q.; Long, L. S.; Al-Thabaiti, S. A.; Hong, M. C., Two polymeric 36-metal pure lanthanide nanosize clusters. *Chem. Sci.* **2013,** *4* (8), 3104-3109.
38. Xiong, J.; Ding, H. Y.; Meng, Y. S.; Gao, C.; Zhang, X. J.; Meng, Z. S.; Zhang, Y. Q.; Shi, W.; Wang, B. W.; Gao, S., Hydroxide-bridged five-coordinate Dy^{III} single-molecule magnet exhibiting the record thermal relaxation barrier of magnetization among lanthanide-only dimers. *Chem. Sci.* **2017,** *8* (2), 1288-1294.
39. Zhou, L. L.; Ding, L.; Wei, K. Y.; Sun, Y. Q.; Chen, Y. P., Novel Lanthanide Cluster Polymers Based on Cubane-like $[Ln_4(OH)_4]^{8+}$ Clusters and Sulfate Anions. *Chinese J. Struc. Chem.* **2016,** *35* (3), 375-382.
40. Zhou, Y.; Zheng, X. Y.; Cai, J.; Hong, Z. F.; Yan, Z. H.; Kong, X. J.; Ren, Y. P.; Long, L. S.; Zheng, L. S., Three Giant Lanthanide Clusters Ln_{37} (Ln = Gd, Tb, and Eu) Featuring A Double-Cage Structure. *Inorg. Chem.* **2017,** *56* (4), 2037-2041.
41. Arliguie, T.; Belkhiri, L.; Bouaoud, S. E.; Thuery, P.; Villiers, C.; Boucekkine, A.; Ephritikhine, M., Lanthanide(III) and Actinide(III) Complexes $[M(BH_4)_2(THF)_5][BPh_4]$ and $[M(BH_4)_2(18\text{-crown-}6)][BPh_4]$ (M = Nd, Ce, U): Synthesis, Crystal Structure, and Density Functional Theory Investigation of the Covalent Contribution to Metal-Borohydride Bonding. *Inorg. Chem.* **2009,** *48* (1), 221-230.

42. Di Pietro, P.; Kerridge, A., Assessing covalency in equatorial U-N bonds: density based measures of bonding in BTP and isoamethyrin complexes of uranyl. *Phys. Chem. Chem. Phys.* **2016,** *18* (25), 16830-9.
43. Gourier, D.; Caurant, D.; Arliguie, T.; Ephritikhine, M., EPR and angle-selected ENDOR study of 5f-ligand interactions in the $[U(\eta^7\text{-}C_7H_7)_2]^-$ anion, an f^1 analogue of uranocene. *J. Am. Chem. Soc.* **1998,** *120* (24), 6084-6092.
44. Huang, Q. R.; Kingham, J. R.; Kaltsoyannis, N., The strength of actinide-element bonds from the quantum theory of atoms-in-molecules. *Dalton Trans.* **2015,** *44* (6), 2554-2566.
45. Kozimor, S. A.; Yang, P.; Batista, E. R.; Boland, K. S.; Burns, C. J.; Clark, D. L.; Conradson, S. D.; Martin, R. L.; Wilkerson, M. P.; Wolfsberg, L. E., Trends in Covalency for d- and f-Element Metallocene Dichlorides Identified Using Chlorine K-Edge X-ray Absorption Spectroscopy and Time-Dependent Density Functional Theory. *J. Am. Chem. Soc.* **2009,** *131* (34), 12125-12136.
46. Minasian, S. G.; Krinsky, J. L.; Williams, V. A.; Arnold, J., A heterobimetallic complex with an unsupported Uranium(III)-Aluminum(I) bond: $(CpSiMe_3)_3U\text{-}AlCp^*$ ($Cp^* = C_5Me_5$). *J. Am. Chem. Soc.* **2008,** *130* (31), 10086-10090.
47. Oelkers, B.; Butovskii, M. V.; Kempe, R., f-Element-Metal Bonding and the Use of the Bond Polarity To Build Molecular Intermetalloids. *Chem. Eur. J.* **2012,** *18* (43), 13566-13579.
48. Parry, J.; Carmona, E.; Coles, S.; Hursthouse, M., Synthesis and Single-Crystal X-Ray-Diffraction Study on the First Isolable Carbonyl Complex of an Actinide, $(C_5Me_4H)_3U(CO)$. *J. Am. Chem. Soc.* **1995,** *117* (9), 2649-2650.
49. Xiao, C. L.; Wang, C. Z.; Mei, L.; Zhang, X. R.; Wall, N.; Zhao, Y. L.; Chai, Z. F.; Shi, W. Q., Europium, uranyl, and thorium-phenanthroline amide complexes in acetonitrile solution: an ESI-MS and DFT combined investigation. *Dalton Trans.* **2015,** *44* (32), 14376-14387.
50. Chatelain, L.; White, S.; Scopelliti, R.; Mazzanti, M., Isolation of a Star-Shaped Uranium(V/VI) Cluster from the Anaerobic Photochemical Reduction of Uranyl(VI). *Angew. Chemie. Int. Ed.* **2016,** *55* (46), 14323-14327.
51. Falaise, C.; Nyman, M., The Key Role of U_{28} in the Aqueous Self-Assembly of Uranyl Peroxide Nanocages. *Chem. Eur. J.* **2016,** *22* (41), 14678-14687.
52. Falaise, C.; Volkringer, C.; Loiseau, T., Mixed Formate-Dicarboxylate Coordination Polymers with Tetravalent Uranium: Occurrence of Tetranuclear $\{U_4O_4\}$ and Hexanuclear $\{U_6O_4(OH)_4\}$ Motifs. *Cryst. Growth. Des.* **2013,** *13* (7), 3225-3231.
53. Knope, K. E.; Vasiliu, M.; Dixon, D. A.; Soderholm, L., Thorium(IV)-Selenate Clusters Containing an Octanuclear Th(IV) Hydroxide/Oxide Core. *Inorg. Chem.* **2012,** *51* (7), 4239-4249.
54. Knope, K. E.; Wilson, R. E.; Vasiliu, M.; Dixon, D. A.; Soderholm, L., Thorium(IV) Molecular Clusters with a Hexanuclear Th Core. *Inorg. Chem.* **2011,** *50* (19), 9696-9704.
55. Sigmon, G. E.; Szymanowski, J. E. S.; Carter, K. P.; Cahill, C. L.; Burns, P. C., Hybrid Lanthanide-Actinide Peroxide Cage Clusters. *Inorg. Chem.* **2016,** *55* (6), 2682-2684.
56. Travia, N. E.; Scott, B. L.; Kiplinger, J. L., A Rare Tetranuclear Thorium(IV) μ_4-Oxo Cluster and Dinuclear Thorium(IV) Complex Assembled by Carbon-Oxygen Bond Activation of 1,2-Dimethoxyethane (DME). *Chem. Eur. J.* **2014,** *20* (51), 16846-16852.

57. Woidy, P.; Kraus, F., $[Th_{10}(\mu\text{-}F_{16})(\mu_3\text{-}O_4)(\mu_4\text{-}O_4)(NH_3)_{32}](NO_3)_8$ 19.6 NH_3 - the Largest Thorium Complex from Solution known to Date. *Z. Anorg. Allg. Chem.* **2014,** *640* (8-9), 1547-1550.
58. Zhang, Y. J.; Karatchevtseva, I.; Kadi, F.; Lu, K.; Yoon, B.; Price, J. R.; Li, F.; Lumpkin, G. R., Synthesis, spectroscopic characterization and crystal structures of thorium(IV) mononuclear lactato and hexanuclear formato complexes. *Polyhedron.* **2015,** *87*, 377-382.
59. Berthet, J. C.; Thuery, P.; Ephritikhine, M., Formation of Uranium(IV) Oxide Clusters from Uranocene $[U(\eta^8\text{-}C_8H_8)_2]$ and Uranyl $[UO_2X_2]$ Compounds. *Inorg. Chem.* **2010,** *49* (17), 8173-8177.
60. Berthet, J. C.; Thuery, P.; Ephritikhine, M., Unprecedented reduction of the uranyl ion $[UO_2]^{2+}$ into a polyoxo uranium(IV) cluster: Synthesis and crystal structure of the first f-element oxide with a $M_6(\mu_3\text{-}O)_8$ core. *Chem. Commun.* **2005,** (27), 3415-3417.
61. Oliveri, A. F.; Pilgrim, C. D.; Qiu, J.; Colla, C. A.; Burns, P. C.; Casey, W. H., Dynamic Phosphonic Bridges in Aqueous Uranyl Clusters. *Eur. J. Inorg. Chem.* **2016,** (6), 797-801.
62. Qiu, J.; Ling, J.; Jouffret, L.; Thomas, R.; Szymanowski, J. E. S.; Burns, P. C., Water-soluble multi-cage super tetrahedral uranyl peroxide phosphate clusters. *Chem. Sci.* **2014,** *5* (1), 303-310.
63. Zhang, Y. J.; Bhadbhade, M.; Price, J. R.; Karatchevtseva, I.; Kong, L. G.; Scales, N.; Lumpkin, G. R.; Li, F., Uranyl peroxide clusters stabilized by dicarboxylate ligands: A pentagonal ring and a dimer with extensive uranyl-cation interactions. *Polyhedron.* **2015,** *92*, 99-104.
64. Biswas, B.; Mougel, V.; Pecaut, J.; Mazzanti, M., Base-Driven Assembly of Large Uranium Oxo/Hydroxo Clusters. *Angew. Chemie. Int. Ed.* **2011,** *50* (25), 5744-5747.
65. Brianese, N.; Casellato, U.; Ossola, F.; Porchia, M.; Rossetto, G.; Zanella, P.; Graziani, R., Reactivity of Dicyclopentadienyluranium(IV) Derivatives - Formation and Structural Characterization of an Oxygen Bridged Cluster Containing Both Inorganic and Organometallic Uranium Atoms. *J. Organomet. Chem.* **1989,** *365* (3), 223-232.
66. Chatelain, L.; Faizova, R.; Fadaei-Tirani, F.; Pecaut, J.; Mazzanti, M., Structural Snapshots of Cluster Growth from $\{U_6\}$ to $\{U_{38}\}$ During the Hydrolysis of UCl_4. *Angew. Chemie. Int. Edit.* **2019,** *58* (10), 3021-3026.
67. Dufaye, M.; Martin, N. P.; Duval, S.; Volkringer, C.; Ikeda-Ohno, A.; Loiseau, T., Time-controlled synthesis of the 3D coordination polymer U(1,2,3-Hbtc)$_2$ followed by the formation of molecular poly-oxo cluster $\{U_{14}\}$ containing hemimellitate uranium(IV). *Rsc Adv.* **2019,** *9* (40), 22795-22804.
68. Falaise, C.; Neal, H. A.; Nyman, M., U(IV) Aqueous Speciation from the Monomer to UO_2 Nanoparticles: Two Levels of Control from Zwitterionic Glycine Ligands. *Inorg. Chem.* **2017,** *56* (11), 6591-6598.
69. Falaise, C.; Volkringer, C.; Vigier, J. F.; Henry, N.; Beaurain, A.; Loiseau, T., Three-Dimensional MOF-Type Architectures with Tetravalent Uranium Hexanuclear Motifs (U_6O_8). *Chem. Eur. J.* **2013,** *19* (17), 5324-5331.
70. Lin, J.; Yue, Z. H.; Silver, M. A.; Qie, M. Y.; Wang, X. M.; Liu, W.; Lin, X.; Bao, H. L.; Zhang, L. J.; Wang, S.; Wang, J. Q., In Situ Reduction from Uranyl Ion into a Tetravalent Uranium Trimer and Hexamer Featuring Ion-Exchange Properties and the Alexandrite Effect. *Inorg. Chem.* **2018,** *57* (11), 6753-6761.

71. Ling, J.; Lu, H. J.; Wang, Y. X.; Johnson, K.; Wang, S., One-dimensional chain structures of hexanuclear uranium(IV) clusters bridged by formate ligands. *Rsc Adv.* **2018,** *8* (61), 34947-34953.
72. Martin, N. P.; Marz, J.; Volkringer, C.; Henry, N.; Hennig, C.; Ikeda-Ohno, A.; Loiseau, T., Synthesis of Coordination Polymers of Tetravalent Actinides (Uranium and Neptunium) with a Phthalate or Mellitate Ligand in an Aqueous Medium. *Inorg. Chem.* **2017,** *56* (5), 2902-2913.
73. Martin, N. P.; Volkringer, C.; Henry, N.; Trivelli, X.; Stoclet, G.; Ikeda-Ohno, A.; Loiseau, T., Formation of a new type of uranium(IV) poly-oxo cluster $\{U_{38}\}$ based on a controlled release of water via esterification reaction. *Chem. Sci.* **2018,** *9* (22), 5021-5032.
74. Mokry, L. M.; Dean, N. S.; Carrano, C. J., Synthesis and structure of a discrete hexanuclear uranium-phosphate complex. *Angew. Chemie. Int. Ed.* **1996,** *35* (13-14), 1497-1498.
75. Nocton, G.; Pecaut, J.; Filinchuk, Y.; Mazzanti, M., Ligand assisted cleavage of uranium oxo-clusters. *Chem. Commun.* **2010,** *46* (16), 2757-2759.
76. Salmon, L.; Thuery, P.; Ephritikhine, M., Polynuclear uranium(IV) compounds with $(\mu_3\text{-oxo})U_3$ or $(\mu_4\text{-oxo})U_4$ cores and compartmental Schiff base ligands. *Polyhedron.* **2006,** *25* (7), 1537-1542.
77. Takao, S.; Takao, K.; Kraus, W.; Ernmerling, F.; Scheinost, A. C.; Bernhard, G.; Hennig, C., First Hexanuclear U(IV) and Th(IV) Formate Complexes - Structure and Stability Range in Aqueous Solution. *Eur. J. Inorg. Chem.* **2009,** (32), 4771-4775.
78. Tamain, C.; Dumas, T.; Hennig, C.; Guilbaud, P., Coordination of Tetravalent Actinides ($An=Th^{IV}$, U^{IV}, Np^{IV}, Pu^{IV}) with DOTA: From Dimers to Hexamers. *Chem. Eur. J.* **2017,** *23* (28), 6864-6875.
79. Vanagas, N. A.; Wacker, J. N.; Rom, C. L.; Glass, E. N.; Colliard, I.; Qiao, Y. S.; Bertke, J. A.; Van Keuren, E.; Schelter, E. J.; Nyman, M.; Knope, K. E., Solution and Solid State Structural Chemistry of Th(IV) and U(IV) 4-Hydroxybenzoates. *Inorg. Chem.* **2018,** *57* (12), 7259-7269.
80. Zehnder, R. A.; Boncella, J. M.; Cross, J. N.; Kozimor, S. A.; Monreal, M. J.; La Pierre, H. S.; Scott, B. L.; Tondreau, A. M.; Zeller, M., Network Dimensionality of Selected Uranyl(VI) Coordination Polymers and Octopus-like Uranium(IV) Clusters. *Cryst. Growth. Des.* **2017,** *17* (10), 5568-5582.
81. Franke, S. M.; Heinemann, F. W.; Meyer, K., Reactivity of uranium(IV) bridged chalcogenido complexes U(IV)-E-U(IV) (E = S, Se) with elemental sulfur and selenium: synthesis of polychalcogenido-bridged uranium complexes. *Chem. Sci.* **2014,** *5* (3), 942-950.
82. Jones, R. G.; Karmas, G.; Martin, G. A.; Gilman, H., Organic Compounds of Uranium. II. Uranium(IV) Amides, Alkoxides and Mercaptides. *J. Am. Chem. Soc.* **1956,** *78* (17), 4285-4286.
83. Leverd, P. C.; Ephritikhine, M.; Lance, M.; Vigner, J.; Nierlich, M., Triscyclopentadienyl uranium thiolates and selenolates. *J. Organomet. Chem.* **1996,** *507* (1-2), 229-237.
84. Mesbah, A.; Prakash, J.; Beard, J. C.; Pozzi, E. A.; Tarasenko, M. S.; Lebegue, S.; Malliakas, C. D.; Van Duyne, R. P.; Ibers, J. A., Positional Flexibility: Syntheses and Characterization of Six Uranium Chalcogenides Related to the 2H Hexagonal Perovskite Family. *Inorg. Chem.* **2015,** *54* (6), 2851-2857.
85. Pinkerton, A. A.; Storey, A. E.; Zellweger, J. M., Dithiophosphinate Complexes of the Actinides .1. Preparation and Characterization of Complexes of

Thorium(IV) and the Crystal-Structures of $[Th(S_2Pr_2)_4]$ R=Me or C_6H_{11}. *J. Chem. Soc., Dalton Trans.* **1981,** (7), 1475-1480.
86. Rosenzweig, M. W.; Scheurer, A.; Lamsfus, C. A.; Heinemann, F. W.; Maron, L.; Andrez, J.; Mazzanti, M.; Meyer, K., Uranium(IV) terminal hydrosulfido and sulfido complexes: insights into the nature of the uranium-sulfur bond. *Chem. Sci.* **2016,** *7* (9), 5857-5866.
87. Smiles, D. E.; Wu, G.; Hrobarik, P.; Hayton, T. W., Use of ^{77}Se and ^{125}Te NMR Spectroscopy to Probe Covalency of the Actinide-Chalcogen Bonding in $[Th(E_n)\{N(SiMe_3)_2\}_3]^-$ (E = Se, Te; n = 1, 2) and Their Oxo-Uranium(VI) Congeners. *J. Am. Chem. Soc.* **2016,** *138* (3), 814-825.
88. Leverd, P. C.; Arliguie, T.; Ephritikhine, M.; Nierlich, M.; Lance, M.; Vigner, J., The first structurally characterized uranium tetrathiolate complex, $U(SPr^i)_4[OP(NMe_2)_3]_2$, and the first uranium-sulfur cluster $U_3(\mu_3\text{-}S)(\mu_3\text{-}SBut)(\mu_2\text{-}SBut)_3(SBut)_6$. *New Journal of Chemistry.* **1993,** *17* (12), 769-771.
89. Leverd, P. C.; Lance, M.; Vigner, J.; Nierlich, M.; Ephritikhine, M., Synthesis and Reactions of Uranium(IV) Tetrathiolate Complexes. *J. Chem. Soc., Dalton Trans.* **1995,** (2), 237-244.
90. Spencer, L. P.; Yang, P.; Scott, B. L.; Batista, E. R.; Boncella, J. M., Uranium(VI) Bis(imido) Chalcogenate Complexes: Synthesis and Density Functional Theory Analysis. *Inorg. Chem.* **2009,** *48* (6), 2693-2700.
91. Gaunt, A. J.; Scott, B. L.; Neu, M. P., U(IV) chalcogenolates synthesized via oxidation of uranium metal by dichalcogenides. *Inorg. Chem.* **2006,** *45* (18), 7401-7407.
92. Arliguie, T.; Thuery, P.; Le Floch, P.; Mezailles, N.; Ephritikhine, M., A homoleptic SPS-based complex and a double-cubane-type sulfur cluster of an actinide element. *Polyhedron.* **2009,** *28* (8), 1578-1582.
93. Brennan, J. G.; Andersen, R. A.; Zalkin, A., Chemistry of Trivalent Uranium Metallocenes - Electron-Transfer Reactions - Synthesis and Characterization of $[(MeC_5H_4)_3U]_2E$ (E = S, Se, Te) and the Crystal Structures of $[(MeC_5H_4)_3U]_2S$ and $(MeC_5H_4)_3UOPPh_3$. *Inorg. Chem.* **1986,** *25* (11), 1761-1765.
94. Camp, C.; Antunes, M. A.; Garcia, G.; Ciofini, I.; Santos, I. C.; Pecaut, J.; Almeida, M.; Marcalo, J.; Mazzanti, M., Two-electron versus one-electron reduction of chalcogens by uranium(III): synthesis of a terminal U(V) persulfide complex. *Chem. Sci.* **2014,** *5* (2), 841-846.
95. Chatelain, L.; Scopelliti, R.; Mazzanti, M., Synthesis and Structure of Nitride-Bridged Uranium(III) Complexes. *J. Am. Chem. Soc.* **2016,** *138* (6), 1784-1787.
96. Evans, W. J.; Montalvo, E.; Ziller, J. W.; DiPasquale, A. G.; Rheingold, A. L., Uranium Metallocene Complexes of the 1,3,4,6,7,8-Hexahydro-*2H*-pyrimido[1,2-*a*]pyrimidinato Ligand, $(hpp)^-$. *Inorg. Chem.* **2010,** *49* (1), 222-228.
97. Lam, O. P.; Heinemann, F. W.; Meyer, K., Activation of elemental S, Se and Te with uranium(III): bridging U-E-U (E = S, Se) and diamond-core complexes U-E_2-U (E = O, S, Se, Te). *Chem. Sci.* **2011,** *2* (8), 1538-1547.
98. Smiles, D. E.; Wu, G.; Hayton, T. W., Reactivity of $[U(CH_2SiMe_2NSiMe_3)(NR_2)_2]$ (R = $SiMe_3$) with elemental chalcogens: towards a better understanding of chalcogen atom transfer in the actinides. *New Journal of Chemistry.* **2015,** *39* (10), 7563-7566.
99. Clark, D. L.; Gordon, J. C.; Huffman, J. G.; Watkin, J. G.; Zwick, B. D., Preparation of mono-pentamethylcyclopentadienyl uranium(IV) sulfido clusters

through oxidation of (η-C_5Me_5)$UI_2(THF)_3$ - X-ray structural characterization of (η-C_5Me_5)$_3U_3$(μ$_3$-I)(μ$_3$-S)(μ$_2$-I)$_3I_3$. *New Journal of Chemistry.* **1995,** *19* (5-6), 495-502.
100. Arliguie, T.; Blug, M.; Le Floch, P.; Mezailles, N.; Thuery, P.; Ephritikhine, M., Organouranium complexes with phosphinine-based SPS pincer ligands. Variations with the substituent at the phosphorus atom. *Organometallics.* **2008,** *27* (16), 4158-4165.
101. Arliguie, T.; Thuéry, P.; Floch, P. L.; Mézailles, N.; Ephritikhine, M., A homoleptic SPS-based complex and a double-cubane-type sulfur cluster of an actinide element. *Polyhedron.* **2009,** *28* (8), 1578-1582.
102. Brunner, H.; Kauermann, H.; Wachter, J., The Reaction of the Sulfur-Rich Compounds (C_5Me_5)$_2Mo_2S_4$ and (C_5Me_5)$_2Cr_2S_5$ with M-M Double Bonding of the Complex [Eta$_5C_5R_5$(CO)M']$_2$ (R=H,CH_3 and M'=Cr,Mo,W) and 2-Nuclear and 3-Nuclear Clusters with M_3S_4 and M_4S_4 Structures. *J. Organomet. Chem.* **1984,** *265* (2), 189-198.
103. Cecconi, F.; Ghilardi, C. A.; Midollini, S.; Orlandini, A., Synthesis and Structure of the New Cubane-Like Cluster [Fe_4Te_4(PEt_3)$_4$]PF_6, Containing Only Terminal Phosphine-Ligands. *J. Chem. Soc., Chem. Commun.* **1992,** (12), 910-911.
104. Li, T. Y.; Baum, Z. J.; Goldberger, J. E., A Vanadium Chalcogenide Dicubane. *Eur. J. Inorg. Chem.* **2016,** (1), 28-32.
105. Mena, M.; Perez-Redondo, A.; Yelamos, C., Heterometallic Cube-Type Molecular Nitrides. *Eur. J. Inorg. Chem.* **2016,** (12), 1762-1778.
106. Mutoh, Y.; Sakigawara, M.; Niiyama, I.; Saito, S.; Ishii, Y., Synthesis of Rhodium-Primary Thioamide Complexes and Their Desulfurization Leading to Rhodium Sulfido Cubane-Type Clusters and Nitriles. *Organometallics.* **2014,** *33* (19), 5414-5422.
107. Rauchfuss, T. B.; Weatherill, T. D.; Wilson, S. R.; Zebrowski, J. P., Stepwise Assembly of Heterometallic M_4S_4 Clusters - the Structure of ($MeCp$)$_2V_2Fe_2(NO)_2S_4$, a 58e Cubane. *J. Am. Chem. Soc.* **1983,** *105* (21), 6508-6509.
108. Seino, H.; Kaneko, T.; Fujii, S.; Hidai, M.; Mizobe, Y., Cubane-type heterometallic sulfido clusters: Incorporation of two metal fragments into a dinuclear ReS(μ-S)$_2$ReS core affording bimetallic M_2Re_2(μ$_3$-S)$_4$ clusters (M = Ru, Pt, Cu) or trimetallic MM'Re_2(μ$_3$-S)$_4$ clusters via incomplete cubane-type MRe_2(μ$_3$-S)(μ$_2$-S)$_3$ intermediates (M = Ru, Rh, Ir; M ' = Mo, W, Pd, Ru, Rh). *Inorg. Chem.* **2003,** *42* (15), 4585-4596.
109. Seino, H.; Mizobe, Y.; Hidai, M., Preparation of hydrosulfido- and hydroselenido-bridged diruthenium complexes with pi-arene co-ligands and their conversion into new cubane-type sulfido or selenido clusters. *New Journal of Chemistry.* **2000,** *24* (11), 907-911.
110. Shibata, R.; Seino, H.; Fujii, S.; Mizobe, Y., Core Conversion Reactions of the Cubane-Type Metal-Sulfido Clusters: Shape Shift, Contraction, and Expansion of the MM'Re_2S_4 Cubanes (M = Ir, Rh, Ru; M' = Pt, Pd). *Inorg. Chem.* **2010,** *49* (15), 6889-6896.
111. Zanello, P., The competition between chemistry and biology in assembling iron-sulfur derivatives. Molecular structures and electrochemistry. Part V. {[Fe_4S_4]($S^{\gamma Cys}$)$_4$} proteins. *Coord. Chem. Rev.* **2017,** *335*, 172-227.
112. Capone, M.; Narzi, D.; Bovi, D.; Guidoni, L., Mechanism of Water Delivery to the Active Site of Photosystem II along the S_2 to S_3 Transition. *J. Phys. Chem. Lett.* **2016,** *7* (3), 592-596.

113. Umena, Y.; Kawakami, K.; Shen, J.-R.; Kamiya, N., Crystal structure of oxygen-evolving photosystem II at a resolution of 1.9 Å. *Nature.* **2011,** *473* (7345), 55-60.
114. Okura, I.; Nakamura, S., Hydrogen Evolution Catalyzed by Fe_4S_4-Albumin as a Hydrogenase Model. *J. Mol. Catal.* **1980,** *9* (1), 125-127.
115. Pedrajas, E.; Sorribes, I.; Gushchin, A. L.; Laricheva, Y. A.; Junge, K.; Beller, M.; Llusar, R., Chemoselective Hydrogenation of Nitroarenes Catalyzed by Molybdenum Sulphide Clusters. *ChemCatChem.* **2017,** *9* (6), 1128-1134.
116. Seino, H.; Hidai, M., Catalytic functions of cubane-type M_4S_4 clusters. *Chem. Sci.* **2011,** *2* (5), 847-857.
117. Nguyen, A. I.; Suess, D. L. M.; Darago, L. E.; Oyala, P. H.; Levine, D. S.; Ziegler, M. S.; Britt, R. D.; Tilley, T. D., Manganese–Cobalt Oxido Cubanes Relevant to Manganese-Doped Water Oxidation Catalysts. *J. Am. Chem. Soc.* **2017,** *139* (15), 5579-5587.
118. Cleaver, W. M.; Spath, M.; Hnyk, D.; McMurdo, G.; Power, M. B.; Stuke, M.; Rankin, D. W. H.; Barron, A. R., Vapor-phase Laser Photochemistry and Determination by Electron-Difraction of the Molecular - Structure of $[(^tBu)GaS]_4$ - Evidence for the Retention of the Ga_4S_4 Cubane Core During the Mocvd Growth of Cubic Gas *Organometallics.* **1995,** *14* (2), 690-697.
119. Macinnes, A. N.; Power, M. B.; Barron, A. R., Chemical-Vapor-Deposition of Gallium Sulfide-Phase-Control by Molecular Design. *Chem. Mater.* **1993,** *5* (9), 1344-1351.
120. An, R.; Chen, X. L.; Hu, H. M.; Ren, Y. L.; Wu, Q. R.; Xue, G. L., Synthesis and characterization of an unprecedented 3D lanthanide coordination polymer assembled by cubane-like clusters and a flexible V-shaped dicarboxylate ligand. *Inorg. Chem. Commun.* **2015,** *61*, 177-180.
121. Banerjee, S.; Sheckelton, J.; Emge, T. J.; Brennan, J. G., Heterometallic Ln/Hg Tellurido Clusters. *Inorg. Chem.* **2010,** *49* (4), 1728-1732.
122. Berthet, J. C.; Thuery, P.; Ephritikhine, M., Polyimido Clusters of Neodymium and Uranium, Including a Cluster with an $M_6(\mu_3\text{-}N)_8$ Core. *Eur. J. Inorg. Chem.* **2008,** (35), 5455-5459.
123. Biswas, S.; Mondal, A. K.; Konar, S., Densely Packed Lanthanide Cubane Based 3D Metal-Organic Frameworks for Efficient Magnetic Refrigeration and Slow Magnetic Relaxation. *Inorg. Chem.* **2016,** *55* (5), 2085-2090.
124. Das, S.; Dey, A.; Biswas, S.; Colacio, E.; Chandrasekhar, V., Hydroxide-Free Cubane-Shaped Tetranuclear $[Ln_4]$ Complexes. *Inorg. Chem.* **2014,** *53* (7), 3417-3426.
125. Freedman, D.; Melman, J. H.; Emge, T. J.; Brennan, J. G., Cubane clusters containing lanthanide ions: $(py)_8Yb_4Se_4(SePh)_4$ and $(py)_{10}Yb_6S_6(SPh)_6$. *Inorg. Chem.* **1998,** *37* (17), 4162-4163.
126. Hu, M.; Wang, Q. L.; Xu, G. F.; Zhao, B.; Deng, G. R.; Zhang, Y. H.; Yang, G. M., Synthesis and characterization of a novel lanthanide coordination polymer with network structure based on $[Er_4(\mu_3\text{-}OH)_4]^{8+}$ cluster and 2,2'-bipyridine-3,3'-dicarboxylate. *Inorg. Chem. Commun.* **2007,** *10* (10), 1177-1180.
127. Ke, H. S.; Gamez, P.; Zhao, L.; Xu, G. F.; Xue, S. F.; Tang, J., Magnetic Properties of Dysprosium Cubanes Dictated by the M-O-M Angles of the $[Dy_4(\mu_3\text{-}OH)_4]$ Core. *Inorg. Chem.* **2010,** *49* (16), 7549-7557.
128. Li, T. T.; Nishiura, M.; Cheng, J. H.; Li, Y.; Hou, Z. M., $M_4(CH_2)_4$ Cubane-Type Rare-Earth Methylidene Complexes: Unique Reactivity toward Unsaturated C-O, C-N, and C-S Bonds. *Chem. Eur. J.* **2012,** *18* (47), 15079-15085.

129. Rohde, A.; Urland, W., Synthesis, crystal structures and magnetic behaviour of dimeric and tetrameric gadolinium carboxylates with trichloroacetic acid. *Dalton Trans.* **2006,** (24), 2974-2978.
130. Wagner, A. T.; Roesky, P. W., Rare-Earth Metal Oxo/Hydroxo Clusters - Synthesis, Structures, and Applications. *Eur. J. Inorg. Chem.* **2016,** (6), 782-791.
131. Yao, R. X.; Xu, X.; Zhang, X. M., Ferromagnetically coupled chiral dysprosium hydroxysulfate and centrosymmetric dysprosium hydroxysulfate-oxalate: $Dy_4(OH)_4$ cubane based high-connected networks via in situ conversion of organosulfur to sulfate. *Rsc Adv.* **2014,** *4* (96), 53954-53959.
132. Baskar, V.; Roesky, P. W., Lanthanide hydroxide cubane clusters anchoring ferrocenes: model compounds for fixation of organometallic fragments on a lanthanide oxide surface. *Dalton Trans.* **2006,** (5), 676-679.
133. Han, S. D.; Miao, X. H.; Liu, S. J.; Bu, X. H., Magnetocaloric effect and slow magnetic relaxation in two dense (3,12)-connected lanthanide complexes. *Inorg. Chem. Front.* **2014,** *1* (7), 549-552.
134. Liu, X. B.; Lin, H.; Xiao, Z. Y.; Fan, W. D.; Huang, A.; Wang, R. M.; Zhang, L. L.; Sun, D. F., Multifunctional lanthanide-organic frameworks for fluorescent sensing, gas separation and catalysis. *Dalton Trans.* **2016,** *45* (9), 3743-3749.
135. Ma, B. Q.; Zhang, D. S.; Gao, S.; Jin, T. Z.; Yan, C. H.; Xu, G. X., From cubane to supercubane: The design, synthesis, and structure of a three-dimensional open framework based on a Ln_4O_4 cluster. *Angew. Chemie. Int. Ed.* **2000,** *39* (20), 3644-3646.
136. Zhou, J. M.; Shi, W.; Li, H. M.; Li, H.; Cheng, P., Experimental Studies and Mechanism Analysis of High-Sensitivity Luminescent Sensing of Pollutional Small Molecules and Ions in Ln_4O_4 Cluster Based Microporous Metal-Organic Frameworks. *J. Phys. Chem. C.* **2014,** *118* (1), 416-426.
137. Kornienko, A.; Emge, T. J.; Kumar, G. A.; Riman, R. E.; Brennan, J. G., Lanthanide clusters with internal Ln ions: Highly emissive molecules with solid-state cores. *J. Am. Chem. Soc.* **2005,** *127* (10), 3501-3505.
138. Norton, K.; Kumar, G. A.; Dilks, J. L.; Emge, T. J.; Riman, R. E.; Brik, M. G.; Brennan, J. G., Lanthanide Compounds with Fluorinated Aryloxide Ligands: Near-Infrared Emission from Nd, Tm, and Er. *Inorg. Chem.* **2009,** *48* (8), 3573-3580.
139. Zhang, W. X.; Wang, Z. T.; Nishiura, M.; Xi, Z. F.; Hou, Z. M., $Ln_4(CH_2)_4$ Cubane-Type Rare-Earth Methylidene Complexes Consisting of "$(C_5Me_4SiMe_3)LnCH_2$)" Units (Ln = Tm, Lu). *J. Am. Chem. Soc.* **2011,** *133* (15), 5712-5715.
140. Stuber, M. A.; Kornienko, A. Y.; Emge, T. J.; Brennan, J. G., Tetrametallic Thorium Compounds with Th_4E_4 (E = S, Se) Cubane Cores. *Inorg. Chem.* **2017,** *56* (17), 10247-10256.
141. Deacon, G. B.; Junk, P. C.; Kelly, R. P.; Wang, J., Exploring the effect of the Ln(III)/Ln(II) redox potential on C-F activation and on oxidation of some lanthanoid organoamides. *Dalton Trans.* **2016,** *45* (4), 1422-1435.
142. Maleev, A. A.; Fagin, A. A.; Ilichev, V. A.; Lopatin, M. A.; Konev, A. N.; Samsonov, M. A.; Fukin, G. K.; Bochkarev, M. N., Lanthanide pentafluorophenolates. Synthesis, structure and luminescent properties. *J. Organomet. Chem.* **2013,** *747*, 126-132.
143. Romero, N.; Dufrois, Q.; Vendier, L.; Dinoi, C.; Etienne, M., Highly Fluorinated Tris(indazolyl)borate Hydrocarbyl Complexes of Calcium and

Magnesium: Synthesis and Structural Studies. *Organometallics.* **2017,** *36* (3), 564-571.
144. Rosca, S. C.; Caytan, E.; Dorcet, V.; Roisnel, T.; Carpentier, J. F.; Sarazin, Y., pi Ligands in Alkaline Earth Complexes. *Organometallics.* **2017,** *36* (7), 1269-1277.
145. Stark, M. J.; Shaw, M. J.; Fadamin, A.; Rath, N. P.; Bauer, E. B., Synthesis, structural characterization and catalytic activity of indenyl complexes of ruthenium bearing fluorinated phosphine ligands. *J. Organomet. Chem.* **2017,** *847*, 41-53.
146. Yin, H. L.; Zabula, A. V.; Schelter, E. J., C-F -> Ln/An interactions in synthetic f-element chemistry. *Dalton Trans.* **2016,** *45* (15), 6313-6323.
147. Fitzgerald, M.; Emge, T. J.; Brennan, J. G., Chalcogen-rich lanthanide clusters with fluorinated thiolate ligands. *Inorg. Chem.* **2002,** *41* (13), 3528-3532.
148. Behrle, A. C.; Barnes, C. L.; Kaltsoyannis, N.; Walensky, J. R., Systematic Investigation of Thorium(IV)- and Uranium(IV)-Ligand Bonding in Dithiophosphonate, Thioselenophosphinate, and Diselenophosphonate Complexes. *Inorg. Chem.* **2013,** *52* (18), 10623-10631.
149. Lam, O. P.; Franke, S. M.; Heinemann, F. W.; Meyer, K., Reactivity of U–E–U (E = S, Se) Toward CO_2, CS_2, and COS: New Mixed-Carbonate Complexes of the Types U–CO_2E–U (E = S, Se), U–CS_2E–U (E = O, Se), and U–COSSe–U. *J. Am. Chem. Soc.* **2012,** *134* (40), 16877-16881.
150. Smiles, D. E.; Wu, G.; Hayton, T. W., Reversible Chalcogen-Atom Transfer to a Terminal Uranium Sulfide. *Inorg. Chem.* **2014,** *53* (24), 12683-12685.
151. Ringgold, M.; Rehe, D.; Hrobarik, P.; Kornienko, A. Y.; Emge, T. J.; Brennan, J. G., Thorium Cubanes-Synthesis, Solid-State and Solution Structures, Thermolysis, and Chalcogen Exchange Reactions. *Inorg. Chem.* **2018,** *57* (12), 7129-7141.
152. Wu, W.; Rehe, D.; Hrobarik, P.; Kornienko, A. Y.; Emge, T. J.; Brennan, J. G., Molecular Thorium Compounds with Dichalcogenide Ligands: Synthesis, Structure, ^{77}Se NMR Study, and Thermolysis. *Inorg. Chem.* **2018,** *57* (23), 14821-14833.
153. Fortney-Zirker, R. G.; Henderson, W.; Tiekink, E. R. T., Mixed-chalcogenide diplatinum complexes; an investigation of ligand exchange processes using ESI mass spectrometry. *Inorg. Chim. Acta.* **2017,** *462*, 83-96.
154. Groom, C. R.; Bruno, I. J.; Lightfoot, M. P.; Ward, S. C., The Cambridge Structural Database. *Acta. Crystallogr. B.* **2016,** *72*, 171-179.
155. Rehe, D.; Kornienko, A. Y.; Emge, T. J.; Brennan, J. G., Thorium Compounds with Bonds to Sulfur or Selenium: Synthesis, Structure, and Thermolysis. *Inorg. Chem.* **2016,** *55* (14), 6961-7.
156. Berg, J. M.; Clark, D. L.; Huffman, J. C.; Morris, D. E.; Sattelberger, A. P.; Streib, W. E.; Vandersluys, W. G.; Watkin, J. G., Early Actinide Alkoxide Chemistry - Synthesis, Characterization, and Molecular-Structures of Th(IV) and U(IV) Aryloxide Complexes. *J. Am. Chem. Soc.* **1992,** *114* (27), 10811-10821.
157. Ren, W. S.; Zi, G. F.; Walter, M. D., Synthesis, Structure, and Reactivity of a Thorium Metallocene Containing a 2,2 '-Bipyridyl Ligand. *Organometallics.* **2012,** *31* (2), 672-679.
158. Zhou, E. W.; Ren, W. S.; Hou, G. H.; Zi, G. F.; Fang, D. C.; Walter, M. D., Small Molecule Activation Mediated by a Thorium Terminal Imido Metallocene. *Organometallics.* **2015,** *34* (14), 3637-3647.

159. Settineri, N. S.; Garner, M. E.; Arnold, J., A Thorium Chalcogenolate Series Generated by Atom Insertion into Thorium-Carbon Bonds. *J. Am. Chem. Soc.* **2017,** *139* (17), 6261-6269.
160. Mesbah, A.; Ringe, E.; Lebegue, S.; Van Duyne, R. P.; Ibers, J. A., $Ba_2An(S_2)_2S_2$ (An=U, Th): Syntheses, Structures, Optical, and Electronic Properties. *Inorg. Chem.* **2012,** *51* (24), 13390-13395.
161. Prakash, J.; Mesbah, A.; Beard, J.; Lebegue, S.; Malliakas, C. D.; Ibers, J. A., Synthesis, crystal structure, optical, and electronic study of the new ternary thorium selenide $Ba_3ThSe_3(Se_2)_2$. *J. Solid. State. Chem.* **2015,** *231*, 163-168.
162. Pyykko, P., Additive covalent radii for single-, double-, and triple-bonded molecules and tetrahedrally bonded crystals: a summary. *J. Phys. Chem. A.* **2015,** *119* (11), 2326-37.
163. Shannon, R. D., Revised Effective Ionic-Radii and Systematic Studies of Interatomic Distances in Halides and Chalcogenides. *Acta. Crystallogr. A.* **1976,** *32* (Sep1), 751-767.
164. Reichenbächer, K.; Süss, H. I.; Hulliger, J., Fluorine in crystal engineering—"the little atom that could". *Chem. Soc. Rev.* **2005,** *34* (1), 22-30.
165. Duddeck, H., Selenium-77 nuclear magnetic resonance spectroscopy. *Progress in Nuclear Magnetic Resonance Spectroscopy.* **1995,** *27* (1-3), 1-323.
166. Huebner, L.; Kornienko, A.; Emge, T. J.; Brennan, J. G., Lanthanide clusters with internal Ln: Fragmentation and the formation of dimers with bridging Se^{2-} and Se_2^{2-} ligands. *Inorg. Chem.* **2005,** *44* (14), 5118-5122.

Chapter 4: Tetrametallic Uranium Compounds with U_4E_4 (E = S, Se) Cubane Cores

4.1 Introduction

Non-aqueous actinide chemistry has been built on research of purely aqueous systems that were directly related to nuclear fuel processes. Using non-aqueous solvents allows for the exploration of compounds with novel actinide-ligand bonds to promote advancements in fields such as catalysis and cluster chemistry. Uranium cluster chemistry[1-9] has focused primarily on systems with oxygen based anions,[9-12] including uranyl[13-17] functionalities in aqueous solutions. Clusters containing hydroxide- or oxo-bridged U(IV) cations usually contain organic ligands on their surfaces which aid in the synthesis and growth of larger oxo-clusters.[18-37] For materials with chalcogen-based ligands, terminal U=E bonds are uncommon,[38-43] dimeric (μ_2-E)-bridged uranium molecular compounds are more common,[44-60] while few (μ_3-E)-bridged uranium clusters are found in the literature.[56, 59, 61-63]

Successful preparations of molecular compounds with uranium-chalcogen bonds have in the past relied on the presence of large sterically demanding multidentate ligands.[44-49, 52-55, 57-62, 64-77] It has become apparent, however, that sterically saturating multidentate ligands are not a prerequisite to the formation of stable cluster products. Several stable uranium chalcogenido compounds have been synthesized with smaller and more labile chalcogen containing ancillary ligands.[50, 56, 78-82]

The identity of larger clusters has been shown to be influenced by the use of monodentate ligands. For example, different sized CuEL clusters (E = Se, Te; L =

PEt_3, PPr^i_3, PBu^t_3, PEt_2Ph, PPh_3) clusters were prepared by using phosphine ligands of various size.[83-85] The same principal could apply in actinide chalcogenide chemistry, since in these materials there has always been at least one solvent molecule (pyridine, THF, etc.) coordinating to every metal.

Fluorinated $EC_6F_5^-$ ligands have been used to form monomeric compounds and multimetallic clusters of the lanthanides and thorium,[86-88] and can permit the direct comparison between the synthesis of these previously explored compounds to the synthesis of novel uranium clusters, as well as a related uranium chalcogenido cluster, $(py)_8U_4(\mu_3\text{-}Se)_4(\mu_2\text{-}SePh)_4(SePh)_4$,[56] that does not incorporate fluorinated ancillary ligands. The increase in solubility of EC_6F_5 compared to EC_6H_5 ligands has been noted in several coordination compounds,[87, 89-95] as well as the fluorinated ligands effect on crystal packing and inter- and intramolecular interactions.[88, 96, 97] Fluorinated ligands that aid in the synthesis of multimetallic uranium clusters also gives the opportunity to study magnetic exchange coupling, as these terminal ligands aid in stabilizing clusters with a variety of chalcogenido bridging ligands.

The characterization of uranium complexes with magnetic moment data has historically been used to aid in determining the oxidation state or uranium when complex ligand environments are present.[98] In magnetic susceptibility studies of molecular uranium compounds, antiferromagnetic exchange coupling has been observed.[99-106] Magnetic susceptibility studies of U(IV) chalcogenolates are rare, with the literature comprising studies of bimetallic uranium compounds bridged by E (E = S, Se, Te).[47, 54, 57, 107, 108] By characterizing and comparing small molecule compounds with magnetic susceptibility data, links can be made amongst compounds ranging from monomeric coordination complexes and nanoscale clusters, to solid state

materials. The studies of such materials are of interests to fields such as quantum computing[109] and data storage.[110]

This chapter outlines the synthesis and characterization of a series of uranium tetrameric cubanes that have both EPh and EC_6F_5 ligands. The first examples of heterochalcogen clusters of uranium are compared the series of heterochalcogen thorium tetrameric cubanes, as well as the selenium containing $(py)_8U_4(\mu_3\text{-}Se)_4(\mu_2\text{-}SePh)_4(SePh)_4$[56] cubane. The series of uranium tetrameric cubanes were characterized for their magnetic properties, which suggest antiferromagnetic coupling. Magnetic moments are in agreement with other U(IV) compounds with bridging chalcogenido ligands.

4.2 Results and Discussion

In-situ prepared solutions of "$U(EPh)_x(E'C_6F_5)_{4-x}$" (E, E' = S, Se) undergo ligand-based redox reactions with elemental E in pyridine or pyridine/toluene mixtures. A trace amount of I_2 is used as a catalyst to reduce the time required for U to be consumed in the reaction. The elemental E is reduced to E^{2-} and EPh^- from "$U(EPh)_3(E'C_6F_5)$" is oxidized to PhEEPh, leading to the formation of $(py)_8U_4(\mu_3\text{-}E)_4(\mu_2\text{-}EPh)_4(E'C_6F_5)_4$ (Figure 4.1). As discussed in Chapter 3, while there are various combinations of S and Se at the E, EPh, and $E'C_6F_5$ sites, many combinations form clusters with disordered products containing irreproducible ratios of S^{2-} and Se^{2-}. It is only when E = (E)Ph that ordered clusters are synthesized, while the $(E')C_6F_5$ site can be modified (E'= S, Se) independently with no chalcogen exchange. Synthesis of the uranium tetramers is informed by the combinations of chalcogen ligands used to synthesize the ordered thorium tetrameric clusters.

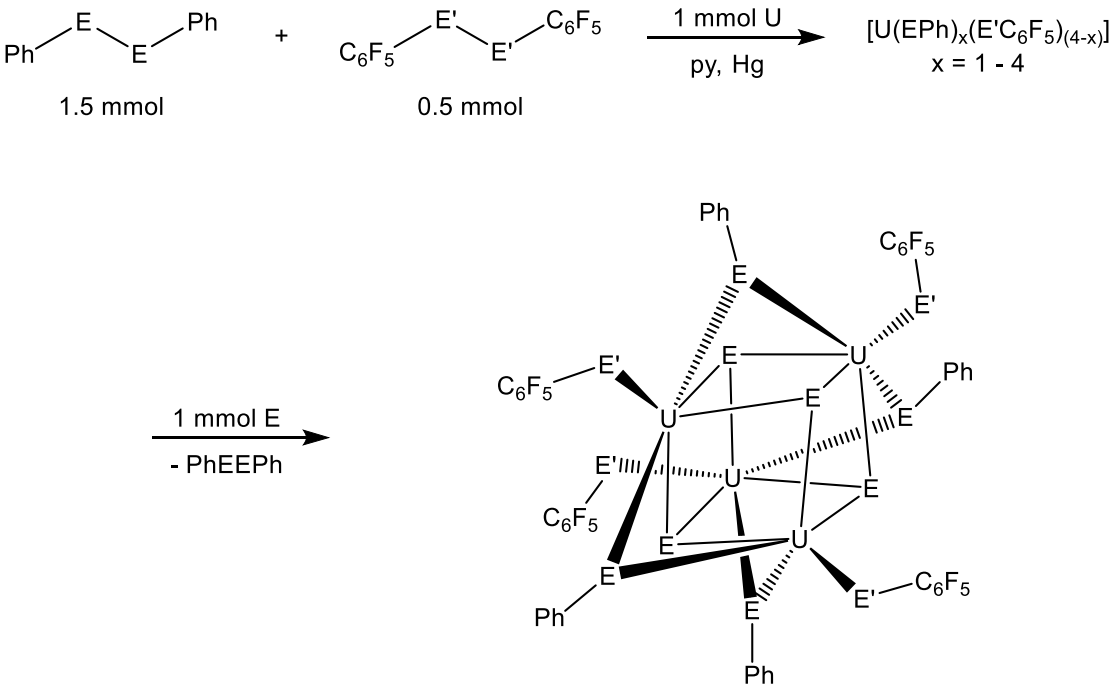

Figure 4.1 Synthesis of the series of $(py)_8U_4(\mu_3\text{-}E)_4(\mu_2\text{-}EPh)_4(E'C_6F_5)_4$ (E, E' = S, Se) with py removed for clarity.

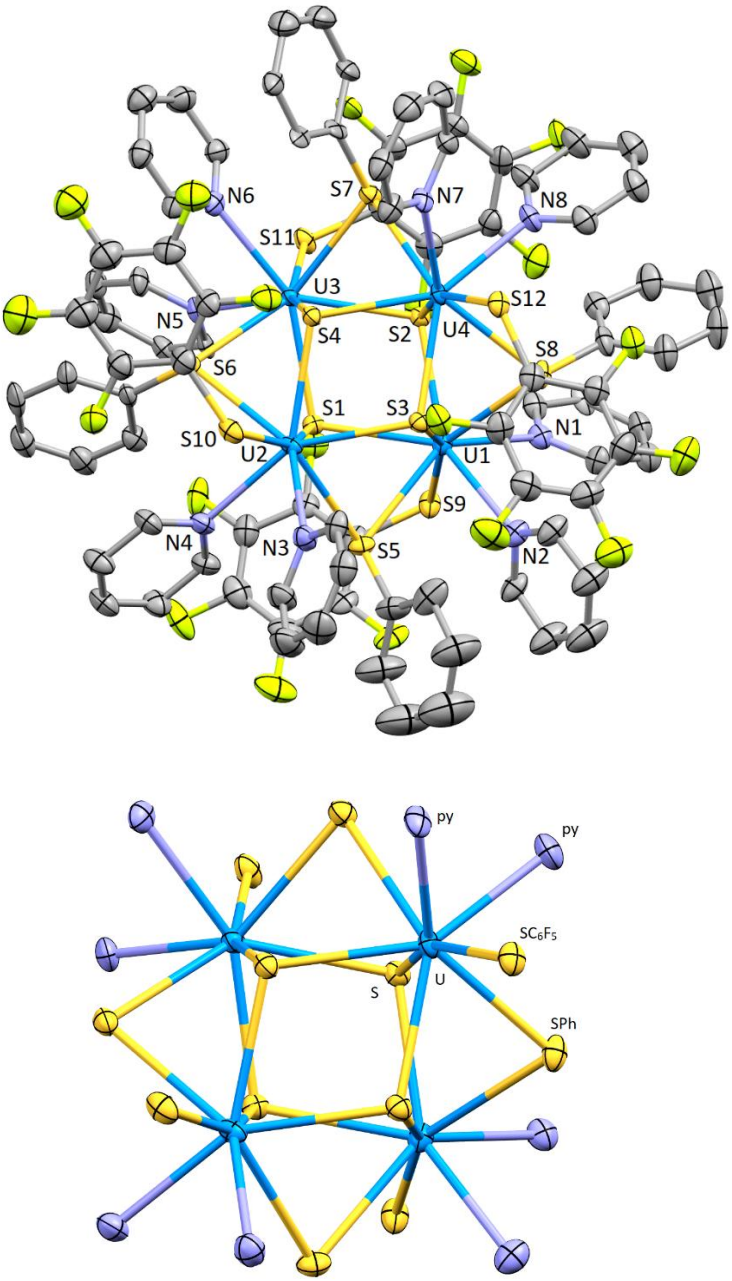

Figure 4.2 (Top) Thermal ellipsoid diagram of $py_8U_4S_4(\mu_2\text{-}SPh)_4(SC_6F_5)_4$ (**11**), with light green F, yellow S, blue U, purple N, gray C, H atoms removed for clarity, and ellipsoids at the 50% probability level. The view is of the top region of the cubane core. (Bottom) Diagram of the cubane core region of **11** in the same orientation as the top figure.

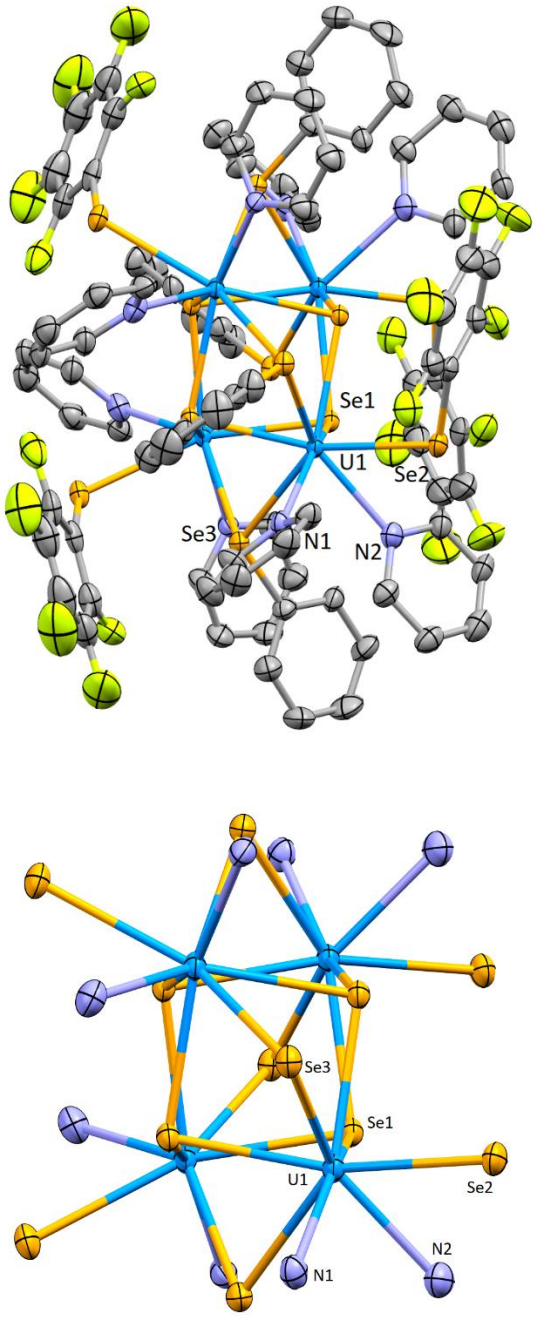

Figure 4.3 (Top) Thermal ellipsoid diagram of $py_8U_4Se_4(\mu_2\text{-}SePh)_4(SeC_6F_5)_4$ (**12**), with light green F, orange Se, blue U, purple N, gray C, H atoms removed for clarity, and ellipsoids at the 50% probability level. The view is of the side of the cubane core. (Bottom) Diagram of the cubane core region of **12** in the same orientation as the top figure.

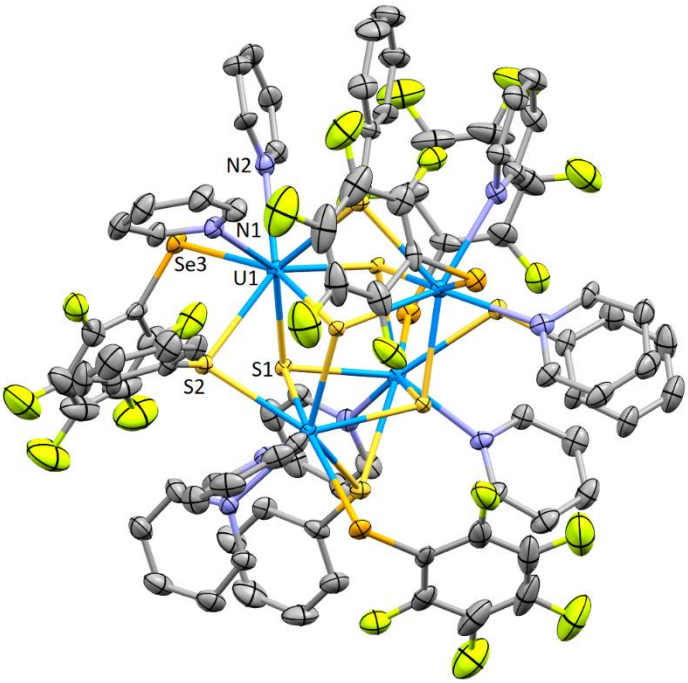

Figure 4.4 Thermal ellipsoid diagram of $py_8U_4S_4(\mu_2\text{-}SPh)_4(SeC_6F_5)_4$ (**13**), with light green F, yellow S, orange Se, blue U, purple N, gray C, H atoms removed for clarity, and ellipsoids at the 50% probability level.

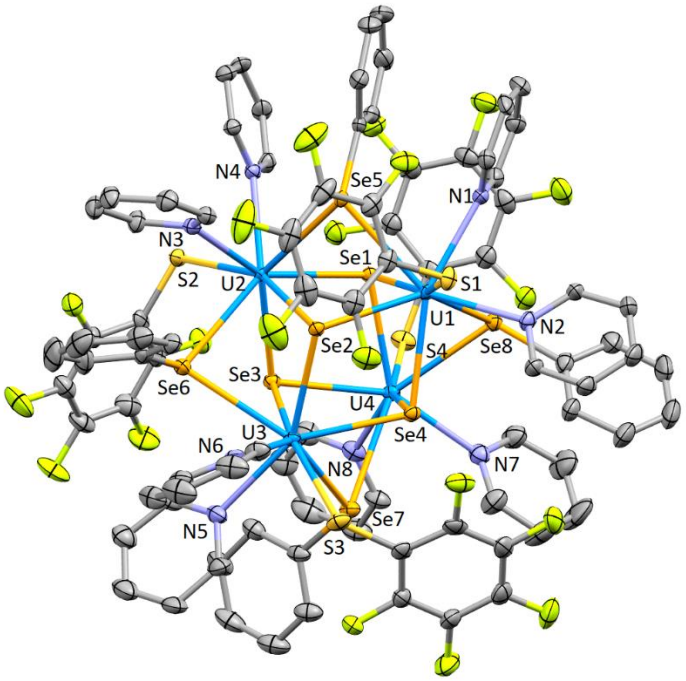

Figure 4.5 Thermal ellipsoid diagram of $py_8U_4S_4(\mu_2\text{-}SPh)_4(SeC_6F_5)_4$ (**14**), with light green F, yellow S, orange Se, light blue Th, purple N, gray C, H atoms removed for clarity, and ellipsoids at the 50% probability level.

Table 4.1 Summary of Crystallographic Details for **11** – **14**.

compound	**11**	**12**	**13**	**14**
empirical formula	$C_{100}H_{72}F_{20}N_{10.4}S_{12}U_4$	$C_{98}H_{70}F_{20}N_{10}Se_{12}U_4$	$C_{98}H_{70}F_{20}N_{10}S_8Se_4U_4$	$C_{105.5}H_{77.50}F_{20}N_{11.5}S_4Se_8U_4$
fw	3136.12	3667.28	3292.08	3598.33
space group (No.)	P-1 (2)	I-4 (82)	I-4 (82)	P-1 (2)
a (Å)	15.254(3)	20.4101(14)	20.1179(19)	14.803(3)
b (Å)	15.404(3)	20.4101(14)	20.1179(19)	15.802(3)
c (Å)	24.000(5)	12.4702(8)	12.4706(12)	24.236(5)
α (deg)	106.411(4)	90	90	84.789(4)
β (deg)	100.180(4)	90	90	89.531(4)
γ (deg)	100.286(4)	90	90	87.224(4)
V ($Å^3$)	5166.3(18)	5194.7(8)	5047.2(11)	5639(2)
Z	2	2	2	2
D(calcd) (Mg/m^3)	2.016	2.345	2.116	2.119
temperature (°K)	120(2)	100(2)	120(2)	120(2)
λ (Å)	0.71073	0.71073	0.71073	0.71073
abs coeff (mm^{-1})	6.582	10.507	8.095	8.467
R(F)[a] [I > 2 σ(I)]	0.0650	0.0388	0.0381	0.0731
$R_W(F^2)$[b] [I > 2 σ(I)]	0.1366	0.0793	0.0856	0.1522

Definitions: [a] $R(F) = \Sigma||F_o| - |F_c||/\Sigma|F_o|$; [b] $R_w(F^2) = [\Sigma[w(F_o^2 - F_c^2)^2]/\Sigma[w(F_o^2)^2]]^{1/2}$

Compounds **11-14** were characterized by spectroscopic methods and by low-temperature single-crystal X-ray diffraction, details given in Table 4.1. While the previously described $(py)_8Th_4(\mu_3\text{-}E)_4(\mu_2\text{-}EPh)_4(E'C_6F_5)_4$ tetrameric compounds[88] discussed in Chapter 3 exclusively crystallized in the tetragonal I-4 cell, compounds **11-14** crystallize in more than one unit cell. All have the same basic structure with varying numbers and orientations of the lattice pyridine molecules. Each cluster in the unit cell exhibits a site symmetry of S_4 with a U_4E_{12} core. This core region consists of

a central distorted $U_4(\mu_3\text{-}E)_4$ cube-like motif, four (μ_2-E) ligands bridging the uranium centers of the cube, and four (η-E') ligands on each uranium in the cube. The cube-like motif is composed of rhomboid U_2E_2 facets and four U_2E_2 side facets that are more regular (e.g. more square) in shape, with the μ_2-EPh ligands bridging two U atoms on each side facet.

Table 4.2 Selected Distances (Å), and Angles (°) for **11** – **14**.

Bond/Angle	**11** (E,E' = S, S)	**12** (E,E' = Se,Se)	**13** (E,E' = S, Se)	**14** (E,E' = Se, S)
U-N	2.603-2.640(11),	2.614(10), 2.654(10)	2.642(8), 2.606(8)	2.605-2.630(10),
U-μ_3E *(side)*	2.668-2.682(3)	2.8092(10)	2.687(2)	2.7976-2.8338(13)
U-μ_3E *(top)*	2.760-2.807(3)	2.9196(11), 2.9203(11)	2.800(2), 2.804(2)	2.8899-2.9281(14)
U-E'(C_6F_5)	2.811-2.828(3)	2.9624(11)	2.967(1)	2.788-2.828(3)
U-E(Ph)	2.872-2.892(4),	2.9975(12), 3.0403(11)	2.888(2), 2.929(2)	2.9826-3.0231(15),
U…U *(side)*	3.906-3.931(10)	4.0628(6)	3.9141(6)	4.048-4.087(1)
U…U *(top)*	4.500-4.504(1)	4.7101(6)	4.5269(7)	4.6630-4.6634(9)
E'-C(E'C_6F_5)*	1.712-1.820(16)	1.895(13)	1.889(10)	1.741-1.770(13)
E-C(EPh)	1.767-1.811(17)	1.914(11)	1.772(9)	1.904-1.936(15)
U- μ_3E-U *(side)*	90.97-92.05(10)	90.30(3), 90.31(3)	90.90(6), 91.00(5)	90.13-91.36(4)
U- μ_3E-U *(top)*	107.52-107.98(12)	107.52(3)	107.76(7)	106.45-107.20(4)
U-E(Ph)-U *(side)*	83.97-84.41(10)	84.58(3)	84.58(6)	83.53-84.59(4)
U-E'-C(E'C_6F_5)*	112.1-114.2(14)	110.0(3)	109.7(3)	111.7-114.1(4)
U-E-C(EPh)	118.0-120.2(6)	116.1(3), 117.4(4)	117.4(3), 120.2(4)	114.5-118.3(1)

* Average of two parts for minor SeC_6F_5 site disorder in compound **1**.

All bond distances are consistent with literature values reflecting the sizes of their individual atomic components,[111] as well as examples of similar structures found in the Cambridge Structural Database.[112] Relevant bond lengths and angles are given in Table 4.2. The range of values for U-N(pyridine) bond lengths here (2.585(12)-2.642(8) Å) are consistent with previously reported U-N(pyridine) bond lengths,[56, 59, 64, 82, 113, 114] including 2.590(5)-2.640(5) Å for the non-fluorinated tetrameric $[U(py)_2(SePh)(\mu_3\text{-}Se)(\mu_2\text{-}SePh)]_4$,[56] and 2.563(5)-2.629(5) Å for monomeric $U(SPh)_4(py)_3$.[56]

The range of values for U-(μ_3-E^{2-}) bond lengths are also consistent amongst scarce literature containing triply bridging chalcogenides to three uranium atom centers.[56, 61, 62] In compounds **11** and **13** the bridging μ_3-S^{2-} distances in the elongated top U_2S_2 facets are 2.760(3)-2.807(3) Å, and in the side U_2S_2 facets are shorter at 2.668(3)-2.687(2) Å, which suggests there is increased strain relative to the U-(μ_3-E^{2-}) bonds in the side facets that are bridged by μ_2-EPh. These are comparable to the U-(μ_3-S^{2-}) bond distances (2.662(4)-2.810(3) Å) in $[[U(COT)]_4[U(THF)_3]_2(\mu_3\text{-}S)_8]$.[61] The uranium metal centers in this compound arrange in an octahedron, where each face of the octahedron contains μ_3-S^{2-} that bridges each uranium.

In compounds **12** and **14** the bridging μ_3-Se^{2-} distances in the elongated top U_2Se_2 facets are 2.8899(14)-2.9396(8) Å, and in the side U_2Se_2 facets are slightly shorter at 2.7976(13)-2.8335(7) Å. The increased lengths of the U-(μ_3-E^{2-}) bonds in the top and bottom facets of the cube-like core region suggest that there is increased strain relative to the U-(μ_3-E^{2-}) bonds in the side facets that are bridged by μ_2-EPh. The U-(μ_3-Se^{2-}) bonds in **12** and **14** are comparable to the U-(μ_3-Se^{2-}) bond distances in the non-fluorinated tetrameric $[U(py)_2(SePh)(\mu_3\text{-}Se)(\mu_2\text{-}SePh)]_4$ cluster (2.7928(6)-2.9482(6) Å).[56] Uranium chalcogenido solid-state materials with comparable U-E^{2-}

distances are known, with UE_3 [defined as $U^{4+}(E^{2-})(E_2^{2-})$] including U-S^{2-} bonds (2.7530(18)-2.825(2) Å),[115] and U-Se^{2-} bonds (2.896(1)-2.969(1) Å).[116]

The range of values for U-(μ_2-EPh) bond lengths are comparable to other bridging U-E-U bonds in the literature.[44-60] In compounds **11** and **13** the bridging μ_2-SPh distances are 2.872(4)-2.965(4) Å. These are comparable to the U-μ_2-SPh distances (2.8667(19)-2.9378(19) Å and terminal U-SPh distance (2.813(2) Å) in $[U(EPh)_2(\mu_2\text{-}EPh)_2(CH_3CN)_2]_2$.[56] In compounds **12** and **14** the bridging μ^2-SePh distances are 2.9826(15)-3.0976(8) Å. These are comparable to the U-μ_2-SePh distances (3.0184(7)-3.1225(7) Å) and terminal U-SePh distances (2.9185(7)-2.9349(7) Å) in the non-fluorinated tetrameric $[U(py)_2(SePh)(\mu_3\text{-}Se)(\mu_2\text{-}SePh)]_4$ cluster.[56]

Each uranium atom center contains one bond to a terminally bound fluorinated phenyl chalcogenolate ligand. While the only example of terminal U-EC_6F_5 bonds are in compound **11** - **14**, there are comparable compounds with non-fluorinated phenyl chalcogenolate ligands.[50, 56, 59, 65-82] The fluorinated analogues are longer than their non-fluorinated counterparts; for example: 2.9624(11)Å for U-SeC_6F_5 in compound **12**, compared to 2.9175(7)-2.9349(7) Å for U-SePh in the isomorphous non-fluorinated $[U(py)_2(SePh)(\mu_3\text{-}Se)(\mu_2\text{-}SePh)]_4$.[56] This lengthening of the U-E(C_6F_5) bond can be rationalized by noting the electron withdrawing nature of the fluorines that effectively decreases the electrostatic interactions between U and E.

Other f-metal clusters containing EC_6F_5 ligands have been synthesized, including the series of lanthanide clusters $(THF)_6Ln_4E(E_2)_4(SC_6F_5)_2$ (Ln = Yb, E = S, Se; Ln = Tm, E = Se).[87] As with the actinide clusters discussed here and in Chapter 3, the fluorinated ligands only bind terminally to a metal cation in the cluster. In contrast to the actinide clusters, the lanthanide cluster series is synthesized in a multistep

approach where Ln metal is oxidized by $Hg(SC_6F_5)_2$ to form $Ln(SC_6F_5)_3$, which is subsequently filtered into a solution of $Ln(EPh)_3$ to form presumed intermediate "$Ln(EPh)_x(EC_6F_5)_{3-x}$".[87] EPh ligands are subsequently displaced via reaction with elemental S or Se. As in the actinide clusters, $EC_6F_5^-$ is not oxidized upon addition of E, while EPh can be replaced by bridging E^{2-}. Yb-S(C_6F_5) bond lengths in $(THF)_6Ln_4S(S_2)_4(SC_6F_5)_2$ (2.675 Å) and $(THF)_6Ln_4Se(Se_2)_4(SC_6F_5)_2$ (2.667 Å) are similar despite the identity of the bridging E^{2-} ligands.[87] This holds true in the Th-(E')C_6F_5 bonds of the Th clusters $(py)_8Th_4E_4(EPh)_4(E'C_6F_5)_4$, **7** (E, E' = S, S) (2.904(2) Å) compared to **10** (E, E' = Se, S) (2.899(2) Å), and **8** (E, E' = Se, Se) (3.020(1) Å) compared to **9** (E, E' = S, Se) (3.030(1) Å). This trend is also present in the U-(E')C_6F_5 bonds of the U clusters $(py)_8U_4E_4(EPh)_4(E'C_6F_5)_4$, **11** (E, E' = S, S) (2.811-2.828(3) Å) compared to **14** (E, E' = Se, S) (2.788-2.828(3) Å), and **12** (E, E' = Se, Se) (2.9624(11) Å) compared to **13** (E, E' = S, Se) (2.967(1) Å).

The temperature-dependent behavior of the four cubane-like tetrameric compounds reveals magnetic moments of μ_{eff} = 2.82(1) (**11**), 3.51(1) (**12**), 2.51(1) (**13**), 3.15(2) (**14**) μ_B/U at 300 K, that decreases to μ_{eff} = 2.07(4) (**11**), 0.78(1) (**12**), 0.22(1) (**13**), 0.16(2) (**14**). This is consistent with the range of reported data for room-temperature and low-temperature magnetic moments for U^{4+} compounds.[98] Table 4.3 shows select bimetallic U(IV) complexes with bridging chalcogenido ligands, with magnetic moments at room-temperature and low-temperature compared to tetrametallic uranium compounds **11** – **14**. There are no other reports in the literature of compounds with more than two U^{4+} ions bridged by chalcogenido ligands. There is a general trend of higher room-temperature magnetic moments for bimetallic compounds with a selenido bridging ligand compared to the sulfur derivatives. The only exception is the lower magnetic moment for $[[((^{t\text{-}Bu}ArO)_3tacn)U]_2(\mu\text{-Se})]$[57]

compared to the sulfur-containing dimer, though still larger than similar [[((^{Ad}ArO)$_3$N)U]$_2$(μ-S)].[57] Room-temperature magnetic moments of UE_3 (E = S, Se, Te) ($ZrSe_3$-type structure) are also noted in Table 4.3 to compare to **11** – **14** as these compounds show bridging E^{2-} between U^{4+} ions [UE_3 is defined as $U^{4+}(E^{2-})(E_2^{2-})$].[115-117] This shows an opposite trend where the magnetic moment for USe_3 is lower compared to US_3, as well as UTe_3.

Table 4.3 Room-temperature (R.T.) and low-temperature (L.T.) magnetic moments (μ_B) of bimetallic U(IV) complexes with bridging chalcogenido ligands, and comparisons to tetrametallic compounds **11** – **14**, as well as solid-state UE_3 (E = S, Se, Te)

Compound	R.T. μ (μ_B)	L.T. μ (μ_B) (temp, K)
$py_8U_4S_4(SPh)_4(SC_6F_5)_4$ (**11**)	2.82	2.07 (1.8)
$py_8U_4Se_4(SePh)_4(SeC_6F_5)_4$ (**12**)	3.51	0.78 (1.8)
$py_8U_4S_4(SPh)_4(SeC_6F_5)_4$ (**13**)	2.51	0.22 (1.8)
$py_8U_4Se_4(SePh)_4(SC_6F_5)_4$ (**14**)	3.15	0.16 (1.8)
[[((^{Ad}ArO)$_3$N)U]$_2$(μ-S_2)$_2$][107]	1.65	0.26 (2)
[[((^{Ad}ArO)$_3$N)U]$_2$(μ-η^3: η^3-Se_4)][107]	2.30	0.39 (2)
[[((^{Ad}ArO)$_3$N)U]2(μ-Se2)(μ-DME)][107]	2.69	0.30 (2)
[[((^{Ad}ArO)$_3$N)U(THF)]$_2$(μ-η^2: η^2-Se_4)][107]	2.82	0.33 (2)
$(Cp_3U)_2S$[108]	2.64	0.58 (4.2)
[Na(DME)$_3$]$_2$[[((^{Ad}ArO)$_3$N)U]$_2$(μ-S)$_2$][57]	3.2	0.4 (2)
[Na(DME)$_3$]$_2$[[((^{Ad}ArO)$_3$N)U]$_2$(μ-Se)$_2$][57]	3.4	0.4 (2)
[[((^{Ad}ArO)$_3$N)U]$_2$(μ-Se)][57]	3.5	0.5 (2)
[Na(DME)$_3$]$_2$[[((^{Ad}ArO)$_3$N)U]$_2$(μ-Te)$_2$][57]	3.5	0.5 (2)
[[((^{Ad}ArO)$_3$N)U]$_2$(μ-S)][57]	3.6	0.6 (2)
[[(($^{t\text{-}Bu}$ArO)$_3$tacn)U]$_2$(μ-Se)][57]	3.8	0.7 (2)
[[(($^{t\text{-}Bu}$ArO)$_3$tacn)U]$_2$(μ-S)][57]	4.0	1.1 (2)
[[((^{Ad}ArO)$_3$N)U]$_2$(μ-SH)$_2$][54]	2.46	0.34
[[((^{Ad}ArO)$_3$N)U]$_2$(μ-SeH)$_2$][54]	2.65	0.33
[[((^{Ad}ArO)$_3$N)U]$_2$(μ-TeH)$_2$][54]	2.44	0.31
US_3[117]	3.08	
USe_3[117]	2.98	
UTe_3[117]	3.09	

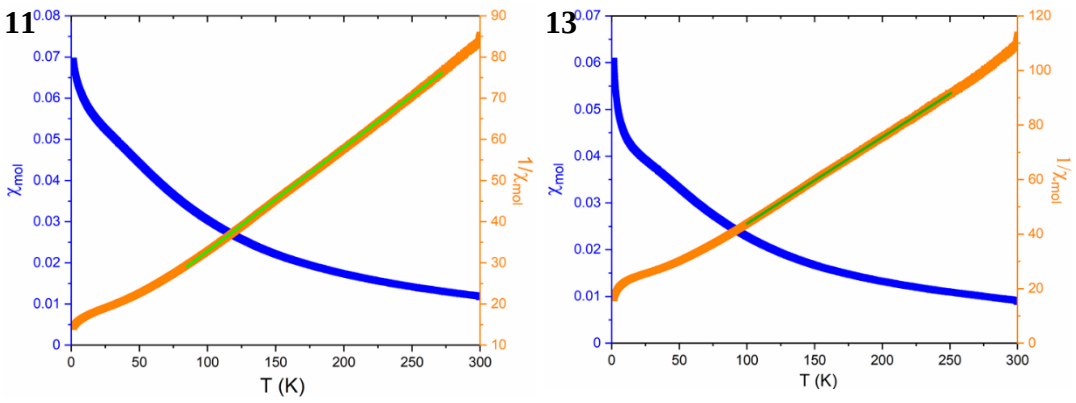

Figure 4.6 The temperature dependence of susceptibility measured in zero field cooling method at 0.3 T for **11** and **13**.

Antiferromagnetic exchange coupling dominating at low temperatures is common in various uranium compounds, and is observed as a maximum at lower temperatures in the plots of χ/mol vs. T.[99-107] The magnetic susceptibilities of **11** – **14** do not show such distinctive maximum at low temperatures (Figure 4.6-blue). Smooth peaks are observed around 20 K in the temperature dependent magnetization data for **11** and **13** with continued increase in χ/mol at temperatures below this point, which can suggest possible paramagnetic impurities, but can possibly be seen as the start of antiferromagnetic ordering in these U_4E_4 compounds.[107] While the magnetic susceptibility plots for **12** and **14** are similar with continuous increase in χ/mol with decreasing temperature, smooth peaks were not observed. This suggests either paramagnetic impurities are more pronounced than in **11** and **13**, or that similar signs of antiferromagnetic ordering in **12** and **14** are not present at lower temperatures compared to **11** and **13**.

The experimental data for **11** – **14** were measured at 0.3 T with zero-field cooling and fitted using the Curie-Weiss law $\chi = \frac{C}{T-\theta}$ between 75 and 250 K (example seen in Figure 4.6-orange), where C is the Curie constant, θ is the Weiss

constant (also known as the Curie temperature, units in K), and T is temperature (K).[118] The fitting yields values of θ = -31(1) K (**11**), -6(1) K (**12**), -39(1) K (**13**), -41(4) K (**14**). The negative sign of paramagnetic Curie temperature (θ) suggests antiferromagnetic interactions in all four compounds with different theoretical antiferromagnetic transition temperatures.

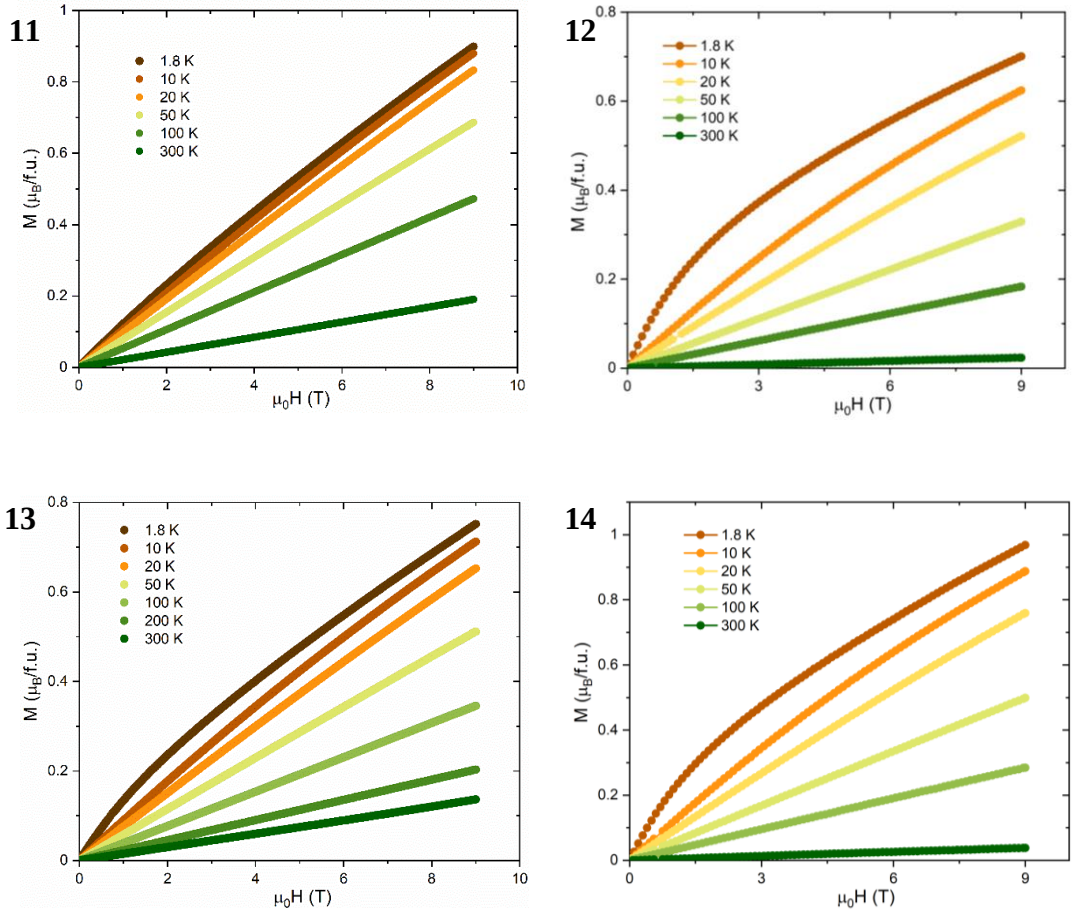

Figure 4.7 Isothermal magnetic field dependence of magnetization for **11** – **14**.

The isothermal magnetic field dependence of magnetization is shown in Figure 4.7. Magnetization increases linearly with increasing magnetic field above 20 K with no sign of saturation up to the highest applied field (9 T). This is consistent with antiferromagnetic local interactions present in **11** – **14**.

4.3 Conclusion

A series of $py_8U_4E_4(\mu_2\text{-}EPh)_4(E'C_6F_5)_4$ cubane clusters (E = S, Se; E' = S, Se) were prepared with varying combinations of E, E' =S, Se via in situ ligand based redox reactions with EPh ligands on intermediate uranium monomers being reduced by elemental E. All four compounds are morphous with the series of thorium cubanes discussed in Chapter 3. Like the thorium series, there is a consistent and unique pattern of terminal $E'C_6F_5$ versus bridging EPh ligand positions. Magnetic susceptibility measurements suggest antiferromagnetic local interactions in the tetramers at low temperatures.

4.4 References

1. Arliguie, T.; Belkhiri, L.; Bouaoud, S. E.; Thuery, P.; Villiers, C.; Boucekkine, A.; Ephritikhine, M., Lanthanide(III) and Actinide(III) Complexes $[M(BH_4)_2(THF)_5][BPh_4]$ and $[M(BH_4)_2(18\text{-crown-6})][BPh_4]$ (M = Nd, Ce, U): Synthesis, Crystal Structure, and Density Functional Theory Investigation of the Covalent Contribution to Metal-Borohydride Bonding. *Inorg. Chem.* **2009,** *48* (1), 221-230.
2. Di Pietro, P.; Kerridge, A., Assessing covalency in equatorial U-N bonds: density based measures of bonding in BTP and isoamethyrin complexes of uranyl. *Phys. Chem. Chem. Phys.* **2016,** *18* (25), 16830-9.
3. Gourier, D.; Caurant, D.; Arliguie, T.; Ephritikhine, M., EPR and angle-selected ENDOR study of 5f-ligand interactions in the $[U(\eta^7\text{-}C_7H_7)_2]^-$ anion, an f^1 analogue of uranocene. *J. Am. Chem. Soc.* **1998,** *120* (24), 6084-6092.
4. Huang, Q. R.; Kingham, J. R.; Kaltsoyannis, N., The strength of actinide-element bonds from the quantum theory of atoms-in-molecules. *Dalton Trans.* **2015,** *44* (6), 2554-2566.
5. Kozimor, S. A.; Yang, P.; Batista, E. R.; Boland, K. S.; Burns, C. J.; Clark, D. L.; Conradson, S. D.; Martin, R. L.; Wilkerson, M. P.; Wolfsberg, L. E., Trends in Covalency for d- and f-Element Metallocene Dichlorides Identified Using Chlorine K-Edge X-ray Absorption Spectroscopy and Time-Dependent Density Functional Theory. *J. Am. Chem. Soc.* **2009,** *131* (34), 12125-12136.
6. Minasian, S. G.; Krinsky, J. L.; Williams, V. A.; Arnold, J., A heterobimetallic complex with an unsupported Uranium(III)-Aluminum(I) bond: $(CpSiMe_3)_3U\text{-}AlCp^*$ ($Cp^* = C_5Me_5$). *J. Am. Chem. Soc.* **2008,** *130* (31), 10086-10090.
7. Oelkers, B.; Butovskii, M. V.; Kempe, R., f-Element-Metal Bonding and the Use of the Bond Polarity To Build Molecular Intermetalloids. *Chem. Eur. J.* **2012,** *18* (43), 13566-13579.
8. Parry, J.; Carmona, E.; Coles, S.; Hursthouse, M., Synthesis and Single-Crystal X-Ray-Diffraction Study on the First Isolable Carbonyl Complex of an Actinide, $(C_5Me_4H)_3U(CO)$. *J. Am. Chem. Soc.* **1995,** *117* (9), 2649-2650.
9. Xiao, C. L.; Wang, C. Z.; Mei, L.; Zhang, X. R.; Wall, N.; Zhao, Y. L.; Chai, Z. F.; Shi, W. Q., Europium, uranyl, and thorium-phenanthroline amide complexes in acetonitrile solution: an ESI-MS and DFT combined investigation. *Dalton Trans.* **2015,** *44* (32), 14376-14387.
10. Chatelain, L.; Scopelliti, R.; Mazzanti, M., Synthesis and Structure of Nitride-Bridged Uranium(III) Complexes. *J. Am. Chem. Soc.* **2016,** *138* (6), 1784-1787.
11. Falaise, C.; Nyman, M., The Key Role of U_{28} in the Aqueous Self-Assembly of Uranyl Peroxide Nanocages. *Chem. Eur. J.* **2016,** *22* (41), 14678-14687.
12. Sigmon, G. E.; Szymanowski, J. E. S.; Carter, K. P.; Cahill, C. L.; Burns, P. C., Hybrid Lanthanide-Actinide Peroxide Cage Clusters. *Inorg. Chem.* **2016,** *55* (6), 2682-2684.
13. Berthet, J. C.; Thuery, P.; Ephritikhine, M., Formation of Uranium(IV) Oxide Clusters from Uranocene $[U(\eta^8\text{-}C_8H_8)_2]$ and Uranyl $[UO_2X_2]$ Compounds. *Inorg. Chem.* **2010,** *49* (17), 8173-8177.
14. Berthet, J. C.; Thuery, P.; Ephritikhine, M., Unprecedented reduction of the uranyl ion $[UO_2]^{2+}$ into a polyoxo uranium(IV) cluster: Synthesis and crystal structure of the first f-element oxide with a $M_6(\mu_3\text{-}O)_8$ core. *Chem. Commun.* **2005,** (27), 3415-3417.

15. Oliveri, A. F.; Pilgrim, C. D.; Qiu, J.; Colla, C. A.; Burns, P. C.; Casey, W. H., Dynamic Phosphonic Bridges in Aqueous Uranyl Clusters. *Eur. J. Inorg. Chem.* **2016,** (6), 797-801.
16. Qiu, J.; Ling, J.; Jouffret, L.; Thomas, R.; Szymanowski, J. E. S.; Burns, P. C., Water-soluble multi-cage super tetrahedral uranyl peroxide phosphate clusters. *Chem. Sci.* **2014,** *5* (1), 303-310.
17. Zhang, Y. J.; Bhadbhade, M.; Price, J. R.; Karatchevtseva, I.; Kong, L. G.; Scales, N.; Lumpkin, G. R.; Li, F., Uranyl peroxide clusters stabilized by dicarboxylate ligands: A pentagonal ring and a dimer with extensive uranyl-cation interactions. *Polyhedron.* **2015,** *92*, 99-104.
18. Biswas, B.; Mougel, V.; Pecaut, J.; Mazzanti, M., Base-Driven Assembly of Large Uranium Oxo/Hydroxo Clusters. *Angew. Chemie. Int. Ed.* **2011,** *50* (25), 5744-5747.
19. Brianese, N.; Casellato, U.; Ossola, F.; Porchia, M.; Rossetto, G.; Zanella, P.; Graziani, R., Reactivity of Dicyclopentadienyluranium(IV) Derivatives - Formation and Structural Characterization of an Oxygen Bridged Cluster Containing Both Inorganic and Organometallic Uranium Atoms. *J. Organomet. Chem.* **1989,** *365* (3), 223-232.
20. Chatelain, L.; Faizova, R.; Fadaei-Tirani, F.; Pecaut, J.; Mazzanti, M., Structural Snapshots of Cluster Growth from $\{U_6\}$ to $\{U_{38}\}$ During the Hydrolysis of UCl_4. *Angew. Chemie. Int. Ed.* **2019,** *58* (10), 3021-3026.
21. Dufaye, M.; Martin, N. P.; Duval, S.; Volkringer, C.; Ikeda-Ohno, A.; Loiseau, T., Time-controlled synthesis of the 3D coordination polymer $U(1,2,3\text{-Hbtc})_2$ followed by the formation of molecular poly-oxo cluster $\{U_{14}\}$ containing hemimellitate uranium(IV). *Rsc Adv.* **2019,** *9* (40), 22795-22804.
22. Falaise, C.; Neal, H. A.; Nyman, M., U(IV) Aqueous Speciation from the Monomer to UO_2 Nanoparticles: Two Levels of Control from Zwitterionic Glycine Ligands. *Inorg. Chem.* **2017,** *56* (11), 6591-6598.
23. Falaise, C.; Volkringer, C.; Loiseau, T., Mixed Formate-Dicarboxylate Coordination Polymers with Tetravalent Uranium: Occurrence of Tetranuclear $\{U_4O_4\}$ and Hexanuclear $\{U_6O_4(OH)_4\}$ Motifs. *Cryst. Growth. Des.* **2013,** *13* (7), 3225-3231.
24. Falaise, C.; Volkringer, C.; Vigier, J. F.; Henry, N.; Beaurain, A.; Loiseau, T., Three-Dimensional MOF-Type Architectures with Tetravalent Uranium Hexanuclear Motifs (U_6O_8). *Chem. Eur. J.* **2013,** *19* (17), 5324-5331.
25. Lin, J.; Yue, Z. H.; Silver, M. A.; Qie, M. Y.; Wang, X. M.; Liu, W.; Lin, X.; Bao, H. L.; Zhang, L. J.; Wang, S.; Wang, J. Q., In Situ Reduction from Uranyl Ion into a Tetravalent Uranium Trimer and Hexamer Featuring Ion-Exchange Properties and the Alexandrite Effect. *Inorg. Chem.* **2018,** *57* (11), 6753-6761.
26. Ling, J.; Lu, H. J.; Wang, Y. X.; Johnson, K.; Wang, S., One-dimensional chain structures of hexanuclear uranium(IV) clusters bridged by formate ligands. *Rsc Adv.* **2018,** *8* (61), 34947-34953.
27. Martin, N. P.; Marz, J.; Volkringer, C.; Henry, N.; Hennig, C.; Ikeda-Ohno, A.; Loiseau, T., Synthesis of Coordination Polymers of Tetravalent Actinides (Uranium and Neptunium) with a Phthalate or Mellitate Ligand in an Aqueous Medium. *Inorg. Chem.* **2017,** *56* (5), 2902-2913.
28. Martin, N. P.; Volkringer, C.; Henry, N.; Trivelli, X.; Stoclet, G.; Ikeda-Ohno, A.; Loiseau, T., Formation of a new type of uranium(IV) poly-oxo cluster $\{U_{38}\}$ based on a controlled release of water via esterification reaction. *Chem. Sci.* **2018,** *9* (22), 5021-5032.

29. Moisan, L.; Le Borgne, T.; Thuery, P.; Ephritikhine, M., An ion pair formed by protonated $Fe(cp^*py)_2$ and the octanuclear cluster $U_8Cl_{24}O_4(cp^*py)_2$ [cp*py is tetramethyl-5-(2-pyridyl)cyclopentadiene]. *Acta. Crystallogr. C.* **2002,** *58*, m98-m101.
30. Mokry, L. M.; Dean, N. S.; Carrano, C. J., Synthesis and structure of a discrete hexanuclear uranium-phosphate complex. *Angew. Chemie. Int. Ed.* **1996,** *35* (13-14), 1497-1498.
31. Nocton, G.; Pecaut, J.; Filinchuk, Y.; Mazzanti, M., Ligand assisted cleavage of uranium oxo-clusters. *Chem. Commun.* **2010,** *46* (16), 2757-2759.
32. Salmon, L.; Thuery, P.; Ephritikhine, M., Crystal structure of the first octanuclear uranium(IV) complex with compartmental Schiff base ligands. *Polyhedron.* **2004,** *23* (4), 623-627.
33. Salmon, L.; Thuery, P.; Ephritikhine, M., Polynuclear uranium(IV) compounds with $(\mu_3\text{-oxo})U_3$ or $(\mu_4\text{-oxo})U_4$ cores and compartmental Schiff base ligands. *Polyhedron.* **2006,** *25* (7), 1537-1542.
34. Takao, S.; Takao, K.; Kraus, W.; Ernmerling, F.; Scheinost, A. C.; Bernhard, G.; Hennig, C., First Hexanuclear U(IV) and Th(IV) Formate Complexes - Structure and Stability Range in Aqueous Solution. *Eur. J. Inorg. Chem.* **2009,** (32), 4771-4775.
35. Tamain, C.; Dumas, T.; Hennig, C.; Guilbaud, P., Coordination of Tetravalent Actinides ($An=Th^{IV}$, U^{IV}, Np^{IV}, Pu^{IV}) with DOTA: From Dimers to Hexamers. *Chem. Eur. J.* **2017,** *23* (28), 6864-6875.
36. Vanagas, N. A.; Wacker, J. N.; Rom, C. L.; Glass, E. N.; Colliard, I.; Qiao, Y. S.; Bertke, J. A.; Van Keuren, E.; Schelter, E. J.; Nyman, M.; Knope, K. E., Solution and Solid State Structural Chemistry of Th(IV) and U(IV) 4-Hydroxybenzoates. *Inorg. Chem.* **2018,** *57* (12), 7259-7269.
37. Zehnder, R. A.; Boncella, J. M.; Cross, J. N.; Kozimor, S. A.; Monreal, M. J.; La Pierre, H. S.; Scott, B. L.; Tondreau, A. M.; Zeller, M., Network Dimensionality of Selected Uranyl(VI) Coordination Polymers and Octopus-like Uranium(IV) Clusters. *Cryst. Growth. Des.* **2017,** *17* (10), 5568-5582.
38. Brown, J. L.; Fortier, S.; Lewis, R. A.; Wu, G.; Hayton, T. W., A Complete Family of Terminal Uranium Chalcogenides, $[U(E)(N\{SiMe_3\}_2)_3]^-$ (E = O, S, Se, Te). *J. Am. Chem. Soc.* **2012,** *134* (37), 15468-15475.
39. Brown, J. L.; Fortier, S.; Wu, G.; Kaltsoyannis, N.; Hayton, T. W., Synthesis and Spectroscopic and Computational Characterization of the Chalcogenido-Substituted Analogues of the Uranyl Ion, $[OUE]^{2+}$ (E = S, Se). *J. Am. Chem. Soc.* **2013,** *135* (14), 5352-5355.
40. Kelly, R. P.; Falcone, M.; Lamsfus, C. A.; Scopelliti, R.; Maron, L.; Meyer, K.; Mazzanti, M., Metathesis of a UV imido complex: a route to a terminal UV sulfide. *Chem. Sci.* **2017,** *8* (8), 5319-5328.
41. Pagano, J. K.; Arney, D. S. J.; Scott, B. L.; Morris, D. E.; Kiplinger, J. L.; Burns, C. J., A sulphur and uranium fiesta! Synthesis, structure, and characterization of neutral terminal uranium(VI) monosulphide, uranium(VI) η^2-disulphide, and uranium(IV) phosphine sulphide complexes. *Dalton Trans.* **2019,** *48* (1), 50-57.
42. Smiles, D. E.; Wu, G.; Hayton, T. W., Synthesis of Uranium–Ligand Multiple Bonds by Cleavage of a Trityl Protecting Group. *J. Am. Chem. Soc.* **2013,** *136* (1), 96-99.
43. Ventelon, L.; Lescop, C.; Arliguie, T.; Ephritikhine, M.; Leverd, P. C.; Lance, M.; Nierlich, M., Synthesis and X-ray crystal structure of [Na(18-crown-

6)][U(Cp*)$_2$(SBu^t)(S)], the first f-element compound containing a metal–sulfur double bond. *Chem. Commun.* **1999,** (7), 659-660.
44. Andrez, J.; Pecaut, J.; Scopelliti, R.; Kefalidis, C. E.; Maron, L.; Rosenzweig, M. W.; Meyere, K.; Mazzanti, M., Synthesis and reactivity of a terminal uranium(IV) sulfide supported by siloxide ligands. *Chem. Sci.* **2016,** *7* (9), 5846-5856.
45. Arnold, P. L.; Stevens, C. J.; Bell, N. L.; Lord, R. M.; Goldberg, J. M.; Nichol, G. S.; Love, J. B., Multi-electron reduction of sulfur and carbon disulfide using binuclear uranium(III) borohydride complexes. *Chem. Sci.* **2017,** *8* (5), 3609-3617.
46. Avens, L. R.; Barnhart, D. M.; Burns, C. J.; Mckee, S. D.; Smith, W. H., Oxidation Chemistry of a Uranium(III) Aryloxide. *Inorg. Chem.* **1994,** *33* (19), 4245-4254.
47. Brennan, J. G.; Andersen, R. A.; Zalkin, A., Chemistry of Trivalent Uranium Metallocenes - Electron-Transfer Reactions - Synthesis and Characterization of [(MeC$_5$H$_4$)$_3$U]$_2$E (E = S, Se, Te) and the Crystal Structures of [(MeC$_5$H$_4$)$_3$U]$_2$S and (MeC$_5$H$_4$)$_3$UOPPh$_3$. *Inorg. Chem.* **1986,** *25* (11), 1761-1765.
48. Brown, J. L.; Wu, G.; Hayton, T. W., Chalcogen Atom Transfer to Uranium(III): Synthesis and Characterization of [(R$_2$N)$_3$U]$_2$(μ-E) and [(R$_2$N)$_3$U]$_2$(μ-η^2:η^2-S$_2$) (R = SiMe$_3$; E = S, Se, Te). *Organometallics.* **2013,** *32* (5), 1193-1198.
49. Camp, C.; Antunes, M. A.; Garcia, G.; Ciofini, I.; Santos, I. C.; Pecaut, J.; Almeida, M.; Marcalo, J.; Mazzanti, M., Two-electron versus one-electron reduction of chalcogens by uranium(III): synthesis of a terminal U(V) persulfide complex. *Chem. Sci.* **2014,** *5* (2), 841-846.
50. Diaconescu, P. L.; Arnold, P. L.; Baker, T. A.; Mindiola, D. J.; Cummins, C. C., Arene-bridged diuranium complexes: Inverted sandwiches supported by delta backbonding. *J. Am. Chem. Soc.* **2000,** *122* (25), 6108-6109.
51. Diaconescu, P. L.; Cummins, C. C., μ-η^6,η^6-Arene-Bridged Diuranium Hexakisketimide Complexes Isolable in Two States of Charge. *Inorg. Chem.* **2012,** *51* (5), 2902-2916.
52. Evans, W. J.; Montalvo, E.; Ziller, J. W.; DiPasquale, A. G.; Rheingold, A. L., Uranium Metallocene Complexes of the 1,3,4,6,7,8-Hexahydro-*2H*-pyrimido[1,2-*a*]pyrimidinato Ligand, (hpp)$^-$. *Inorg. Chem.* **2010,** *49* (1), 222-228.
53. Evans, W. J.; Takase, M. K.; Ziller, J. W.; DiPasquale, A. G.; Rheingold, A. L., Reductive Reactivity of the Tetravalent Uranium Complex [η^5-C$_5$Me$_5$)(η^8-C$_8$H$_8$)U]$_2$(μ-η^3:η^3-C$_8$H$_8$). *Organometallics.* **2009,** *28* (1), 236-243.
54. Franke, S. M.; Rosenzweig, M. W.; Heinemann, F. W.; Meyer, K., Reactivity of uranium(III) with H$_2$E (E = S, Se, Te): synthesis of a series of mononuclear and dinuclear uranium(IV) hydrochalcogenido complexes. *Chem. Sci.* **2015,** *6* (1), 275-282.
55. Gardner, B. M.; King, D. M.; Tuna, F.; Wooles, A. J.; Chilton, N. F.; Liddle, S. T., Assessing crystal field and magnetic interactions in diuranium-μ-chalcogenide triamidoamine complexes with U(IV)-E-U(IV) cores (E = S, Se, Te): implications for determining the presence or absence of actinide-actinide magnetic exchange. *Chem. Sci.* **2017,** *8* (9), 6207-6217.
56. Gaunt, A. J.; Scott, B. L.; Neu, M. P., U(IV) chalcogenolates synthesized via oxidation of uranium metal by dichalcogenides. *Inorg. Chem.* **2006,** *45* (18), 7401-7407.
57. Lam, O. P.; Heinemann, F. W.; Meyer, K., Activation of elemental S, Se and Te with uranium(III): bridging U-E-U (E = S, Se) and diamond-core complexes U-E$_2$-U (E = O, S, Se, Te). *Chem. Sci.* **2011,** *2* (8), 1538-1547.

58. Leverd, P. C.; Arliguie, T.; Lance, M.; Nierlich, M.; Vigner, J.; Ephritikhine, M., Monocyclooctatetraene Uranium Thiolate Complexes - Crystal-Structure of $[(U(\eta\text{-}C_8H_8)(\mu\text{-}SPr^i)_2)_2]$. *J. Chem. Soc., Dalton Trans.* **1994,** (4), 501-504.
59. Leverd, P. C.; Lance, M.; Vigner, J.; Nierlich, M.; Ephritikhine, M., Synthesis and Reactions of Uranium(IV) Tetrathiolate Complexes. *J. Chem. Soc., Dalton Trans.* **1995,** (2), 237-244.
60. Shinomoto, R.; Zalkin, A.; Edelstein, N. M., Preparation and Crystal-Structures of Tetrakis-(Methyltrihydroborato)Uranium(IV)Bis(Tetrahydrofuranate) and Tetrakis(Methyltrihydroborato)-Uranium(IV)Tetrahydrothiophenate. *Inorg. Chim. Acta.* **1987,** *139* (1-2), 91-95.
61. Arliguie, T.; Blug, M.; Le Floch, P.; Mezailles, N.; Thuery, P.; Ephritikhine, M., Organouranium complexes with phosphinine-based SPS pincer ligands. Variations with the substituent at the phosphorus atom. *Organometallics.* **2008,** *27* (16), 4158-4165.
62. Arliguie, T.; Thuery, P.; Le Floch, P.; Mezailles, N.; Ephritikhine, M., A homoleptic SPS-based complex and a double-cubane-type sulfur cluster of an actinide element. *Polyhedron.* **2009,** *28* (8), 1578-1582.
63. Clark, D. L.; Gordon, J. C.; Huffman, J. G.; Watkin, J. G.; Zwick, B. D., Preparation of mono-pentamethylcyclopentadienyl uranium(IV) sulfido clusters through oxidation of $(\eta\text{-}C_5Me_5)UI_2(THF)_3$ - X-ray structural characterization of $(\eta\text{-}C_5Me_5)_3U_3(\mu_3\text{-}I)(\mu_3\text{-}S)(\mu_2\text{-}I)_3I_3$. *New Journal of Chemistry.* **1995,** *19* (5-6), 495-502.
64. Arliguie, T.; Thuery, P.; Fourmigue, M.; Ephritikhine, M., Reduction of dithiocarbonates as a novel route to dithiolene compounds of uranium. Crystal structure of the first bimetallic dithiolene complex of an f-element. *Organometallics.* **2003,** *22* (14), 3000-3003.
65. Evans, W. J.; Miller, K. A.; Hillman, W. R.; Ziller, J. W., Two-electron reductive reactivity of trivalent uranium tetraphenylborate complexes of $(C_5Me_5)^{1-}$ and $(C_5Me_4H)^{1-}$. *J. Organomet. Chem.* **2007,** *692* (17), 3649-3654.
66. Evans, W. J.; Miller, K. A.; Kozimor, S. A.; Ziller, J. W.; DiPasquale, A. G.; Rheingold, A. L., Actinide hydride complexes as multielectron reductants: Analogous reduction chemistry from $[(C_5Me_5)_2UH]_2$, $[(C_5Me_5)_2UH_2]_2$, and $[(C_5Me_5)_2ThH_2]_2$. *Organometallics.* **2007,** *26* (14), 3568-3576.
67. Evans, W. J.; Miller, K. A.; Ziller, J. W.; DiPasquale, A. G.; Heroux, K. J.; Rheingold, A. L., Formation of $(C_5Me_5)_2U(EPh)Me$, $(C_5Me_5)_2U(EPh)_2$, and $(C_5Me_5)_2U(\eta^2\text{-}TeC_6H_4)$ from $(C_5Me_5)_2UMe_2$ and PhEEPh (E = S, Se, Te). *Organometallics.* **2007,** *26* (17), 4287-4293.
68. Evans, W. J.; Walensky, J. R.; Ziller, J. W., Reaction Chemistry of the U^{3+} Metallocene Amidinate $(C_5Me_5)_2[^iPrNC(Me)N^iPr]U$ Including the Isolation of a Uranium Complex of a Monodentate Acetate. *Inorg. Chem.* **2010,** *49* (4), 1743-1749.
69. Graves, C. R.; Scott, B. L.; Morris, D. E.; Kiplinger, J. L., Facile access to pentavalent uranium organometallics: One-electron oxidation of Uranium(IV) imido complexes with copper(I) salts. *J. Am. Chem. Soc.* **2007,** *129* (39), 11914-11915.
70. Graves, C. R.; Scott, B. L.; Morris, D. E.; Kiplinger, J. L., Selenate and tellurate complexes of pentavalent uranium. *Chem. Commun.* **2009,** (7), 776-778.
71. Karmazin, L.; Mazzanti, M.; Pecaut, J., Unique crown thioether complexes of f elements: the crystal structure of U(III) and La(III) complexes of 1,4,7-trithiacyclononane. *Chem. Commun.* **2002,** (6), 654-655.

72. Leverd, P. C.; Ephritikhine, M.; Lance, M.; Vigner, J.; Nierlich, M., Triscyclopentadienyl uranium thiolates and selenolates. *J. Organomet. Chem.* **1996,** *507* (1-2), 229-237.
73. Rosenzweig, M. W.; Hummer, J.; Scheurer, A.; Lamsfus, C. A.; Heinemann, F. W.; Maron, L.; Mazzanti, M.; Meyer, K., A complete series of uranium(IV) complexes with terminal hydrochalcogenido (EH) and chalcogenido (E) ligands E = O, S, Se, Te. *Dalton Trans.* **2019,** *48* (29), 10853-10864.
74. Santos, I. G.; Abram, U., Synthesis and structures of dioxouranium complexes with 2-pyridineformamide thiosemicarbazones. *Inorg. Chem. Commun.* **2004,** *7* (3), 440-442.
75. Sitran, S.; Fregona, D.; Casellato, U.; Vigato, P. A.; Graziani, R.; Faraglia, G., Dioxouranium(VI) Complexes with Pentadentate Bases Containing Acetal Groups. *Inorg. Chim. Acta.* **1987,** *132* (2), 279-288.
76. Thomson, R. K.; Graves, C. R.; Scott, B. L.; Kiplinger, J. L., Synthesis and Molecular Structure of $(C_5Me_5)_2U(O^tBu)(SePh)$: A Mixed-Ligand Alkoxide-Selenide Uranium(IV) Metallocene Complex Resulting from tert-Butoxy-Trimethylsilane Elimination. *J. Chem. Crystallogr.* **2011,** *41* (8), 1241-1244.
77. Zalkin, A.; Brennan, J. G., A Trivalent-Uranium Thioether Coordination Compound. *Acta. Crystallogr. C.* **1985,** *41* (Sep), 1295-1297.
78. Clark, D. L.; Miller, M. M.; Watkin, J. G., Synthesis, Characterization, and X-Ray Structure of the Uranium Thiolate Complex $U(S\text{-}2,6\text{-}Me_2C_6H_3)[N(SiMe_3)_2]_3$. *Inorg. Chem.* **1993,** *32* (5), 772-774.
79. Leverd, P. C.; Lance, M.; Nierlich, M.; Vigner, J.; Ephritikhine, M., Synthesis and Crystal-Structure of Homoleptic Uranium Hexathiolates - $[NEt_2H_2]_2[U(SPh)_6]$ and $[(Ph_3P)Cu(\mu\text{-}SPh)_3\text{-}U(\mu\text{-}SPh)_3Cu(PPh_3)]$. *J. Chem. Soc. Dalton.* **1994,** (24), 3563-3567.
80. Spencer, L. P.; Yang, P.; Scott, B. L.; Batista, E. R.; Boncella, J. M., Oxidative Addition to U(V)-U(V) Dimers: Facile Routes to Uranium(VI) Bis(imido) Complexes. *Inorg. Chem.* **2009,** *48* (24), 11615-11623.
81. Spencer, L. P.; Yang, P.; Scott, B. L.; Batista, E. R.; Boncella, J. M., Uranium(VI) Bis(imido) Chalcogenate Complexes: Synthesis and Density Functional Theory Analysis. *Inorg. Chem.* **2009,** *48* (6), 2693-2700.
82. Tomson, N. C.; Anderson, N. H.; Tondreau, A. M.; Scott, B. L.; Boncella, J. M., Oxidation of uranium(IV) mixed imido-amido complexes with PhEEPh and to generate uranium(VI) bis(imido) dichalcogenolates, $U(NR)_2(EPh)_2(L)_2$. *Dalton Trans.* **2019,** *48* (29), 10865-10873.
83. Fenske, D.; Kraustscheid, H.; Balter, S., Synthese und Struktur neuer Cu-Cluster: $[Cu_{30-x}Se_{15}(P^iPr_3)_{12}]$ (x = 0,1) und $[Cu_{36}Se_{18}(P^tBu_3)_{12}]$. *Angew. Chemie.* **1990,** *102* (7), 799-801.
84. Fenske, D.; Krautscheid, H., Neue Kupfercluster mit Se und PEt_3 als Liganden: $[Cu_{70}Se_{35}(PEt_3)_{22}]$ und $[Cu_{20}Se_{13}(PEt_3)_{12}]$. *Angew. Chemie.* **1990,** *102* (12), 1513-1516.
85. Krautscheid, H.; Fenske, D.; Baum, G.; Semmelmann, M., A New Copper Selenide Cluster with PPh_3 Ligands: $[Cu_{146}Se_{73}(PPh_3)_{30}]$. *Angew. Chemie. Int. Ed.* **1993,** *32* (9), 1303-1305.
86. Rehe, D.; Kornienko, A. Y.; Emge, T. J.; Brennan, J. G., Thorium Compounds with Bonds to Sulfur or Selenium: Synthesis, Structure, and Thermolysis. *Inorg. Chem.* **2016,** *55* (14), 6961-7.
87. Fitzgerald, M.; Emge, T. J.; Brennan, J. G., Chalcogen-rich lanthanide clusters with fluorinated thiolate ligands. *Inorg. Chem.* **2002,** *41* (13), 3528-3532.

88. Stuber, M. A.; Kornienko, A. Y.; Emge, T. J.; Brennan, J. G., Tetrametallic Thorium Compounds with Th_4E_4 (E = S, Se) Cubane Cores. *Inorg. Chem.* **2017,** *56* (17), 10247-10256.
89. Banerjee, S.; Emge, T. J.; Brennan, J. G., Heterometallic Ln/Hg Compounds with Fluorinated Thiolate Ligands. *Inorg. Chem.* **2004,** *43* (20), 6307-6312.
90. De Mel, V. S. J.; Kumar, R.; Oliver, J. P., Synthesis and characterization of alkylaluminum compounds of pentafluorothiophenol. Crystal and molecular structure of $[Me_2Al(\mu\text{-}SC_6F_5)]_2$. *Organometallics.* **1990,** *9* (4), 1303-1307.
91. Hendershot, D. G.; Kumar, R.; Barber, M.; Oliver, J. P., Phenoxides and thiophenoxides of aluminum and gallium. Evidence of a ^1H-^{19}F coupling in $(R_2MOC_6F_5)_2$ in solution. Crystal and molecular structures of $(Me_2AlOC_6F_5)_2$ and $(Me_2GaSC_6F_5)_2$. *Organometallics.* **1991,** *10* (6), 1917-1922.
92. Melman, J. H.; Emge, T. J.; Brennan, J. G., Fluorinated thiolates of divalent and trivalent lanthanides. Ln-F bonds and the synthesis of LnF_3. *Inorg. Chem.* **2001,** *40* (5), 1078-1083.
93. Melman, J. H.; Rohde, C.; Emge, T. J.; Brennan, J. G., Trivalent Lanthanide Compounds with Fluorinated Thiolate Ligands: Ln−F Dative Interactions Vary with Ln and Solvent. *Inorg. Chem.* **2002,** *41* (1), 28-33.
94. Müller, B.; Schneider, A.; Tesmer, M.; Vahrenkamp, H., Alcohol and Aldehyde Adducts of Zinc Thiolates: Structural Modeling of Alcoholdehydrogenase. *Inorg. Chem.* **1999,** *38* (8), 1900-1907.
95. Peach, M. E., Some reactions of pentafluorothiophenol. Preparation of some pentafluoro-phenylthio metal derivatives. *Canadian Journal of Chemistry.* **1968,** *46* (16), 2699-2706.
96. Moreno-Alcántar, G.; Romo-Islas, G.; Flores-Álamo, M.; Torrens, H., Aurophilicity vs. thiophilicity: directing the crystalline supramolecular arrangement in luminescent gold compounds. *New Journal of Chemistry.* **2018,** *42* (10), 7845-7852.
97. Moreno-Alcántar, G.; Turcio-García, L.; Guevara-Vela, J. M.; Romero-Montalvo, E.; Rocha-Rinza, T.; Pendás, Á. M.; Flores-Álamo, M.; Torrens, H., Directing the Crystal Packing in Triphenylphosphine Gold(I) Thiolates by Ligand Fluorination. *Inorg. Chem.* **2020,** *59* (13), 8667-8677.
98. Kindra, D. R.; Evans, W. J., Magnetic Susceptibility of Uranium Complexes. *Chem. Rev.* **2014,** *114* (18), 8865-8882.
99. Chatelain, L.; Mougel, V.; Pécaut, J.; Mazzanti, M., Magnetic communication and reactivity of a stable homometallic cation–cation trimer of pentavalent uranyl. *Chem. Sci.* **2012,** *3* (4).
100. Gardner, B. M.; Stewart, J. C.; Davis, A. L.; McMaster, J.; Lewis, W.; Blake, A. J.; Liddle, S. T., Homologation and functionalization of carbon monoxide by a recyclable uranium complex. *Proceedings of the National Academy of Sciences.* **2012,** *109* (24), 9265-9270.
101. Jones, E. R.; Hendricks, M. E.; Stone, J. A.; Karraker, D. G., Magnetic properties of the trichlorides, tribromides, and triiodides of U(III), Np(III), and Pu(III). *J. Chem. Phys.* **1974,** *60* (5), 2088-2094.
102. Lam, O. P.; Heinemann, F. W.; Meyer, K., Activation of elemental S, Se and Te with uranium(III): bridging U–E–U (E = S, Se) and diamond-core complexes U–$(E)_2$–U (E = O, S, Se, Te). *Chem. Sci.* **2011,** *2* (8).
103. Mougel, V.; Horeglad, P.; Nocton, G.; Pécaut, J.; Mazzanti, M., Stable Pentavalent Uranyl Species and Selective Assembly of a Polymetallic Mixed-Valent Uranyl Complex by Cation-Cation Interactions. *Angew. Chemie. Int. Ed.* **2009,** *48* (45), 8477-8480.

104. Nocton, G. g.; Horeglad, P.; Pécaut, J.; Mazzanti, M., Polynuclear Cation−Cation Complexes of Pentavalent Uranyl: Relating Stability and Magnetic Properties to Structure. *J. Am. Chem. Soc.* **2008,** *130* (49), 16633-16645.
105. Rosen, R. K.; Andersen, R. A.; Edelstein, N. M., $[(MeC_5H_4)_3U]_2[\mu\text{-}1,4\text{-}N_2C_6H_4]$: a bimetallic molecule with antiferromagnetic coupling between the uranium centers. *J. Am. Chem. Soc.* **1990,** *112* (11), 4588-4590.
106. Spencer, L. P.; Schelter, E. J.; Yang, P.; Gdula, R. L.; Scott, B. L.; Thompson, J. D.; Kiplinger, J. L.; Batista, E. R.; Boncella, J. M., Cation-Cation Interactions, Magnetic Communication, and Reactivity of the Pentavalent Uranium Ion $[U(N^tBu)_2]^+$. *Angew. Chemie.* **2009,** *121* (21), 3853-3856.
107. Franke, S. M.; Heinemann, F. W.; Meyer, K., Reactivity of uranium(IV) bridged chalcogenido complexes U(IV)-E-U(IV) (E = S, Se) with elemental sulfur and selenium: synthesis of polychalcogenido-bridged uranium complexes. *Chem. Sci.* **2014,** *5* (3), 942-950.
108. Spirlet, M.-R.; Rebizant, J.; Apostolidis, C.; Dornberger, E.; Kanellakopulos, B.; Powietzka, B., Oxo-bridged bimetallic organouranium complexes: The crystal structure of μ-oxo-bis[tris(cyclopentadienyl)uranium(IV)]. *Polyhedron.* **1996,** *15* (9), 1503-1508.
109. Ran, S.; Eckberg, C.; Ding, Q.-P.; Furukawa, Y.; Metz, T.; Saha, S. R.; Liu, I. L.; Zic, M.; Kim, H.; Paglione, J.; Butch, N. P., Nearly ferromagnetic spin-triplet superconductivity. *Science.* **2019,** *365* (6454), 684-687.
110. Mills, D. P.; Moro, F.; McMaster, J.; van Slageren, J.; Lewis, W.; Blake, A. J.; Liddle, S. T., A delocalized arene-bridged diuranium single-molecule magnet. *Nature Chemistry.* **2011,** *3* (6), 454-460.
111. Shannon, R. D., Revised Effective Ionic-Radii and Systematic Studies of Interatomic Distances in Halides and Chalcogenides. *Acta. Crystallogr. A.* **1976,** *32* (Sep1), 751-767.
112. Groom, C. R.; Bruno, I. J.; Lightfoot, M. P.; Ward, S. C., The Cambridge Structural Database. *Acta. Crystallogr. B.* **2016,** *72*, 171-179.
113. Roger, M.; Arliguie, T.; Thuery, P.; Ephritikhine, M., Homoleptic 2-mercapto benzothiazolate uranium and lanthanide complexes. *Inorg. Chem.* **2008,** *47* (9), 3863-3868.
114. Tourneux, J. C.; Berthet, J. C.; Cantat, T.; Thuery, P.; Mezailles, N.; Ephritikhine, M., Exploring the Uranyl Organometallic Chemistry: From Single to Double Uranium-Carbon Bonds. *J. Am. Chem. Soc.* **2011,** *133* (16), 6162-6165.
115. Kwak, J. E.; Gray, D. L.; Yun, H.; Ibers, J. A., Uranium trisulfide, US_3. *Acta. Crystallogr. E.* **2006,** *62*, I86-I87.
116. Ben Salem, A.; Meerschaut, A.; Rouxel, J., Étude structurale du triséléniure d'uranium. *C R Acad Sci Sér II.* **1984,** *299*, 617-619.
117. Noel, H., Magnetic susceptibility of the uranium trichalcogenides US_3, USe_3 and UTe_3. *Journal of the Less Common Metals.* **1986,** *121*, 265-270.
118. West, A. R., *Solid State Chemistry and its Applications*. Second edition, student edition. ed.; John Wiley & Sons, Inc.: Chichester, West Sussex, 2014; p xxiv, 556 pages.

Chapter 5: Materials and Methods

5.1 General Methods

Depleted thorium (Th-232) and depleted uranium (U-238) are radioactive as weak α-emitters with half-lives of 1.41×10^{10} years and 4.47×10^{9} years, respectively. Thorium and uranium should be handled by individuals trained for radiation safety in controlled fume hoods and gloveboxes with inert atmospheres in a laboratory equipped to handle such equipment.

All syntheses were performed under ultrapure nitrogen (Welco Praxair), using conventional drybox or Schlenk techniques. Pyridine (Aldrich) and hexane (Aldrich) were purified with a dual column Solv-Tek solvent purification system and collected immediately prior to use. $(SC_6F_5)_2$[1] and $(SeC_6F_5)_2$[2] were prepared according to literature procedures. PhSeSePh (Aldrich) was purchased and recrystallized from hexanes. PhSSPh (Acros), thorium chips and uranium turnings (International Bioanalytical Industries Inc.), mercury (Strem Chemicals), 2,2'-bipyridine (Aldrich), sulfur (Aldrich), selenium (Aldrich), silver(I) fluoride (Aldrich), 2,2'-dipyridyl disulfide (Aldrich) were purchased and used as received. Melting points were recorded in sealed capillaries and are uncorrected. IR spectra were recorded on a Thermo Nicolet Avatar 360 FTIR spectrometer from 4000 to 450 cm^{-1} as mineral oil mulls on CsI plates. UV−vis absorption spectra were recorded on a Varian DMS 100S spectrometer with the samples dissolved in pyridine, placed in either a 1.0 mm × 1.0 cm Spectrosil quartz cell or a 1.0 cm^2 special optical glass cuvette, and scanned from 200 to 1000 nm – all four thorium tetrameric compounds were found to be optically transparent from 400-1000 nm. All NMR data were collected on a Varian VNMRS 500 spectrometer at 25 °C with the compounds dissolved in NC_5D_5, C_6D_6, or toluene-

d8. ^{1}H and ^{19}F NMR spectra were obtained at 499 and 476 MHz, respectively; ^{77}Se NMR spectra were acquired with a longer relaxation delay (7.0 s) together with an extended number of scans (4096) in hydrogen or fluorine decoupled mode at 95 MHz using $(SeC_6F_5)_2$ as an external standard. Elemental analyses were performed by Quantitative Technologies, Inc. (Whitehouse, NJ).

5.2 Single Crystal X-Ray Structure Determination

Data for each compound were collected on a Bruker Smart APEX CCD diffractometer with graphite monochromatized Mo Kα radiation (λ = 0.71073 Å).[3] Crystals were immersed in mineral oil and examined at low temperatures. The data were corrected for Lorenz effects and polarization, and absorption, the latter by a multi-scan method or by a numerical method when the multi-scan method appeared insufficient.[3] The structures were solved by direct methods, and all non-hydrogen atoms were refined based upon F_{obs}^2.[4-6] All structures were visualized via the Mercury v4.3.1 program.[7]

5.3 Magnetic Susceptibility Measurements

Magnetic properties of $py_8U_4E_4(EPh)_4(E'C_6F_5)_4$ (E, E' = S and Se) were measured with a Quantum Design DynaCool Physical Property Measurement System (PPMS) equipped with vibrating-sample magnetometer (VSM) option, which operates over a temperature range of 1.8–300 K and applied magnetic fields up to 9 T. Both zero-field cooling and field-cooling modes were conducted to measure the magnetic susceptibility. The polycrystalline samples (~12mg) were packed in the plastic straw to perform the measurements.

5.4 Syntheses

Synthesis of $(bipy)_2Th(SeC_6F_5)_4 \bullet 2THF$ (1)

Th (0.116 g, 0.50 mmol) and $(SeC_6F_5)_2$ (0.492 g, 1.00 mmol) were combined with Hg (0.020 g, 0.10 mmol) in pyridine (11 mL). The solution was stirred for 24 h. The solvent was removed under vacuum, 2,2′-bipyridine (0.156 g, 1.00 mmol) and THF (14 mL) were added and the mixture was stirred for 24 h. The resulting red solution was filtered to remove trace greenish precipitate and layered with hexane (10 mL) to form pale yellow (0.77 g, 46%) crystals that turn brown-deep orange at 101 °C, melt at 105 °C and decompose at 173 °C. Anal. calcd for $C_{52}H_{32}F_{20}O_2N_4Se_4Th$: C, 37.3; H, 1.93; N, 3.35 (lattice desolvated $C_{44}H_{16}F_{20}N_4Se_4Th$: C, 34.6; H, 1.05; N, 3.67). Found: C, 36.7; H, 1.63; N, 3.36. UV-vis: this compound does not show an optical absorption maximum from 400 to 1000 nm. IR: 2957 (s), 2923 (s), 2853 (s), 2361 (w), 1598 (w), 1462 (m), 1376 (m), 1261 (m), 1153 (w), 1081 (m), 1013 (m), 967 (w), 800 (m), 722 (w) cm^{-1}. ^1H NMR (pyridine-d_5): 10.2 (d, 2H, J = 5.0 Hz, bipy), 8.47 (dt, 2H, J = 8.5, 1.0 Hz, bipy), 8.21 (td, 2H, J = 7.7, 1.6 Hz, bipy), 7.73 (ddd, 2H, J = 7.5, 5.5, 1.1 Hz, bipy), 3.64 (m, 3H,THF), 1.61 (m, 3H, THF). ^{19}F NMR (pyridine-d_5): −124 (m, 2F), −161 (s, 1F), −163 (m, 2F). ^{77}Se NMR (pyridine-d_5): 361 (s).

Synthesis of $pyTh(Spy)_4 \bullet 0.5py$ (2)

Th (0.232 g, 1.00 mmol) and 2,2'-dithiodipyridine (0.441 g, 2.0 mmol) were combined with Hg (0.017 g, 0.085 mmol) in pyridine (10 mL). The solution was stirred for 3 days, after which toluene (5 mL) was added to the cloudy green solution, and the mixture was stirred briefly (about 15 minutes). After all precipitate settled, the resulting red solution was filtered (10 mL) and layered with hexane (5 mL) to form colorless crystals that melt at 180°C and decompose at 300°C. IR: 2924 (s), 2854 (s),

2361 (m), 1727 (m), 1641 (w), 1584 (w), 1460 (m), 1412 (w), 1376 (m), 1261 (m), 1129 (w), 1037 (w), 890 (w), 804 (w), 750 (w), 725 (w), 638 (w), 624 (w), 482 (w), 447 (w) cm^{-1}. Anal. Calcd for lattice desolvated $C_{25}H_{21}N_5S_4Th$: C, 39.9; H, 2.82; N, 9.32. Found: C, 39.8; H, 2.63; N, 9.25.

Synthesis of $pyU(Spy)_4$ (3)

U (0.220 g, 0.924 mmol) and 2,2'-dithiodipyridine (0.407 g, 1.85 mmol) were combined with Hg (0.021 g, 0.11 mmol) in pyridine (10 mL). The solution was stirred for 6 days, after which toluene (5 mL) and pyridine (5 mL) was added to the dark cloudy green solution, and the mixture was stirred briefly (about 15 minutes). After all prcipitate settled, the resulting dark green solution was filtered (15 mL) and layered with hexane (10 mL) at 0°C to form yellow crystals that melt at 180°C and decompose at 250°C. IR: 2923 (s), 2853 (s), 1644 (w), 1577 (w), 1574 (w), 1539 (w), 1505 (w) , 1463 (m), 1455 (m), 1373 (m), 1260 (w), 1219 (w), 1183 (w), 1129 (w), 1085 (w), 1067 (w), 1037 (w), 1002 (w), 725 (w) cm^{-1}. Anal. Calcd for $C_{25}H_{21}N_5S_4U$: C, 39.6; H, 2.79; N, 9.24. Found: C, 39.7; H, 2.81; N, 9.30.

Synthesis of $py_4Th_2(Se_2)_2I_2(Spy)_2 \cdot 4py$ (4)

Th (0.233 g, 1.00 mmol), $(SePh)_2$ (0.314 g, 1.01 mmol), 2,2'-dithiodipyridine (0.114 g, 0.517 mmol), and I_2 (0.130 g, 0.512 mmol) were combined with Hg (0.019 g, 0.095 mmol) in pyridine (10 mL). The solution was stirred for 1 day, after which pyridine (10 mL) and selenium (0.160 g, 2.03 mmol) was added to the cloudy green solution and stirred for 2 hours. After all precipitate settled, the resulting orange solution was filtered (10 mL) and layered with hexane (7 mL) at 0°C to form orange crystals that melt at 150°C and decompose at 215°C. IR: 2964 (s), 2723 (m), 1597 (w), 1459 (s), 1377 (s), 1263 (w), 1220 (w) , 1151 (w), 1132 (w), 1065 (w), 1037 (w),

1001 (w), 724 (w), 700 (w), 622 (w), 465 (w), 421 (w) cm^{-1}. Anal. Calcd for $C_{50}H_{48.35}N_{10}S_{1.66}Se_4Th_4$: C, 25.2; H, 2.04; N, 5.87. Found: C, 25.7; H, 1.72; N, 5.23.

Synthesis of $py_2UI_2(Spy)_2 \bullet 0.5py$ (5)

U (0.248 g, 1.04 mmol), 2,2'-dithiodipyridine (0.230 g, 1.04 mmol) and I_2 (0.264 g, 1.04 mmol) were combined in pyridine (10 mL). The solution was stirred for 4 days, after which toluene (5 mL) was added to the dark red solution, and the mixture was stirred briefly (about 15 minutes). After all prcipitate settled, the resulting dark red solution was filtered (15 mL) and layered with hexane (15 mL) at 0°C to form orange-red crystals that melt at 140°C and decompose at 200°C. IR: 2924 (s), 2854 (s), 1633 (w), 1599 (w), 1583 (w), 1544 (w), 1459 (m) , 1442 (m), 1412 (m), 1377 (m), 1263 (w), 1217 (w), 1134 (w), 1085 (w), 1065 (w), 1037 (w), 1002 (w), 878 (w), 802 (w) 759 (w), 728 (w), 700 (w), 693 (w), 623 (w), 481 (w) cm^{-1}. Anal. Calcd for $C_{22.5}H_{20.5}I_2N_{4.5}S_2U$: C, 29.7; H, 2.27; N, 6.93. Found: C, 29.4; H, 2.54; N, 6.68.

Synthesis of $(py)_7Th_2F_5(SC_6F_5)_3 \cdot 2py$ (6)

Th (0.232 g, 1.00 mmol), $(SPh)_2$ (0.330 g, 1.51 mmol), $(SC_6F_5)_2$ (0.200 g, 0.503 mmol), and Hg (0.019 g, 0.095 mmol) were combined in pyridine (20 mL) and the solution was stirred for 5 d at 25°C. AgF (0.190 g, 1.50 mmol) was added to the cloudy gray solution and stirred for additional 24 h. The resulting red solution (15 mL) was filtered and layered with hexane (20 mL) to form colorless crystals (0.219 g, 23%), that melt at 155°C and decompose at 275°C. Anal. Calcd for $C_{63}H_{45}F_{20}N_9S_3Th_2$: C, 40.5; H, 2.43; N, 6.75. Found: C, 39.8; H, 2.56; N, 6.64. IR: 2926 (s), 1620 (w), 1505 (m), 1463 (s), 1377 (s), 1260 (w), 1225 (w), 1153 (w), 1071 (w), 1039 (w), 1008 (w), 968 (w), 861 (w), 810 (w), 754 (w), 744 (w), 700 (m), 623

(w) cm^{-1}. ^{1}H NMR (toluene-d_8): 8.33 (m, 2H), 6.88 (m, 1H), 6.56 (m, 2H). ^{19}F NMR (toluene-d_8): -137 (d, 2F), -159 (t, 1F), -162 (td, 2F).

Synthesis of $(py)_8Th_4S_4(SPh)_4(SC_6F_5)_4 \bullet 2py$ (7)

Th (0.232 g, 1.00 mmol), $(SPh)_2$ (0.328 g, 1.50 mmol), and $(SC_6F_5)_2$ (0.200 g, 0.503 mmol) were combined with Hg (0.023 g, 0.11 mmol) in pyridine (15 mL). The solution was stirred for 2 days, elemental S (0.032 g, 1.0 mmol) was added, and the mixture was stirred for 1 h. The resulting red solution (15 mL) was filtered and layered with hexane (20 mL) to form colorless crystals (0.20 g, 26 %) that melt at 140°C and decompose at 200°C. IR: 2925 (s), 2854 (s), 2360 (m), 2342 (m), 1600 (w), 1577 (w), 1499 (w), 1459 (m), 1377 (m), 1263 (w), 1221 (w), 1153 (w), 1081 (w), 1066 (w), 1037 (w), 1002 (w), 968 (w), 860 (w), 737 (w), 691 (w), 668 (w), 621 (w) cm^{-1}. Anal. Calcd for $C_{98}H_{70}F_{20}N_{10}S_{12}Th_4$: C, 38.2; H, 2.29; N, 4.55. Found: C, 37.8; H, 2.35; N, 4.37. ^{1}H NMR: 8.70 (m, 2H, py), 7.55 (m, 1H, py), 7.18 (m, 2H, py), 6.91 (d, 2H, SePh), 6.43 (m, 1H, SePh), 6.39 (m, 2H, SePh). ^{19}F NMR: -128 (d, 2F), -166 (t, 1F), -167 (t, 2F).

Synthesis of $(py)_8Th_4Se_4(SePh)_4(SeC_6F_5)_4 \bullet 2py$ (8)

Th (0.232 g, 1.00 mmol), $(SePh)_2$ (0.469 g, 1.50 mmol), and $(SeC_6F_5)_2$ (0.246 g, 0.500 mmol) were combined with Hg (0.023 g, 0.11 mmol) in pyridine (20 mL). The solution was stirred for 24 h, then elemental Se (0.080 g, 1.0 mmol) was added and the mixture was stirred for 2 h. The resulting red solution (12 mL) was filtered from grey precipitate and layered with hexane (14 mL) to form colorless crystals (0.51 g, 56%) that melt at 160°C and decompose at 200°C. IR: 3730 (s), 2924 (s), 2854 (s), 2360 (m), 2341 (m), 1600 (w), 1498 (w), 1459 (m), 1376 (m), 964 (w), 730 (w), 690 (w), 668 (w) cm^{-1}. Anal. Calcd for $C_{98}H_{70}F_{20}N_{10}Se_{12}Th_4$: C, 32.3; H, 1.94; N, 3.84.

Found: C, 33.0; H, 2.09; N, 4.31. ^{1}H NMR: 8.70 (m, 2H, py), 7.55 (m, 1H, py), 7.18 (m, 2H, py), 6.96 (d, *J* = 10.0 Hz, 2H, SePh), 6.57 (m, H, SePh), 6.45 (t, J = 4.99 Hz, 2H, SePh). ^{19}F NMR: -120 (d, 2F), -164 (t, 1F), -166 (t, 2F). ^{77}Se NMR: 915 (s, μ_3-Se), 480 (s, μ_2-SePh), 369 (s, η-SeC_6F_5). For comparison, the ^{77}Se resonance for $(py)_4Th(SeC_6F_5)_4$ (pyridine-d_5, 25°C) is 400 ppm and the ^{77}Se peak for $(SeC_6F_5)_2$ in pyridine is 377 ppm.

Synthesis of $(py)_8Th_4S_4(SPh)_4(SeC_6F_5)_4 \bullet 2py$ (9)

Th (0.233 g, 1.00 mmol), $(SPh)_2$ (0.329 g, 1.51 mmol), and $(SeC_6F_5)_2$ (0.247 g, 0.502 mmol) were combined with Hg (0.017 g, 0.085 mmol) in pyridine (20 mL). The mixture was stirred for 4 days, elemental sulfur (0.032 g, 1.0 mmol) was added, and the mixture was stirred for 1 h. The resulting orange solution (20 mL) was filtered and layered with hexane (17 mL) to form colorless crystals (0.33 g, 41%) that melt at 130 °C and decompose at 220 °C. IR: 2924 (s), 2283 (w), 1600 (w), 1462 (m), 1377 (m), 1222 (w), 1067 (w), 1037 (w), 1002 (w), 965 (w), 814 (w), 692 (w) cm^{-1}. Anal. Calcd for $C_{98}H_{70}F_{20}N_{10}S_8Se_4Th_4$: C, 36.0; H, 2.16; N, 4.29. Found: C, 35.8; H, 2.01; N, 4.04. ^{1}H NMR: 8.70 (m, 2H, py), 7.55 (m, 1H, py), 7.18 (m, 2H, py), 6.88 (d,, 2H, SePh), 6.46 (m, 1H, SePh), 6.42 (m, 2H, SePh). ^{19}F NMR: -121 (d, 2F), -163 (t, 1F), -166 (t, 2F). This compound was not sufficiently soluble to give ^{77}Se NMR data.

Synthesis of $(py)_8Th_4Se_4(SePh)_4(SC_6F_5)_4 \bullet 2py$ (10)

Th (0.233 g, 1.00 mmol), $(SePh)_2$ (0.470 g, 1.51 mmol), $(SC_6F_5)_2$ (0.200 g, 0.503 mmol) and Hg (0.019 g, 0.095 mmol) were combined in pyridine (15 mL). The solution was stirred for 24 h, elemental Se (0.080 g, 1.0 mmol) was added to the grey/green solution, and the mixture was stirred for 2 h. The resulting yellow/green solution (12 mL) was filtered from grey precipitate and layered with hexane (18 mL)

to form colorless crystals (0.46g, 53%) that melt at 100°C and decompose at 200°C. IR: 2922 (m), 1632 (w), 1601 (w), 1573 (w), 1504 (m), 1455 (m), 1378 (m), 1222 (w), 1154 (w), 1080 (w), 1066 (w), 1021 (w), 1003 (w), 967 (w), 860 (w), 735 (w), 691 (w), 624 (w) cm^{-1}. Anal. Calcd for $C_{98}H_{70}F_{20}N_{10}S_4Se_8Th_4$: C, 34.1; H, 2.04; N, 4.05. Found: C, 34.5; H, 2.12; N, 3.93. ^1H NMR: 8.70 (m, 2H, py), 7.55 (m, 1H, py), 7.18 (m, 2H, py), 7.00 (d, 2H, SePh), 6.55 (m, H, SePh), 6.42 (t, 2H, SePh). ^{19}F NMR: -127 (d, 2F), -166 (t, 1F), -167 (t, 2F). ^{77}Se NMR: 904 (s, μ_3-Se), 479 (s, μ_2-SePh).

Synthesis of $(py)_8U_4S_4(SPh)_4(SC_6F_5)_4 \bullet 2py$ (11)

U (0.24 g, 1.00 mmol), $(SPh)_2$ (0.34 g, 1.50 mmol), and $(SC_6F_5)_2$ (0.20 g, 0.500 mmol) were combined with I_2 (0.030 g, 0.12 mmol) in pyridine (10 mL). The solution was stirred for 2 weeks, after which toluene (10 mL) and elemental S (0.032 g, 1.0 mmol) were added, and the mixture was stirred for 1 h. The resulting red solution (20 mL) was filtered and layered with hexane (20 mL) to form red crystals that melt at 130°C and decompose at 240°C. IR: 2924 (s), 2854 (s), 1600 (m), 1577 (m), 1600 (w), 1500 (w), 1459 (w), 1377 (m), 1377 (m), 1222 (w), 1153 (w), 1082 (w), 1068 (w), 1037 (w), 1037 (w), 1025 (w), 1004 (w), 969 (w), 860 (w), 738 (w), 693 (w), 621 (w), 482 (w) cm^{-1}. Anal. Calcd for $C_{98}H_{70}F_{20}N_{10}S_{12}U_4$: C, 37.9; H, 2.27; N, 4.51. Found: C, 37.5; H, 2.36; N, 3.95.

Synthesis of $(py)_8U_4Se_4(SePh)_4(SeC_6F_5)_4 \bullet 4py$ (12)

U (0.24 g, 1.00 mmol), $(SePh)_2$ (0.47 g, 1.50 mmol), and $(SeC_6F_5)_2$ (0.25 g, 0.500 mmol) were combined with I_2 (0.030 g, 0.12 mmol) in pyridine (10 mL). The solution was stirred for 7 days, then toluene (10 mL) and elemental Se (0.080 g, 1.0 mmol) was added and the mixture was stirred for 2 h. The resulting red solution (15 mL) was filtered from grey precipitate and layered with hexane (20 mL) and stored at

0°C for one week to yield red crystals that melt at 120°C and decompose at 230°C. IR: 2918 (m), 2854 (m), 1937 (m), 1861 (m), 1628 (w), 1599 (w), 1574 (m), 1440 (m), 1378 (w), 1267 (w), 1223 (w), 1178 (w), 1151 (w), 1131 (w), 1067 (w), 1038 (w), 964 (w), 872 (w), 811 (w), 693 (w), 664 (w), 624 (w), 603 (w), 581 (w), 468 (w), 421 (w) cm^{-1}. Anal. Calcd for 2py solvate $C_{98}H_{70}F_{20}N_{10}Se_{12}U_4$: C, 32.1; H, 1.92; N, 3.82. Found: C, 32.6; H, 1.88; N, 3.67.

Synthesis of $(py)_8U_4S_4(SPh)_4(SeC_6F_5)_4 \bullet 2py$ (13)

U (0.238 g, 1.00 mmol), $(SPh)_2$ (0.328 g, 1.50 mmol), and $(SeC_6F_5)_2$ (0.246 g, 0.500 mmol) were combined with I_2 (0.030 g, 0.12 mmol) in pyridine (10 mL). The mixture was stirred for 7 days, then toluene (10 mL) and elemental sulfur (0.032 g, 1.0 mmol) was added, and the mixture was stirred for 1 h. The resulting red solution (15 mL) was filtered and layered with hexane (25 mL) to form colorless crystals (0.331 g, 40.2%) that melt at 150 °C and decompose at 200 °C. IR: 2924 (s), 2854 (s), 1600 (m), 1500 (m), 1459 (m), 1377 (m), 1261 (m), 1222 (m), 1079 (m), 1024 (m), 966 (w), 801 (w), 737 (w), 693 (w), 621 (w), 482 (w) cm^{-1}. Anal. Calcd for $C_{98}H_{70}F_{20}N_{10}S_8Se_4U_4$: C, 35.8; H, 2.14; N, 4.25. Found: C, 35.1; H, 2.27; N, 3.66.

Synthesis of $(py)_8U_4Se_4(SePh)_4(SC_6F_5)_4 \bullet 3.5py$ (14)

U (0.233 g, 1.00 mmol), $(SePh)_2$ (0.468 g, 1.50 mmol), $(SC_6F_5)_2$ (0.200 g, 0.503 mmol) and I_2 (0.030 g, 0.12 mmol) were combined in pyridine (10 mL). The solution was stirred for 4 days, then toluene (10 mL) and elemental Se (0.080 g, 1.0 mmol) was added to the red solution, and the mixture was stirred for 2 h. The resulting red solution (10 mL) was filtered from grey precipitate and layered with hexane (25 mL) to form red crystals that melt at 150°C and decompose at 220°C. IR: 2922 (m), 1626 (w), 1600 (w), 1573 (w), 1501 (m), 1463 (m), 1377 (m), 1261 (w), 1153 (w), 1221

(w), 1067 (w), 1021 (w), 1036 (w), 1021 (w), 1003 (w), 968 (w), 860 (w), 800 (w), 735 (w), 701 (w), 691 (w), 622 (w) cm^{-1}. Anal. Calcd for 2 py solvate $C_{98}H_{70}F_{20}N_{10}S_4Se_8U_4$: C, 33.8; H, 2.03; N, 4.03. Found: C, 33.5; H, 2.24; N, 4.04. ^1H NMR:

Attempted synthesis of U/$(SeC_6F_5)_2$/I_2/py

U (0.119 g, 0.50 mmol), $(SeC_6F_5)_2$ (0.984 g, 2.0 mmol), and catalytic amount of I_2 were combined in pyridine (20 mL). The solution was stirred for 7 days, heating in an oil bath at 60°C for 24 h. The resulting dark black solution (10 mL) was filtered from grey precipitate and dark oil precipitate crashed out of solution after a few days.

Attempted synthesis of U/$(SC_6F_5)_2$/I_2/py

U (0.249 g, 1.05 mmol), $(SC_6F_5)_2$ (0.630 g, 1.58 mmol), and catalytic amount of I_2 were combined in pyridine (20 mL). The solution was stirred for 4 days in 0°C freezer. The resulting dark green solution (8 mL) was filtered from green precipitate and 10 mL py was added. Layered with 20 mL hexanes and placed in 0°C freezer. No crystal formation.

Attempted synthesis of U/$(SeC_6F_5)_2$/I_2/py

U (0.116 g, 0.487 mmol), $(SeC_6F_5)_2$ (0.364 g, 0.740 mmol), and catalytic amount of I_2 were combined in pyridine (20 mL). The solution was stirred for 4 days in 0°C freezer. The resulting dark black solution (10 mL) was filtered from dark black precipitate and layered with 20 mL hexanes and placed in 0°C freezer. A dark oil precipitated.

Attempted synthesis of Th/$(SePh)_2$/Hg/bipy/py/THF

Th (0.232 g, 1.00 mmol), $(SePh)_2$ (0.468 g, 1.50 mmol), and bipy (0.312 g, 2.00 mmol) were combined in THF (15 mL) with a catalytic amount of Hg. The

solution was stirred for 5 days, but metal did not dissolve so THF was evaporated under vacuum and pyridine added. The solution stirred in 70°C oil bath for 1 week. Filtered 10 mL deep red solution once all metal dissolved and layered with 10 mL hexanes, forming a deep red oil.

Attempted synthesis of U/$(SePh)_2$/I_2/bipy/THF

U (0.229 g, 0.962 mmol), $(SePh)_2$ (0.450 g, 1.44 mmol), and bipy (0.301 g, 1.93 mmol) were combined in THF (15 mL) with a catalytic amount of I_2. The solution was stirred for 7 days. Filtered 15 mL deep black/red solution and layered with 25 mL hexanes, forming an oil.

Attempted synthesis of Th/$(SePh)_2$/Hg/bipy/py

Th (0.232 g, 1.00 mmol), $(SePh)_2$ (0.468 g, 1.50 mmol), and bipy (0.312 g, 2.00 mmol) were combined in py (15 mL) with a catalytic amount of Hg. The solution was stirred for 10 days. The deep red solution (15 mL) was filtered once all metal dissolved and layered with 10 mL hexanes, forming a deep red oil.

Attempted synthesis of U/$(SeC_6F_5)_2$/I_2/bipy/py/THF

U (0.111 g, 0.466 mmol), $(SeC_6F_5)_2$ (0.460 g, 0.934 mmol), and I_2 (0.018 g, 0.07 mmol) were combined in pyridine (20 mL). The solution was stirred for 5 days, heating in an oil bath at 60°C for 24 h. The resulting dark black/green solution was evaporated on Schlenk line and sample redissolved in THF and added bipy (0.147 g, 0.942 mmol). Let stir overnight. Filtered red solution and layered with 20 mL hexanes forming a powdery product.

Attempted synthesis of Th/$(SePh)_2$/Hg/$(Ph)_2PP(Ph)_2$/Hg/py

Th (0.116 g, 0.50 mmol) and $(SePh)_2$ (0.312 g, 1.00 mmol) were combined in py (12 mL) with a catalytic amount of Hg and stirred for 1 d. Pyridine was evaporated

via vacuum and sample was redissolved in 12 mL toluene and added $(Ph)_2PP(Ph)_2$ (0.185 g, 0.5 mmol), which was then stirred in 70°C oil bath for 1 d. Evaporated all toluene from the flask via vacuum and redissolved sample in THF to form an orange solution (15 mL). The solution was filtered and layered with 15 mL hexanes, forming a powdery product.

Attempted synthesis of U/$(SePh)_2$/Hg/$(Ph)_2PP(Ph)_2$/py

U (0.119 g, 0.50 mmol) and $(SePh)_2$ (0.312 g, 1.00 mmol) were combined in py (12 mL) with a catalytic amount of I_2 and stirred for 1 week, heating in 70°C oil bath for 1 d. Pyridine was evaporated via vacuum and sample was redissolved in 12 mL THF and added $(Ph)_2PP(Ph)_2$ (0.185 g, 0.5 mmol), which was then stirred for 1 d, yielding a black solution. Added ~8 mL of a THF/py mixture, and the 20 mL solution was filtered and layered with 15 mL hexanes, forming a powdery product.

Attempted synthesis of Th/$(SPh)_2$/Hg/Ph_3PS/py

Th (0.233 g, 1.00 mmol) and $(SePh)_2$ (0.437 g, 2.00 mmol) were combined in py (20 mL) with a catalytic amount of I_2 and stirred for 4 d. Added Ph_3PS (0.294 g, 1.00 mmol) to a cloudy green reaction, which was then stirred for 1 d. Filtered 20 mL of the yellow solution and layered with 15 mL hexanes. Crystals formed were $(py)_4Th(SPh)_4$.

Attempted synthesis of Th/$(SePh)_2$/Hg/Ph_3PS/py

Th (0.233 g, 1.00 mmol) and $(SePh)_2$ (0.624 g, 2.00 mmol) were combined in py (20 mL) with a catalytic amount of I_2 and stirred for 3 d. Added Ph_3PS (0.295 g, 1.00 mmol) to a cloudy green reaction, which was then stirred for 2 d. Filtered 20 mL of the yellow solution and layered with 20 mL hexanes, not forming any crystals.

Attempted synthesis of U/$(SePh)_2$/Hg/Ph_3PS/py

U (0.119 g, 0.50 mmol) and $(SePh)_2$ (0.624 g, 2.00 mmol) were combined in py (20 mL) with a catalytic amount of I_2 and stirred for 1 week. Added Ph_3PS (0.300 g, 1.02 mmol), which was then stirred for 1 d, yielding a dark red solution. Filtered 20 mL of the dark red solution and layered with 20 mL hexanes and allowed to crystallize at -16°C. No crystals formed.

Attempted synthesis of U/I_2/Ph_3PS/Et_2O/toluene

U (0.238 g, 1.00 mmol) and I_2 (0.381 g, 1.50 mmol) were combined in Et_2O (20 mL) and stirred for 1 month at 2°C. Evaporated all Et_2O and dissolved the sample in 15 mL toluene and added Ph_3PS (0.294 g, 1.00 mmol), which was then stirred for 1 week, yielding a dark burgundy solution. Filtered 10 mL of the solution and layered with 10 mL hexanes and allowed to crystallize at -16°C. Crystals formed but contained only Ph_3PS.

Attempted synthesis of U/$(SC_6F_5)_2$/I_2/AgF_2/py

U (0.274 g, 1.15 mmol) and $(SC_6F_5)_2$ (0.688 g, 1.73 mmol) were combined in py (20 mL) with a catalytic amount of I_2 and stirred at 0°C. The solution was stirred for 5 days and became dark black. AgF_2 (0.215 g, 1.17 mmol) was added and stirred overnight. A 5 mL orange solution was filtered from 15 mL green precipitate and layered with 10 mL hexanes. No crystals formed.

Attempted synthesis of U/$(SPh)_2$/$(SC_6F_5)_2$/I_2/AgF/py

U (0.238 g, 1.00 mmol), $(SPh)_2$ (0.330 g, 1.51 mmol), and $(SC_6F_5)_2$ (0.199 g, 1.50 mmol) were combined in py (20 mL) with a catalytic amount of I_2. The solution was stirred for 3 weeks and became dark black. AgF (0.215 g, 1.69 mmol) was added and stirred overnight with no observed change in the dark black solution. 15 mL was filtered and layered with 25 mL hexanes cooled to -30°C. No crystals formed.

Reaction of Th/$(SePh)_2$/$(SeC_6F_5)_2$/Hg/AgF/py

Th (0.232 g, 1.00 mmol), $(SePh)_2$ (0.469 g, 1.50 mmol), and $(SeC_6F_5)_2$ (0.427 g, 1.50 mmol) were combined in py (10 mL) with a catalytic amount of Hg. The solution was stirred for 24 h. AgF (0.190 g, 1.5 mmol) was added and stirred overnight to yield a deep burgundy solution with dark grey precipitate. 10 mL was filtered and layered with 10 mL hexanes, forming crystals of $(py)_8Th_4Se_4(SePh)_4(SeC_6F_5)_4$ (**8**).

Attempted synthesis of Th/$(SePh)_2$/$(SeC_6F_5)_2$/Hg/NH_4F/py

Th (0.233 g, 1.00 mmol), $(SePh)_2$ (0.468 g, 1.50 mmol), and $(SeC_6F_5)_2$ (0.246 g, 0.50 mmol) were combined in py (15 mL) with a catalytic amount of Hg. The solution was stirred for 3 d. NH_4F (0.056 g, 1.5 mmol) was added and stirred 2 weeks to yield a deep burgundy solution with dark grey precipitate. 15 mL was filtered and layered with 15 mL hexanes, forming a thick gel substance.

Attempted synthesis of Th/$(SPh)_2$/Hg/AgF/py

Th (0.232 g, 1.00 mmol) and $(SPh)_2$ (0.437 g, 2.00 mmol) were combined in py (15 mL) with a catalytic amount of Hg. The solution was stirred for 1 week. AgF (0.191 g, 1.51 mmol) was added and stirred overnight to yield a dark black/green solution with dark grey precipitate. 5 mL was filtered from a dark grey precipitate and concentrated in vacuo to 3 mL and cooled to -30°C. No crystals formed.

Attempted synthesis of Th/$(SeC_6F_5)_2$/Hg/AgF/py

Th (0.232 g, 1.00 mmol) and $(SeC_6F_5)_2$ (0.984 g, 2.00 mmol) were combined in py (20 mL) with a catalytic amount of Hg. The solution was stirred for 3 d. AgF (0.190 g, 1.5 mmol) was added and stirred overnight to yield a deep burgundy

solution with dark grey precipitate. 20 mL was filtered and concentrated in vacuo to 15 mL and layered with 20 mL hexanes, forming a dark black oil.

Attempted synthesis of Th/$(SePh)_2$/I_2/Hg/AgF/py

Th (0.232 g, 1.00 mmol), $(SePh)_2$ (0.469 g, 1.50 mmol), and I_2 (0.128 g, 0.50 mmol) were combined in py (10 mL) with a catalytic amount of Hg. The solution was stirred for 5 d. AgF (0.130 g, 1.02 mmol) was added and stirred overnight to yield an orange solution with dark grey precipitate. 10 mL was filtered and layered with 20 mL hexanes, forming crystals that were highly disordered. Unable to determine structure.

Attempted synthesis of Th/$(SPh)_2$/I_2/$(SC_6F_5)_2$/Hg/AgF/py

Th (0.232 g, 1.00 mmol), $(SPh)_2$ (0.218 g, 1.00 mmol), I_2 (0.128 g, 0.50 mmol), and $(SC_6F_5)_2$ (0.199 g, 0.50 mmol) were combined in py (10 mL) with a catalytic amount of Hg. The solution was stirred for 4 d. AgF (0.130 g, 1.02 mmol) was added to the red reaction and stirred overnight to yield a burgundy solution with dark grey precipitate. 10 mL was filtered and layered with 20 mL hexanes, forming very small black crystals unsuitable for single crystal X-ray diffraction.

Attempted synthesis of U/$(SPh)_2$/I_2/$(SC_6F_5)_2$/Hg/AgF/py

U (0.238 g, 1.00 mmol), $(SPh)_2$ (0.218 g, 1.00 mmol), I_2 (0.130 g, 0.502 mmol), and $(SC_6F_5)_2$ (0.199 g, 0.50 mmol) were combined in py (15 mL) with a catalytic amount of Hg. The solution was stirred for 3 weeks. AgF (0.220 g, 1.73 mmol) was added to the dark black reaction and stirred overnight. 15 mL was filtered and layered with 25 mL hexanes. No crystals formed.

Attempted synthesis of Th/$(SePh)_2$/$(SeC_6F_5)_2$/$(SC_6F_5)_2$/Hg/AgF/py

Th (0.232 g, 1.00 mmol), $(SePh)_2$ (0.312 g, 1.00 mmol), $(SeC_6F_5)_2$ (0.369 g, 0.75 mmol), and $(SC_6F_5)_2$ (0.100 g, 0.25 mmol) were combined in py (12 mL) with a catalytic amount of Hg. The solution was stirred for 3 d. AgF (0.160 g, 1.26 mmol) was added to the cloudy dark green reaction and stirred overnight to yield a burgundy solution with dark grey precipitate. 10 mL was filtered and layered with 15 mL hexanes, forming a powdery product.

Reaction of Th/$(SePh)_2$/$(SeC_6F_5)_2$/$(SC_6F_5)_2$/Hg/AgF/py

Th (0.232 g, 1.00 mmol), $(SePh)_2$ (0.468 g, 1.50 mmol), $(SeC_6F_5)_2$ (0.246 g, 0.50 mmol), and $(SC_6F_5)_2$ (0.040 g, 0.10 mmol) were combined in py (10 mL) with a catalytic amount of Hg. The solution was stirred for 5 d. AgF (0.190 g, 1.50 mmol) was added to the cloudy dark green reaction and stirred overnight to yield a burgundy solution with dark grey precipitate. 10 mL was filtered and layered with 10 mL hexanes, forming crystals of a tetrameric thorium cubane with mixed E'C_6F_5 ligands (E' = S, Se) near 50/50%.

Reaction of Th/$(SePh)_2$/$(SeC_6F_5)_2$/Hg/AgF/py/acetonitrile

Th (0.232 g, 1.00 mmol), $(SePh)_2$ (0.468 g, 1.50 mmol), and $(SeC_6F_5)_2$ (0.248 g, 1.50 mmol) were combined in py (10 mL) with a catalytic amount of Hg. The solution was stirred for 3 d. Pyridine was removed under vacuum and the sample was redissolved in 20 mL toluene and 0.5 mL acetonitrile. AgF (0.190 g, 1.5 mmol) was added and stirred overnight to yield a red/brown solution with dark grey precipitate. 20 mL dark red solution was filtered and layered with 20 mL hexanes. Small poor-quality crystals formed; possible tetramer with toluene and acetonitrile as lattice solvents.

Attempted synthesis of Th/$(SPh)_2$/$(SC_6F_5)_2$/Hg/AgCl/py

Th (0.232 g, 1.00 mmol), $(SPh)_2$ (0.330 g, 1.51 mmol), $(SC_6F_5)_2$ (0.200 g, 0.503 mmol), and Hg (0.019 g, 0.095 mmol) were combined in pyridine (20 mL) and the solution was stirred for 3 d. AgCl (0.215 g, 1.50 mmol) was added to the cloudy gray solution and stirred for additional 24 h. The resulting orange solution (15 mL) was filtered and layered with hexane (20 mL), forming a powdery product.

Attempted synthesis of Th/$(SPh)_2$/Zn/$(SC_6F_5)_2$/Hg/AgF/py

Th (0.232 g, 1.00 mmol) and $(SPh)_2$ (0.437 g, 2.00 mmol) were combined in py with a catalytic amount of Hg and stirred for 6 days. In a separate flask, Zn (0.067 g, 1.0 mmol) and $(SC_6F_5)_2$ (0.398 g, 1.00 mmol) were combined in py with a catalytic amount of Hg and stirred for 6 days. The solution with Th was filtered into the solution with Zn and AgF (0.195 g, 1.50 mmol) was added and left to stir for 24 h. Filtered 25 mL dark black/green reaction and concentrated in vacuo to 20 mL. Layered this solution with 15 mL hexanes. No crystal formation.

Synthesis of U/Cu/$(SPh)_2$/$(SC_6F_5)_2$/I_2/AgF/py/DME

U (0.220 g, 0.924 mmol), Cu (0.030 g, 0.47 mmol), $(SPh)_2$ (0.202 g, 0.925 mmol), $(SC_6F_5)_2$ (0.276 g, 0.693 mmol), and I_2 (0.170 g, 0.670 mmol) were combined in 15 mL py. Stirred for 5 days. Added AgF (0.180 g, 1.42 mmol) to the black/brown solution and let stir 1 day. Evaporated py and dissolved sample in DME. Filtered 10 mL dark black solution and layered with 20 mL hexanes to yield very few crystals of $(py)_2UF_2(SC_6F_5)_2$(DME). This structure was unable to be reproduced.

Synthesis of Th/$(SPh)_2$/Hg/py/HOC_6F_5/AgF

Th (0.233 g, 1.01 mmol) and $(SPh)_2$ (0.437 g, 2.00 mmol) were combined in 20 mL py and a catalytic amount of Hg and stirred for 10 days. Added HOC_6F_5 (0.043 g, 0.50 mmol) to the very cloudy pink/grey solution and stirred for 1 d. Added AgF

(0.200 g, 1.13 mmol) and stirred 1 d. Filtered 15 mL yellow solution from grey precipitate. Concentrated in vacuo to 10 mL and layered with 20 mL hexanes to form crystals of $py_4Th(SPh)_4$.

Synthesis of Th/$(SePh)_2$/PhSeCl/Hg/py/AgF

Th (0.232 g, 1.00 mmol), $(SePh)_2$ (0.312 g, 1.00 mmol), and PhSeCl (0.192 g, 1.00 mmol) were combined in 20 mL py with a catalytic amount of Hg and stirred for 1 day. Added AgF (0.200 g, 1.58 mmol) and stirred 24 h. Filtered 20 mL yellow solution from grey precipitate. Concentrated in vacuo to 15 mL nd layered with 25 mL hexanes. Crystals formed of $(py)_4ThCl_4$.

Attempted synthesis of Th/$(SePh)_2$/PhSeBr/Hg/py/AgF

Th (0.232 g, 1.00 mmol), $(SePh)_2$ (0.312 g, 1.00 mmol), and PhSeBr (0.236 g, 1.00 mmol) were combined in 20 mL py with a catalytic amount of Hg and stirred for 1 day. Added AgF (0.200 g, 1.58 mmol) and stirred 24 h. Filtered 20 mL yellow solution from grey precipitate. Concentrated in vacuo to 15 mL nd layered with 25 mL hexanes, forming powdery product.

Synthesis of Th/$(SePh)_2$/PhSeCl/$(SC_6F_5)_2$/Hg/py/AgF

Th (0.233 g, 1.01 mmol), $(SePh)_2$ (0.156 g, 0.50 mmol), PhSeCl (0.192 g, 1.00 mmol), and $(SC_6F_5)_2$ (0.199 g, 0.500 mmol) were combined in 20 mL py with a catalytic amount of Hg and stirred for 7 days. Added AgF (0.210 g, 1.66 mmol) and stirred 24 h. Filtered 18 mL orange solution from yellow precipitate. Concentrated in vacuo to 15 mL nd layered with 25 mL hexanes. Crystals formed of $(py)_7Th_2F_5(SC_6F_5)_3$ (**6**).

Attempted synthesis of Th/$(SePh)_2$/PhSeBr/$(SC_6F_5)_2$/Hg/py/AgF

Th (0.240 g, 1.03 mmol), $(SePh)_2$ (0.160 g, 0.513 mmol), PhSeBr (0.240 g, 1.02 mmol), and $(SC_6F_5)_2$ (0.210 g, 0.527 mmol) were combined in 20 mL py with a catalytic amount of Hg and stirred for 2 days. Added AgF (0.190 g, 1.50 mmol) and stirred 24 h. Filtered 20 mL orange solution from yellow precipitate. Concentrated in vacuo to 15 mL nd layered with 25 mL hexanes. Powdery product formed.

Attempted synthesis of Th/$(SPh)_2$/$(SC_6F_5)_2$/Hg/py/AgF/bipy

Th (0.232 g, 1.00 mmol), $(SPh)_2$ (0.330 g, 1.51 mmol), and $(SC_6F_5)_2$ (0.200 g, 0.502 mmol) were combined in 15 mL py with a catalytic amount of Hg and stirred for 8 days. Added AgF (0.210 g, 1.66 mmol) and stirred 24 h. Filtered 15 mL orange solution from grey precipitate. Added bipy (0.156 g, 1.00 mmol) and stirred 1 d. Filtered 15 mL orange/red solution and layered with 25 mL hexanes. Powdery product formed.

Attempted synthesis of Th/FeI_2/$(SePh)_2$/Hg/py

Th (0.232 g, 1.00 mmol), FeI_2 (0.156 g, 0.504 mmol), and $(SePh)_2$ (0.624 g, 2.00 mmol) were combined in 20 mL py with a catalytic amount of Hg. Stirred 2 days. Filtered 14 mL orange solution from yellow precipitate and layered with 20 mL hexanes. Small crystals of FeI_2 formed.

Attempted synthesis of Th/$(SPh)_2$/$(SC_6F_5)_2$/$(SeC_6F_5)_2$/Hg/S/py

Th (0.232 g, 1.00 mmol), $(SPh)_2$ (0.218 g, 1.00 mmol), $(SC_6F_5)_2$ (0.199 g, 0.50 mmol), and $(SeC_6F_5)_2$ (0.246 g, 0.50 mmol) were combined in py (20 mL) with a catalytic amount of Hg. The solution was stirred for 2 d. Elemental S (0.035 g, 1.09 mmol) was added and stirred 1 h to yield a red solution with dark grey precipitate. 15 mL was filtered and layered with 20 mL hexanes, with a grey precipitate forming.

Attempted synthesis of Th/$(SePh)_2$/$(SPh)_2$/$(SC_6F_5)_2$/Hg/Se/py

Th (0.232 g, 1.00 mmol), (SePh)2 (0.156 g, 0.5 mmol), $(SPh)_2$ (0.218 g, 1.00 mmol), and $(SC_6F_5)_2$ (0.199 g, 0.50 mmol) were combined in py (20 mL) with a catalytic amount of Hg. The solution was stirred for 5 d. Elemental Se (0.082 g, 1.04 mmol) was added and stirred 2 h to yield a dark red solution with dark grey precipitate. 15 mL was filtered and layered with 10 mL hexanes, with a grey precipitate forming.

Reaction of Th/$(SePh)_2$/$(SC_6F_5)_2$/Hg/Se/SeO_2/py

Th (0.232 g, 1.00 mmol), (SePh)2 (0.468 g, 1.5 mmol) and $(SC_6F_5)_2$ (0.200 g, 0.51 mmol) were combined in py (20 mL) with a catalytic amount of Hg. The solution was stirred for 3 d. Elemental Se (0.080 g, 1.01 mmol) was added and stirred 2 h to yield a dark brown/red solution with dark grey precipitate. Added SeO_2 (0.030 g, 0.25 mmol) and stirred 1 h. 15 mL red solution was filtered from black precipitate and layered with 20 mL hexanes. Crystals of $(py)_8Th_4Se_4(SePh)_4(SC_6F_5)_4$ (**10**) formed.

Attempted synthesis of Th/$(SePh)_2$/$(SeC_6F_5)_2$/Hg/Se/SeO_2/py

Th (0.232 g, 1.00 mmol), (SePh)2 (0.470 g, 1.51 mmol) and $(SeC_6F_5)_2$ (0.247 g, 0.51 mmol) were combined in py (20 mL) with a catalytic amount of Hg. The solution was stirred for 3 d. Elemental Se (0.080 g, 1.01 mmol) was added and stirred 2 h to yield a dark brown/red solution with dark grey precipitate. Added SeO_2 (0.030 g, 0.25 mmol) and stirred 1 h. 15 mL red solution was filtered from black precipitate and layered with 20 mL hexanes, with a grey precipitate forming.

Reaction of Th/$(SePh)_2$/$(SeC_6F_5)_2$/Hg/SeO_2/py

Th (0.232 g, 1.00 mmol), (SePh)2 (0.468 g, 1.50 mmol) and $(SeC_6F_5)_2$ (0.246 g, 0.50 mmol) were combined in py (20 mL) with a catalytic amount of Hg. The solution was stirred for 3 d. Added SeO_2 (0.030 g, 0.25 mmol) and stirred 2.5 h to

yield a dark red solution. 20 mL red solution was filtered from black precipitate and concentrated in vacuo to 15 mL. The solution was layered with 25 mL hexane, forming crystals of $(py)_8Th_4Se_4(SePh)_4(SeC_6F_5)_4$ (**8**).

Synthesis of Th/$(SPh)_2$/Hg/py/HOC_6F_5/AgF

Th (0.232 g, 1.00 mmol) and $(SPh)_2$ (0.437 g, 2.00 mmol) were combined in 15 mL py and a catalytic amount of Hg and stirred for 6 days. Added HOC_6F_5 (0.190 g, 1.03 mmol) to the very cloudy grey solution and stirred for 1 week. Added AgF (0.210 g, 0.166 mmol) and stirred 1 d. Filtered 10 mL yellow solution from grey precipitate and layered with 30 mL hexanes to and placed in 0°C freezer. Formed crystals of $(py)_4Th(OC_6F_5)_4$.

Attempted synthesis of Th/$(SPh)_2$/Hg/py/HOC_6F_5/S

Th (0.232 g, 1.00 mmol) and $(SPh)_2$ (0.440 g, 2.02 mmol) were combined in 20 mL py and a catalytic amount of Hg and stirred for 5 days. Added HOC_6F_5 (0.190 g, 1.03 mmol) to the very cloudy pink/grey solution and stirred for 1 week. Added S (0.033 g, 1.0 mmol) and stirred 1 h. Filtered 15 mL yellow solution from grey precipitate. Concentrated in vacuo to 10 mL and layered with 25 mL hexanes to and placed in 0°C freezer. Formed very few poor-quality crystals.

Attempted synthesis of Th/$(SPh)_2$/$(Spy)_2$/Hg/py/AgF

Th (0.232 g, 1.00 mmol), $(SPh)_2$ (0.330 g, 1.51 mmol), and $(Spy)_2$ (0.115 g, 0.522 mmol) were combined with a catalytic amount of Hg in pyridine (20 mL). The solution was stirred for 1 week. AgF (0.210 g, 1.66 mmol) was added to the cloudy green solution, and the mixture was stirred for 2 h. The resulting light green solution (18 mL) was filtered and concentrated in vacuo to 15 mL before being layered with hexane (25 mL). Powdery product formed.

Attempted synthesis of Th/$(SePh)_2$/$(Spy)_2$/Hg/py/Se

Th (0.233 g, 1.01 mmol), $(SePh)_2$ (0.470 g, 1.51 mmol), and $(Spy)_2$ (0.115 g, 0.522 mmol) were combined with a catalytic amount of Hg in pyridine (20 mL). The solution was stirred for 1 day, elemental Se (0.080 g, 1.01 mmol) was added, and the mixture was stirred for 2 h. The resulting yellow solution (20 mL) was filtered and concentrated in vacuo to 15 mL before being layered with hexane (25 mL). Powdery product formed.

Attempted synthesis of Th/$(SePh)_2$/$(Spy)_2$/Hg/py/Se

Th (0.232 g, 1.00 mmol), $(SePh)_2$ (0.315 g, 1.01 mmol), and $(Spy)_2$ (0.220 g, 1.00 mmol) were combined with a catalytic amount of Hg in pyridine (20 mL). The solution was stirred for 5 days. Elemental Se (0.160 g, 2.03 mmol) was added, and the mixture was stirred for 2 h. The resulting orange solution (8 mL) was filtered and concentrated in vacuo to 3 mL and placed in -16°C freezer. Orange powdery precipitate formed.

Attempted synthesis of U/$(SePh)_2$/$(Spy)_2$/Hg/py/Se

U (0.245 g, 1.03 mmol), $(SePh)_2$ (0.325 g, 1.04 mmol), and $(Spy)_2$ (0.228 g, 1.03 mmol) were combined with a catalytic amount of I_2 in pyridine (10 mL). The solution was stirred for 10 days. Elemental Se (0.160 g, 2.03 mmol) was added, and the mixture was stirred for 2 h. The resulting dark black solution (8 mL) was filtered and concentrated in vacuo to 5 mL and placed in -16°C freezer. Black powdery precipitate formed.

Attempted synthesis of Th/$(SePh)_2$/$(Spy)_2$/I_2/Hg/py/AgF

Th (0.233 g, 1.01 mmol), $(SePh)_2$ (0.315 g, 1.02 mmol), $(Spy)_2$ (0.115 g, 0.520 mmol), and I2 (0.127 g, 0.50 mmol) were combined in pyridine (20 mL) with a

catalytic amount of Hg. The solution was stirred for 1 day. AgF (0.270 g, 2.13 mmol) was added to the cloudy green solution and stirred for additional 24 h. The resulting red solution (15 mL) was filtered and layered with hexane (10 mL) and placed in a 0°C freezer. Very small crystals and a lot of powder formed.

Attempted synthesis of U/$(SePh)_2$/$(Spy)_2$/I_2/Hg/py/AgF

U (0.240 g, 1.01 mmol), $(SePh)_2$ (0.315 g, 1.02 mmol), $(Spy)_2$ (0.115 g, 0.520 mmol), and I2 (0.127 g, 0.50 mmol) were combined in pyridine (20 mL) with a catalytic amount of I_2. The solution was stirred for 4 days. AgF (0.260 g, 2.05 mmol) was added to the dark black solution and stirred for additional 24 h. The resulting red solution (12 mL) was filtered and layered with hexane (8 mL) and placed in a 0°C freezer. Crystals of UI_2F_2 formed. This compound has been previously synthesized by others in the laboratory.

Attempted synthesis of Th/$(SC_6F_5)_2$/$(Spy)_2$/Hg/py

Th (0.233 g, 1.01 mmol), $(SC_6F_5)_2$ (0.398 g, 1.00 mmol), and $(Spy)_2$ (0.220 g, 1.00 mmol) were added to 10 mL py with a catalytic amount of Hg and stirred for 2 d. Added about 10 mL toluene. Filtered 18 mL of red solution from grey precipitate and concentrated in vacuo to 15 mL. Layered solution with 20 mL hexanes and placed in 0°C freezer, producing very few small crystals.

Attempted synthesis of Th/$(Spy)_2$/CuF_2/Hg/py

Th (0.232 g, 1.00 mmol), (Spy)2 (0.220 g, 1.00 mmol), and CuF_2 (0.051 g, 0.50 mmol) were added to 10 mL py with a catalytic amount of Hg. Let stir at room temperature for 1 day and then transferred to 60°C oil bath and stirred for 1 day, and then let stir at room temperature for 3 months. No reaction.

Attempted synthesis of U/$(Spy)_2$/CuF_2/Hg/py

U (0.245 g, 1.03 mmol), (Spy)2 (0.227 g, 1.03 mmol), and CuF_2 (0.052 g, 0.50 mmol) were added to 10 mL py with a catalytic amount of Hg. Let stir at room temperature for 1 day and then transferred to 60°C oil bath and stirred for 1 day, and then let stir at room temperature for 3 months. Most U went into solution. Added 10 mL py and filtered 20 mL dark green solution from dark green/black precipitate and layered with 20 mL hexanes. Formation of green precipitate.

5.5 References

1. Mckillop, A.; Koyuncu, D.; Krief, A.; Dumont, W.; Renier, P.; Trabelsi, M., Efficient, High-Yield Oxidation of Thiols and Selenols to Disulfides and Diselenides. *Tetrahedron Lett.* **1990,** *31* (35), 5007-5010.
2. Klapötke, T. M.; Krumm, B.; Polborn, K., Synthesis, Chemistry, and Characterization of Perfluoroaromatic Selenium Derivatives. *Eur. J. Inorg. Chem.* **1999,** *1999* (8), 1359-1366.
3. Bruker., *SMART v.5.625 (2001), SHELXTL v.6.14 (2003), and SAINT v.6.45A (2003). Programs for Single Crystal Data Collection, Data Processing and Structure Determination*. Bruker-AXS Inc.: Madison, Wisconsin, USA.
4. Sheldrick, G. M., A short history of SHELX. *Acta. Crystallogr.* **2008,** *64(1)*, 112-120.
5. Sheldrick, G. M., *SHELXS v.2013/1 and SHELXL v.2013/4 ; Programs for Crystal Structure Analysis*. University of Göttingen Göttingen, Germany, 2013.
6. Sheldrick, G. M., Crystal structure determination with SHELX. *Acta. Crystallog.* **2015,** *C71*, 3-8.
7. Macrae, C. F.; Sovago, I.; Cottrell, S. J.; Galek, P. T. A.; McCabe, P.; Pidcock, E.; Platings, M.; Shields, G. P.; Stevens, J. S.; Towler, M.; Wood, P. A., Mercury 4.0: from visualization to analysis, design and prediction. *Journal of Applied Crystallography*. **2020,** *53* (1), 226-235.